Vol. 1 I Issue 2 I January 2020

CHARUSAT JOURNAL

BY CHAROTAR UNIVERSITY OF SCIENCE AND TECHNOLOGY

CHARUSAT
CHAROTAR UNIVERSITY OF SCIENCE AND TECHNOLOGY

www.charusat.ac.in/charusatjournal

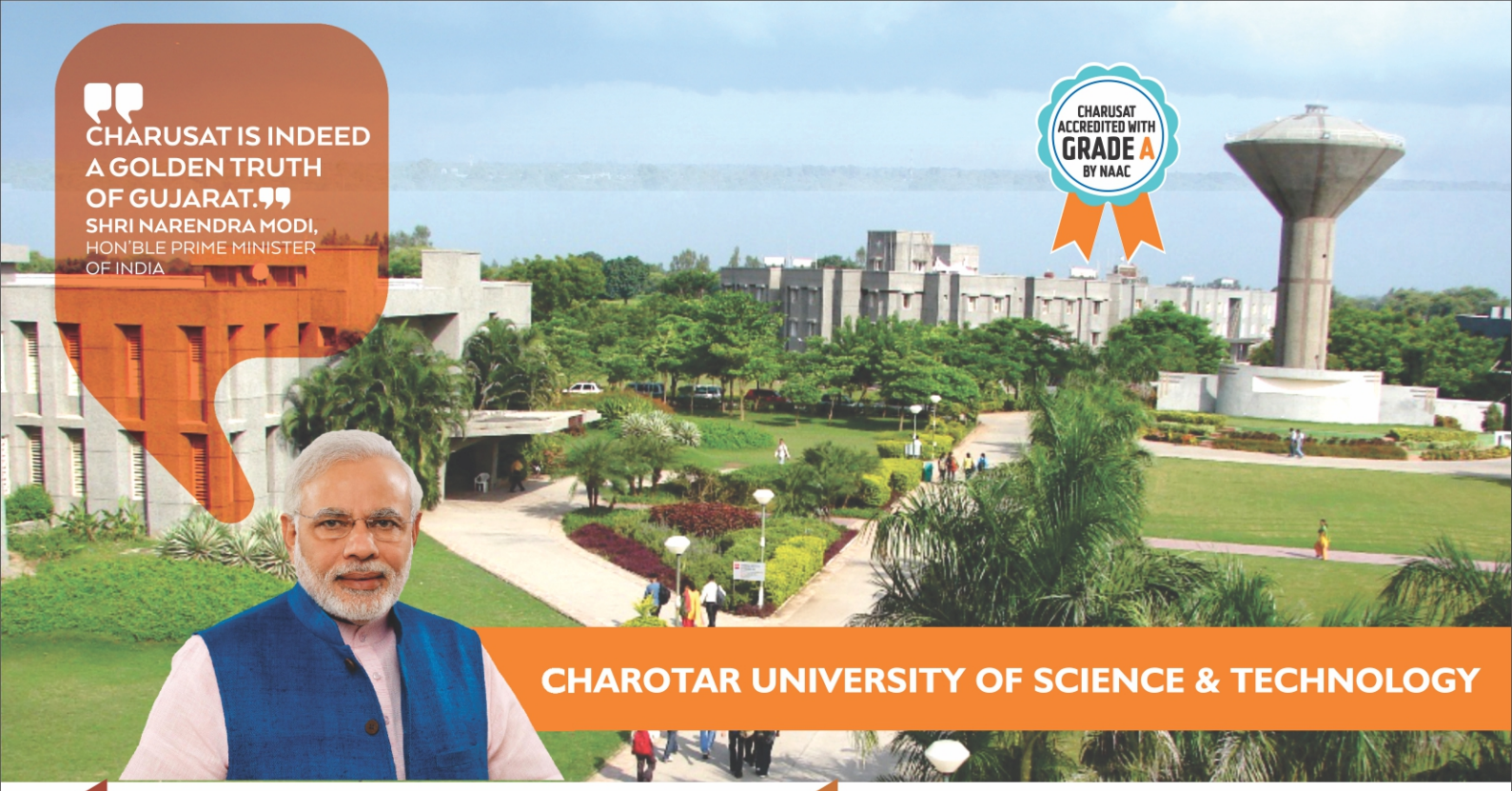

CHAROTAR UNIVERSITY OF SCIENCE & TECHNOLOGY

CHANDUBHAI S PATEL INSTITUTE OF TECHNOLOGY

- **B.Tech Programs**
  Mech. Engg. • Information Technology • Electronics & Communication Engg.
  Civil Engg. • Computer Engg. • Electrical Engg.
- **M.Tech Programs**
  Electronics & Communication Engg.
  (Communication Systems • VLSI & Embedded System)
  Mechanical Engg. (CAD/CAM • Advanced Manufacturing Tech.)
  Electrical Engg. (Power System) • Computer Engg. • Information Technology
  Civil Engineering(Structures)

P D PATEL INSTITUTE OF APPLIED SCIENCES

- **B Sc Program**
- **M Sc Programs**
  Biotechnology • Microbiology • Advanced Organic Chemistry
  Biochemistry • Physics • Mathematics

MANIKAKA TOPAWALA INSTITUTE OF NURSING

- **B Sc Nursing Program** • GNM Program
- **M Sc Nursing Programs**
  Medical Surgical • Obstetric & Gynecological • Community Health
  Paediatrics • Mental Health

SMT CHANDABEN MOHANBHAI PATEL INSTITUTE OF COMPUTER APPLICATIONS

- **BCA Program** • B Sc(IT)
- **MCA Program** • M Sc(IT)
- **PGDCA**

DEVANG PATEL INSTITUTE OF ADVANCE TECHNOLOGY AND RESEARCH

- **B.Tech Programs**
  Computer Science & Engineering • Information Technology
  Computer Engineering

RAMANBHAI PATEL COLLEGE OF PHARMACY

- **B.Pharm Program**
- **M.Pharm Programs**
  Pharmaceutical Technology • Quality Assurance • Clinical Pharmacy
  Pharmaceutics-Drug Regulatory Affairs • Pharmacology & Toxicology

INDUKAKA IPCOWALA INSTITUTE OF MANAGEMENT

• BBA Program • PGDM Program • MBA Program

CHAROTAR INSTITUTE OF PARAMEDICAL SCIENCES

- B. Optometry Program
- **B.Sc Program**
  Medical Radiology & Imaging Technology (BRIT)
  Operation Theatre and Anesthesia Technology (BOPTAT)
- **M.Sc Program**
  Medical Lab Technology
- **PG Diploma**
  Clinical Hypnosis(PGDCH) • Medical Lab Technology(PGDMLT)

ASHOK & RITA PATEL INSTITUTE OF PHYSIOTHERAPY

- **BPT Program**
- **MPT Programs**
  Musculoskeletal Sciences • Women's Health • Paediatrics
  Neurological Sciences • Cardiopulmonary Sciences • Rehabilitation

Ph D PROGRAM IN ALL FACULTIES

CENTERS

- DR. K. C. PATEL RESEARCH & DEVELOPMENT CENTER
- CHARUSAT SPACE RESEARCH & TECHNOLOGY CENTER
- PRAMUKH SWAMI CENTER OF EXCELLENCE IN RENEWBLE ENERGY
- PRI. B. I. PATEL HUMAN RESOURCE DEVELOPMENT CENTRE
- CHARUSAT RURAL EDUCATION DEVELOPMENT PROGRAM (CREDP)

CHARUSAT
CHAROTAR UNIVERSITY OF SCIENCE AND TECHNOLOGY

Accredited with Grade "A" by NAAC, Govt. of India

CHARUSAT
Campus-Changa.
Off Nadiad-Petlad Highway,
Gujarat-388421, INDIA.

Call: (02697), 265011,265021,
E: admissions@charusat.ac.in
Website: www.charusat.ac.in
Help line : 8905 500 500

CHARUSAT is a member of ACU,UK and AIU,New Delhi • Established Under Gujarat State Act No.8 of 2009

Aegis: **Shri Charotar Moti Sattavis Patidar Kelavani Mandal**
President : Shri Surendra M Patel **Secretary :** Dr. M. C. Patel

Edited by Dr. Palash Mandal, Printed and Published by Dr. Devang Joshi, On behalf of Charotar University of Science and Technology, Changa-388421, Gujarat, India and Printed at Reprography Centre, 1st floor, Administration Block, Charotar University of Science and Technology, CHARUSAT Campus, Changa-388421, Gujarat, India.

Vol. 1 I Issue 2 I January 2020

CHARUSAT JOURNAL

BY CHAROTAR UNIVERSITY OF SCIENCE AND TECHNOLOGY

CHARUSAT
CHAROTAR UNIVERSITY OF SCIENCE AND TECHNOLOGY

www.charusat.ac.in/charusatjournal

CHARUSAT JOURNAL : General Information

General

The CHARUSAT JOURNAL aims principally at publishing papers/articles resulting from original research whether pure or applied of disciplines broadly classified as Physical, Biological and Chemical Sciences, Medical & Pharmaceutical Sciences, Engineering, Technology and Management. The primary criteria will be that these articles/papers contribute to the advancement of knowledge in the respective fields of Science and Technology. Papers submitted to other publishing agencies will not be accepted. However manuscripts published in un-refereed magazines, proceedings etc. may be accepted subject to satisfying the requirements for publishing in the CHARUSAT JOURNAL. The journal will publish peer-reviewed full length research papers and review articles under broad category of above mentioned fields.

Instruction to Author

Manuscript Preparation and Submission: Manuscripts should generally be arranged in the following order: title page, abstract, introduction, literature review, materials and methods (or Methodology or Procedure), results, discussion (or results and discussions), conclusion (or conclusion and recommendations) acknowledgements, and references.

Submission: Manuscripts in English (Prepare in Microsoft Word 2007 or a later version word document-DOC/DOCX), should be submitted via the online system of CHARUSAT JOURNAL or through Email to Chief Editor (Email:editor.journal @ charusat.ac.in). The Manuscript should be prepared as per the specification/style given in the "Manuscript Specification/Style". During manuscript submission, the submitting author (corresponding author) must provide contact information (full name, email address, institutional affiliation and mailing address) for all of the co-authors. The author who submits the manuscript for publication accepts the responsibility of notifying all co-authors that the manuscript is being submitted. Deletion of an author after the manuscript has been submitted requires a confirming letter to the Editor-in-Chief from the author whose name is being deleted.

Agreements: Authors intending to publish the article/papers to CHARUSAT JOURNAL should submit properly completed and signed Copyright Transfer Agreement (CTA) and Declaration of Conflicts of Interest & Author Agreement Form (DCIAA). These must be submitted for each manuscript either electronically or through PDF version by the corresponding author. If the PDF version is used, all pages of the signed PDF Agreement must be submitted. Submission of articles/papers to CHARUSAT JOURNAL is understood to mean that the author(s) agree to transfer copyright of the article solely to the publisher to facilitate the widest possible dissemination.

Manuscript Specification/Style: The Manuscript should be prepared as per the specification/style given below. Papers/Articles that fail to meet the CHARUSAT JOURNAL style and form will be rejected outright. Manuscripts must be typed double column (0.8 cm column spacing) single spaced on A4 size paper with 2 cm margins on both side of the paper. It is recommended that prospective authors use numbered pages on right bottom corner.

Length of the Paper: Full length research papers should have maximum 4000 words including an abstract, keywords, an introduction, materials and methods, results, discussion, conclusion, up to a maximum of 6 pages. Review articles should not exceed 5000 words. Title page: The first page of any manuscript shall include the title, name(s) of authors, their institutional affiliations, city and country. Corresponding author should give their address and Email ID in the footnote of the first page.

Title: Titles should clearly and concisely reflect the importance and content of the manuscript and be accessible to a broad audience. The title of the article is typed in bold leading capitals using font size 14 Times New Roman; abbreviations are not allowed. Title must be within one hundred characters (including spaces), descriptive of the contents of the manuscripts and to be accommodated in maximum two lines with single spacing. Author List: Include all those who have made substantial contributions to the work. To facilitate

indexing and retrieval and for unique identification, authors should be listed with surnames first followed by their first name and initials (eg: Smith James K) in font size 10 Times New Roman. At least one author must be designated with an asterisk as the "Corresponding Author"—the person to whom correspondence should be addressed. In case of ambiguity, Chief Editor may ask details of contribution of each author from the corresponding author.

Author (s) affiliation: Addresses (including emails) should be listed under the names of authors with font size 8 Times New Roman Italic. Where authors work at different addresses, they should be identified by numbered superscripts against their names. References to professional qualifications/titles are not required. The first author will be assumed to be the contact person unless otherwise stated.

Abstract: A summation of the most important results and conclusions not exceeding 200 words and to be written in a single section. The abstract heading should be typed in font size 10 Times New Roman in bold leading capital. The text of the abstract should be typed in font size 10 Times New Roman and in italics. The abstract is a concise abbreviated version of the paper which must be informative with respect to aim, methods, procedures, results, discussion, and conclusion.

Keywords: Heading should be 10 points Times New Roman bold. A maximum of five keywords (10 points Times New Roman, leading capital, separated by comma) that best describe the material being presented must follow the abstract.

Body Text Subtitles: The heading of main sections should be typed with font size10 Times New Roman and in bold capital. Subsection titles should be typed with font size10 Times New Roman and in bold leading capital

Body Text: Suitably paragraphed and written with font size 10 Times New Roman, single

spaced.

Tables: Tables are to be numbered according to their sequence in the text and should also be referred to in the text before they are placed. The Tables should be inserted at the exact positions where they belong in the body of the paper. Size and layout limitations of CHARUSAT JOURNAL do not allow for large tables. All Tables must have short but self- explanatory titles. Table numbers and titles should be placed at the top left of the Tables (10 Roman). Tables should be numbered from Table 1 and continued serially to 2, 3, etc. As much as possible avoid numbering unrelated tables as (a), (b), e.g. Table 3(a), Table 3(b).

Figures: Figures should be inserted at the exact positions where they belong in the body of the paper and should also be referred to in the text before they are placed. They should be clearly captioned and numbered in sequence below each figure. Line drawings must be done in black ink. Photographs (good, glossy black and white) and line drawings should not be mounted. Figures may not be used to duplicate data already presented in tables or text or vice versa. Photographs and illustrations other than tables are considered as figures and should be referred to as such. Figure numbers and titles should be placed at the bottom left of the figure (10 Roman). Figures should be numbered from 1 and continued serially to 2, 3, etc. As much as possible avoid numbering unrelated figures as (a), (b), e.g. Fig. 3(a), Fig. 3(b).

Footnotes: Footnotes should be labeled with superscript numbers (1). Footnotes should be used sparingly and only if absolutely required, otherwise the information should be embodied in the text of the paper.

Acknowledgment: This section should acknowledge financial support, technical assistance, advice from colleagues, gifts, etc. (if any)

References:

Harvard Referencing Style should be followed.

References to literature in the body of the manuscript are cited by author(s), followed by year. Authors are cited by their surnames only depending on sentence structure.

Single author: Albert (2007) developed this method of …… Subsequently other researchers have adopted this technique (Premkrishna, 2009; Bhaskar, 2010).

Two Authors: Albert and Ram (2008) developed the model of …….. Subsequently other researchers adopted this technique (Premkrishna, 2009; Rao and Ram, 2011)

Multiple Authors: Ram et al. (2008) has developed a model…..the efficiency of such model is questioned by many researchers further (Premkrishna et al., 2009; Robert, 2010)

Addresses:

Printed by
Dr. Devang Joshi
Registrar,
Charotar University of Science and Technology

Published by
Dr. Devang Joshi
Registrar,
Charotar University of Science and Technology
Phone: 91-02697-265001

On behalf of
Charotar University of Science and Technology,
Changa

Printed at
Reprography Centre

1st floor, Administration Block,

Charotar University of Science and Technology

CHARUSAT Campus, Changa

Published at
Charotar University of Science and Technology
CHARUSAT Campus,
Off. Nadiad-Petlad Highway, Changa,
District: Anand
Gujarat- 388 421

Edited by

Dr. Palash Mandal
Associate Professor,
PDPIAS, Charotar University of Science and Technology
Email: editor.journal@charusat.ac.in
Phone: +91 9666164654

CHARUSAT Journal

A Scientific Publication of CHARUSAT

Editorial Board

Contents

Preface
Research at CHARUSAT
Pankaj Joshi 01

Research Articles

Simultaneous determination of Bimatoprost and Timolol Maleate by Chemometric assisted Ultra-Violet Visible spectrophotometric methods in its pure drugs and it's combined dosage form
Priyanka P. Bhat , Vyomesh P. Nandurbarkar , Samir G. Patel 05

A facile synthesis of Iron Sulfide thin films by Chemical Bath Deposition
Abey M Abraham , Jaimini V Patel1, C. K. Sumesh 13

Screening of significant medium components for enhanced elicitor production using Plackett-Burman Design
Janki N. Thakker, Pinakin C. Dhandhukia, M. Kumari, I. L. Kothari 19

Impact Assessment of Reactive Power Capabilities of Distributed Generating Units in Radial Distribution Network
Pankita Mehta , Praghnesh Bhatt, Vivek Pandya 26

Dissolution Enhancement of Quetiapine Fumarate by Liquisolid Compacts Technique
Dharmang Pandya, Rajesh Parikh, Balram Gajra, Gaytri Patel 33

Comparative study of various beam-column connections under progressive collapse mechanism
Parth Senjalia, V. R. Panchal , Dhaval D. Patel 43

Effect of Parameter Variations on Sensorless Control of BLDC Motor Using Disturbance Torque Estimation
Mitesh B. Astik, Praghnesh Bhatt, Bhavesh R. Bhalja 49

Isolation and characterization of bacteria associated with sunscald-affected Capsicum annuum L.
Vaishnawi Gupta, Aditi D Buch 58

Review Articles

Analytical Methods for Quantitative Estimation of Montelukast Sodium: A Review
Kunti Shah, Vijaykumar Parmar 64

Microbial Chitinase and its potential application for biological control of plant parasites
Farhat Z Marchawala , Seema R Amin 79

Preface

Research at CHARUSAT

Dear Readers, It is my great pleasure to present to you the second issue of the CHARUSAT Journal of the Charotar University of Science and Technology, Anand. Taking advantage of this opportunity, I would like to share with you some news about the research at CHARUSAT University.

Research is a process which involves the application of multiple fields to understand and get solutions to one problem. CHARUSAT offers the students a platform to do research in various disciplines and hence the chances and ease of doing multi-disciplinary research is at it's best in the campus.

CHARUSAT highlights and encourages research projects. Research-oriented M.Sc., M.Pharm. and M.Tech. programs have been started and quality research has always been an vital criterion in faculty selection.

An important goal of the research activity at CHARUSAT is to improve the excellence of interaction between the institute and industry for resolving technical problems in the broad field of Engineering and Sciences.

Similarly important is the aim of stimulating and enhancing the research ability and potential of CHARUSAT students who have the interest and aptitude to carry out innovative research.

At present dynamic research is being carried out within the institutes into various aspects of science and engineering, and also into the many ways in which technology and science impact society and culture.

The CHARUSAT institutes are provided with well-equipped laboratories, specialized equipments, the full range of required infrastructure, including campus-wide networking and high-speed internet access, subscription to hundreds of print and online journals, and more.

In Gujarat, there are no such research institutes where budding researchers and students could go for great quality science education at the undergraduate level. One thing is unquestionably clear: students should learn science in an atmosphere where thrilling research is being conducted simultaneously. In fact, it is considered important that there must be a new system where the students themselves would participate in research. Moreover, an interdisciplinary coordination of learning is sought in which students would get a stable foundation in all the sciences before choosing to specialize in one.

We hope this concept will break down fake barriers between research and undergraduate teaching, as well as barriers between foremost scientific disciplines. Once the comprehensive objectives will be clear, things will move very rapidly.

Here at CHARUSAT, Students doing their masters programme are always encouraged to appear and clear national entrances like CSIR-NET, GATE, etc.

I think the better research output can come by involving more students to do research as that will provide more ideas and deeper understanding for any particular research problem. Hence we are encouraging more students to enroll for Ph.D. programme. Also, all Ph.D. students are provided with fellowship as per the UGC norms to keep them motivated throughout the Ph.D. tenure. This will motivate more students to enroll for Ph.D.

We are organizing conferences and lecture series very often in every departments to provide a platform to interact with scientists and researchers from across India and Globe.

We are offering statrtup grant from university to the research guides to do some preliminary work, which is a mandatory requirement for any project to be

submitted to any national funding agency like DBT/DST.

A good piece of research work is impossible without involving the expertise of different disciplines, and hence we are encouraging collaborative research and possibly industrial collaboration.

The instrument facilities on campus does not have any charge for the students doing Ph.D. from CHARUSAT.

About the CHARUSAT Journal

It is a peer-reviewed journal publishing articles in open ground to promote the author and building capacity on various multidisciplinary research issues. This Journal would like to devote its point to recognize research ideas through the potential young researchers for our country's development. It is a knowledge base platform to uplift regular practice through writing, publishing and disseminates research findings to gather new knowledge interacting with other researchers in respective fields. Thus, students and young researchers can find a path to grow expertise in respective fields as per their standpoint and interest and more significant positive gains in attitude and motivation will be grown gradually.

Objectives of the Journal

The foremost objective of this journal is to promote authors and researchers to grow expertise in respective fields through the publication of diverse articles. Moreover, it tries to establish a platform in which people's voice can be raised by the views of young researchers for country's well being, benefit and development. In this regards, this platform assists several programs for the promotion of research activities, publication of findings and newly collected knowledge.

Goal of the Journal

This journal will work for the continuation of publishing and promoting young researchers through capacity building in field base article writing and gathering of new knowledge with proper innovations and guidelines.

Subject Area of the Journal

CHARUSAT Journal publishes research articles, literature review articles, etc. Manuscripits are welcome from all fields of life sciences. The typical topics include, but are not limited to the following fields: Biology, Cosmology, Physics, Nanotechnology, Chemical Sciences, Artificial intelligence, Communication Studies, Paramedical Science, Nursing, Physiotherapy, Computer Sciences, and Environmental engineering.

The CHARUSAT Journal was intended and founded to signify the increasing needs of computational science as an emerging and progressively vital field, now widely recognized as an integral part of scientific and technical investigations. Its operation is to become an opinion of the Biological sciences, computational science community, addressing researchers and practitioners in areas extending from cosmology to biochemistry, from electronics to environmental sciences, from mathematics to software architecture, giving demonstrable computational methods, findings, and solutions.

CURRENT TRENDS IN SCIENTIFIC RESEARCH

Science and the scientific research are crucial for the development of any country and its economy. Every country has its own amount of funds being allocated for the research and development that encompasses various fields of research, including physical, biological, chemical sciences, along with space research. In current years, the scientific community and affiliated professions have toyed with the idea of generating a "lab of the future." Vendors, research organizations, and engineering and design firms have all begun to explore how contemporary scientists work within research environments and how the physical layout of labs can better support their endeavors. This process has been driven by a desire to substitute more effective collaboration among scientists, rise the number of new ideas entering the pipeline, and permit for more elasticity over the life cycle of a research facility.

One matter that can't be overlooked is that these initial considerations have unfolded during a time when scientific labs were less in comparition with the space allotted for equipment and analysis.

The work patterns, in general, have changed, and shall still continue to change. The type of research that is currently being conducted worldwide is not limited to a single principle investigator and involves various collaborators instead. This is the demand of the time and the type of research which requires different types of analysis to the same issue. This helps giving a clear and better understanding of any issue being addressed. Scientific research used to comprise basic requirements for personal space. Researchers required a six foot long work bench and a four foot long desk. Earlier, the research used to be limited to wet lab

experiments, which have now been replaced by dry lab experiments that involve use of bio-informatic tools, docking studies for understanding the receptor-ligand interactions in a better way, and also the most recent artificial intelligence (AI), which shows better collaboration of all disciplines of science towards one scientific problem.

As we all know that scientific community including research organizations and technological firms have started dreaming about Virtual and intelltual science from physical hard science. This will provide research organizations with unswearing data hubs and better communication connectivity in the field of technology. With new format of visualizing and analysing techniques, data will continue to hoard more rapidly that researchers can analyze it with accurate and reasonable automated analytical software endorsing collaboration among scientific communities. With changing technology, new ideas and approaches for designing automated labs requires sufficient space to do upgraded research in this new emerging world. From our current vantage point, it may be difficult to predict how the scientific and modern lab will look and function in what manner! Till now, science and technology has evolved way ahead. Presently, through flow chip technology, over a billion compounds can process per day rather than automated genome sequencing processing 10,000 compounds per day.

Now-a-days, enterprises are shifting the consumer focus towards more emerging trends and technologies which makes consumer lives more easy and affordable to extent. The field of nanotechnology is going to be evolved to the most by 2025 and shall be applied from toothpastes to car tyres to clothing, which will aid to betterment of individual's life. Other such evolvement is Artificial Intelligence (AI) which is a new hangout among the consumers. According to David Sackman, CEO of Lieberman Research Worldwide, Amazon's Echo, Google Home, and other chat bots are making artificial intelligence at success which in near future will ease the task of engagement, survey, and questionnaire development. According to data, scientists, AI will significantly aid in market analysis, but it will be a challenging task to eliminate traditional research methods altogether. In a field of medicinal/ digital pharmaceutical technology, scientists develop 3D printer- computer for producing any prescription drug accurately in a short time by inputting formulaic quantities of chemicals. This will provide society more accurate and effective treatment towards individual's illness as the computer will allow drugs to personalize according to respective need of an individual. Therefore, with varied forms of 3D printing technologies in medicine, it could transform the digital health industry, and eventually help society to live healthier and better life. The world's first bioeleccetric medicine (wireless device) have been successfully launched which speeds up the nerve regeneration and heal the damaged brain nerves. In the field of Cosmology, scientists have found 12 new moons orbiting around Jupiter, bringing its total number of moons to 79 in the solar system. Therefore, a key part of this assignment is confirming that the scientific community is well equipped with tools and technologies which are needed to evolve the digital science towards new heights.

The medical research these days is no more related to biochemical testing. Various genetic testings have taken the market by storm. Genetic testing has been possible due to the boon of human genome sequencing, which was one of the major breakthroughs in scientific research. Research in the field of genetics of various hereditary diseases has identified major polymorphisms in the genetic make-up of individuals which can render them susceptibility towards any genetic disease. Hence, this tool could be used to progress towards personalized medicine, which could involve testing a person's genetic make-up for any disease, thereby taking measures to prevent the disease development.

Various pharmaceutical companies throughout the world have channeled their research funds towards development of innovative molecules that could be used as a drug, which requires a synthesis of novel molecules. This is where chemistry in the wet lab and docking in the dry lab needs to collaborate for giving better and accurate results.

CHARUSAT Journal welcomes the research from various fields of science and technology, which adds in for the welfare of the society.

Pankaj Joshi
Provost
Charotar University of
Science and Technology (CHARUSAT)
Changa-388 421, Anand, Gujarat
E-mail :psjprovost@charusat.ac.in

Simultaneous determination of Bimatoprost and Timolol Maleate by Chemometric assisted Ultra-Violet Visible spectrophotometric methods in its pure drugs and it's combined dosage form

Priyanka P. Bhat[1], Vyomesh P. Nandurbarkar[2], Samir G. Patel[1]*

[1]Department of Pharmaceutical Chemistry and Analysis, Ramanbhai Patel College of Pharmacy, CHARUSAT Campus, Changa, Gujarat- 388 421, India
[2]Department of Mathematics, P.D. Patel Institute, CHARUSAT Campus, Changa, Gujarat- 388 421, India

Received: 07/02/2017
Revised: 19/07/2017
Accepted: 28/08/2017

Correspondence to:
*Samir G. Patel:
samirpatel.ph@charusat.ac.in

Abstract:

Chemometric methods including Classical Least Square (CLS), Principal Component Regression (PCR) and Partial Least Square (PLS) were developed for simultaneous determination of Bimatoprost and Timolol Maleate in ophthalmic solution using UV-spectrophotometry. A set of 25 standard mixtures containing both drugs were prepared in range of 1-3 µgmL-1 for Bimatoprost and 16.67-50 µgmL-1 for Timolol Maleate. The developed methods were validated as per IUPAC guidelines. Analytical figure of merit (FOM), such as sensitivity, selectivity, limit of detection and limit of quantitation were determined for Chemometric methods. The proposed methods were applied for determination of two components from combined dosage form.

Keywords: Bimatoprost, Timolol Maleate, Partial Least Square, Principal Component Regression, Classical Least Square.

INTRODUCTION

Bimatoprost (BIM) (Figure 1) {5Z)-7-[(1R, 2R, 3R, 5S)-3,5-dihydroxy-2-[(1E,3S)-3-hydroxy-5-phenylpent-1-en-1-yl]cyclopentyl]-N-ethylhept-5-enamide}[1] having chemical formula $C_{25}H_{37}NO_4$ is a prostamide or synthetic prostaglandin analog, thought to lower intraocular pressure (IOP) by increasing the outflow of aqueous humor through both the trabecular meshwork and uveoscleral drainage systems. BIM is not official in any of the pharmacopoeias.

Timolol Maleate (TM) (Fig. 2) {tert-butyl (2-hydroxy-3-{[4-(morpholin-4-yl)-1,2,5-thiadiazol-3-yl]oxy}propyl)amine}[2] having chemical formula $C_{13}H_{24}N_4O_3S$, is an Anti glucomatic agent, causes a reduction in the production of the liquid (aqueous humor) within the eye, thus decreasing intraocular pressure (IOP) Timolol is official in Indian Pharmacopoeia, 2010 [3].

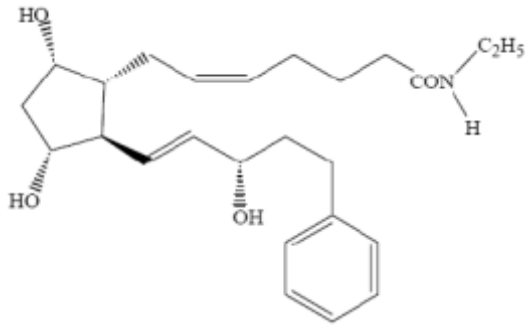

Figure 1 Structure of Bimatoprost

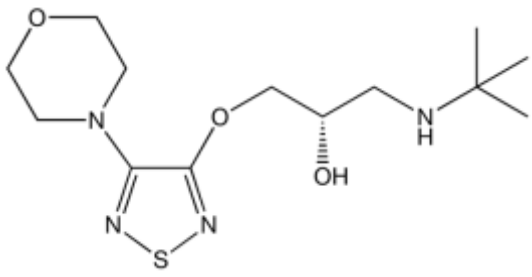

Figure 2 Structuure of Timolol Maleate

The marketed formulation CAREPROST PLUS containing BIM and TM 0.03 and 0.5% respectively (Sun pharmaceuticals Pvt. Ltd., Vadodara) was used throughout the study. Based on literature review it was found that number of methods are available for the estimation of BIM and TM individually as well as in combination with other drugs. Chemometric [4,5], spectrophotometric [6-8]; Near IR and Raman Spectroscopy [9], HPTLC [10] Capillary Zone Electrophoresis [11], UPLC [12] and RP-HPLC [13-18] methods have been used for the estimation of TM and RP-HPLC(by using ELSD Detector) [19,20] methods have been used for the estimation of BIM. As per the literatire non e of the method is available to estimate both the drug simalteniously, hence our thought of interest to develop and validate an analytical method to identified both the drug simalteniopusly.

UV/VIS spectroscopy is a preferred analytical technique as it is easy to operate and interpret the results easily. The various methods UV-spectrophotometry available are:

- Simultaneous Equation estimation Method
- Derivative Spectrophotometry Method
- Absorbance ratio method
- Absorbance Correction method.

But the limitation of UV spectrophotometric methods is its Sensitivity. This limitation could be overcome by use of Chemometric techniques [21-24] that have been reported to be more sensitive than Chromatographic techniques. It was thought of interest to combine the advantage of statistics and UV spectroscopy to develop a simple yet sensitive method for analysis of these drugs. In recent years, multivariate calibrations such as classical least square (CLS), Principal Component Regression (PCR) and Partial lest square (PLS) have been employed extensively in quantitative spectral analysis to get selective information from the unselective data. These methods can be applied for the simultaneous spectrophotometric estimation of drugs in pharmaceutical formulation containing two or more drug compounds. CLS is one of the simplest methods having multivariate least square procedure based directly on Beer's law. PCR and PLS [25-27] are factor analysis methods which are used to establish a relationship between matrices of the chemical data. PLS is related to PCR in that spectral decomposition is performed. PCR decomposition is significantly influenced by variations, which have no relevance to analyte concentration, where as PLS spectral decomposition is weighted to concentration.

METHODS/MATERIALS AND METHODS

Material and Methods

Standards for drugs and reagents

Pure standard sample of BIM and TM were procured as a gratis sample from the Sun pharmaceuticals Pvt. Ltd., Vadodara. Methanol AR grade were purchased from Loba Chemie (Laboratory Chemicals and Fine Reagents).

Instrument and Software

A double beam UV-spectrophotometer, UV-1800 (Shimadzu, Japan) equipped with 1 cm quartz cells and 2 nm fixed slit width connected to a computer loaded with Shimadzu UVPC software was used. An analytical balance New Classic MF (Model No. ML204/A01 METLET TOLEDO Made in Switzerland) was used to weigh accurately the standard and test samples. The additional SOLO software (EIGENVECTOR) was used for various Chemometric methods. The zero order spectra was recorded over 200–400 nm wavelength with one data point per nanometer for Chemometric method.

Pharmaceutical Formulation

Eye drop Careprost Plus, containing 0.03% Bimatoprost and 0.5% TM was taken for the study.

CHEMOMETRIC METHOD[27,28,29,30,31]

Preparation of Stock Solutions

BIM powder (10 mg) was accurately weighed and transferred to a 100 mL volumetric flask. It was dissolved and diluted up to the mark of 100 mL with methanol to obtain a stock solution of BIM with final concentration of 0.1 mg/mol (100µg/ml). TM powder (100 mg) was accurately weighed and transferred to a 100 mL volumetric flask. It was dissolved and diluted up to the mark of 100 mL with methanol to obtain a stock solution of TM with final concentration of 1 mg/mol (1000µg/ml).

Preperation of Working Standard Solution:

Stock solution of BIM (1 mL) was transferred to 10 mL volumetric flask and diluted up to the mark of 10 mL with Methanol to obtain working standard solution of BIM with final concentration of 10 µg/mL. Stock solution of TM (1 mL) was transferred to 10 mL volumetric flask and diluted up to the mark of 10 mL with Methanol to obtain working standard solution of TM with final concentration of 100 µg/mL.

Preparation of Calibration set:

Working standard solutions having concentration range of 1-3 µg mL^{-1} and 16.67-50 µg mL^{-1} for BIM and

TM were prepared by withdrawing 0.1-0.3mL of BIM and 0.16-0.50mL of TM from the above prepared standard stock solutions by using (Tarsons Accupipet, INDIA) micropipette having capacity of 10-100 µL.

Experimental design for CLS, PLS and PCR calibration

A dataset of standard mixture solutions containing 1-3 µg mL^{-1} and 16.67-50 µg mL^{-1} for BIM and TM were prepared from standard stock solution. A set design of concentration data corresponding to the BIM and TM mixture was organized statistically to maximize the information content in the spectra and to minimize the error of multivariate calibrations. The set of 25 standard mixture solutions, with different concentration ratios as mentioned above were systematically prepared (Table 1). From the data set, 9 mixtures have been randomly selected for the validation purpose. The UV absorption spectra were recorded over selected wavelength points. The computations were made using EIGENVECTOR SOLO software for PLS, PCR, CLS methods.

Data Processing

Classical Least Square Method

The Beer–Lambert's law of UV–Vis spectroscopy applied to multiple linear regressions lead to CLS.

* indicates Validation data set

Table 1: Concentration matrix of mixtures containing both drugs BIM and TM (Calibration data set)

S.No.	Concentration (µg mL^{-1})	S.No.	Concentration (µg mL^{-1})		
	BIM	TM		BIM	TM
1	1	16.67	14	2	41.67
2	1	24.99	15	2	50
3*	1	33.34	16	2.5	16.67
4	1	41.67	17*	2.5	24.99
5*	1	50	18	2.5	33.34
6*	1.5	16.67	19	2.5	41.67
7*	1.5	24.99	20*	2.5	50
8	1.5	33.34	21	3	16.67
9*	1.5	41.67	22	3	24.99
10	1.5	50	23	3	33.34
11*	2	16.67	24*	3	41.67
12	2	24.99	25	3	50
13	2	33.34			

* indicates Validation data set

The mathematical formulation of this method, in the matrix compact form can be written as

$$A = K \times C \text{----------(1)}$$

for CLS. Here A is the zero order absorbance, C is the concentration matrix and K is the calibration coefficients.

Partial Least Square and Principal Component Regression Method

An appropriate choice of number of principal components or factors is necessary for PCR and PLS calibrations. Various criteria have been developed to select the optimum parameters. Cross validation methods leaving out one sample at a time was employed with a calibration set of 25 calibration spectra. Then PLS and PCR calibration on 24 calibration spectra were performed, and using this calibration, the concentration of the sample left out during the calibration set was determined. The process was repeated 25 times until each calibration sample had been left once.

ppropriate selection of number of factors to be used to construct model is the key to achieving correct quantitation in PLS and PCR calibrations.

Analysis of Marketed Formulation

0.1 mL of formulation were withdrawn 5 times and diluted upto 10 mL with methanol to get a concentration of 3 µg mL^{-1} of BIM and 50 µg mL^{-1} of TM. The absorbance of the test solution was taken at the selected wavelength and concentration was determined using Chemometric method without using any maximum excitation wavelength and absorbtivity.

Validation of Chemometric method[28,29,30,32]

Developed analytical method was ferther validated by IUPAC guideline. For the validation of mathematical models of CLS, PCR and PLS, statistical analysis were applied. Various Parameters like Root mean standard error of calibration (RMSEC), Root mean standard error of cross validation (RMSECV), Root mean standard error of prediction (RMSEP), Predicted Residual Error Sum of Square (PRESS) and correlation coefficient (r^2) were determined. Figure of merits (FOM) is necessary for the validation of Chemometric methods. FOM such as Sensitivity (SEN), Limit of Detection (LOD) and Limit of Quantitation (LOQ) can be estimated and used to compare analytical methods.

RESULTS AND DISCUSSION

Selection of Solvent

The solvent mentioned in the literatures for the analysis of BIM and TM individually or with other drug combinations are methanol, acetonitrile, and phosphate buffers of different pH. TM is very soluble

in water and BIM is sparingly soluble in water, but mixture of both drugs are not stable in water when kept overnight whereas it is stable in methanol and both drugs are freely soluble in methanol. So, methanol was used in the analysis of BIM and TM in eye drops.

Development and Validation of Chemometric assisted UV Spectrophotometric Method

The calibration data set and validation data set were prepared as shown in Table 1. Zero order spectra were scanned in the whole range of 200-400nm.(Figure 3) The spectra range of 200-220 nm was omitted because of the noise and the region from 341 to 400 nm was also omitted because of the zero absorbance in this range and showed high RMSEC, RMSECV value when model was developed. So, wavelength region selected for the analysis was 220-341nm with minimum values of RMSEC, RMSECV for model developed.

CLS, PLS and PCR method

Absorbance matrix (A) was constructed using recording zero order spectra between 220 nm and 341 nm at 10 nm intervals. Thus, 12 wavelength points were selected. CLS, PLS, PCR models was created by introducing absorbance (A) and concentration matrix (C) data in EIGENVECTOR SOLO software. Absorbance values of samples at 12 different wavelength points have been incorporated in Figure 3 Selection of Spectral wavelength region for Chemometric assisted UV spectroscopic method.

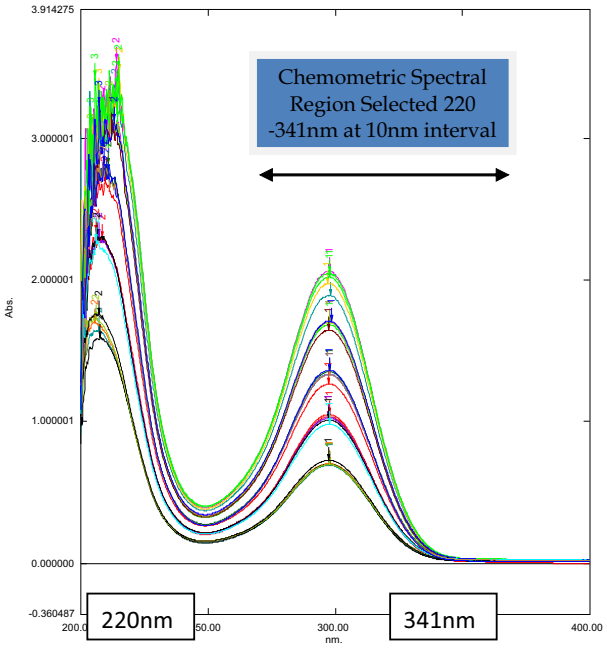

Figure 3 Selection of Spectral wavelength region for Chemometric assisted UV spectroscopic method.

Constructed model and quantities of BIM and TM in validation data set as well as in formulation were predicted as per Table 2.

Table 2: Composition and results of the prediction set by CLS, PLS, PCRPredicted set Concentration

Predicted set Concentration (µg mL^{-1})			Amount of drugs (µg mL^{-1})					
			CLS		PLS		PCR	
Sr. No.	BIM	TM	BIM	TM	BIM	TM	BIM	TM
1	1	33.34	0.9	33.1	0.91	33.1	0.9	33.14
2	1	50	0.94	49.65	0.95	49.6	0.95	49.64
3	1.5	16.67	1.53	16.94	1.53	17.0	1.55	17.01
4	1.5	24.99	1.46	24.97	1.47	25.0	1.47	25.02
5	1.5	41.67	1.49	41.42	1.5	41.4	1.5	41.42
6	2	16.67	2	16.92	2	16.9	2	16.98
7	2.5	24.99	2.59	25.15	2.59	25.16	2.6	25.16
8	2.5	50	2.55	50	2.55	49.93	2.58	49.91
9	3	41.67	3	41.53	2.99	41.47	2.99	41.47

Statistical Analysis in selecting the number of principle components and factors[19]. Various criteria like RMSEC, RMSECV and PRESS have been used to select the optimum parameters. CLS, PCR and PLS calibration on 25 mixtures were performed using this calibration model. The predicted concentrations were calculated and compared with the known concentration of compounds in each calibration sample.(Figure 4). To validate the model, both PRESS and RMSEP values were considered. Both values must be as low as possible for a particular model. Both the values were calculated as follows [19,20,21]:

$$PRESS = S(Ypre - Ytrue)2 \ldots\ldots\ldots\ldots\ldots(2)$$

Y_{pre} and Y_{true} are predicted and true concentrations in µg/ml respectively.

$$RMSECV = \sqrt{\frac{PRESS}{n}} \quad \ldots\ldots\ldots\ldots\ldots(3)$$

Where n is the number of training samples.

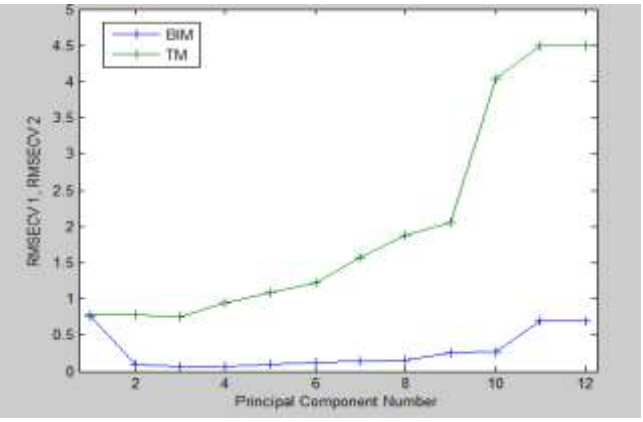

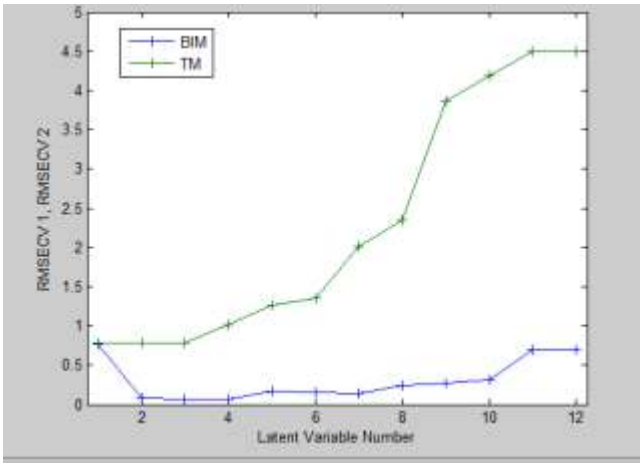

Figure 4 Plot of RMSECV Vs. Number of Components for calibration set prediction using cross-validation of (A) PCR model and (B) PLS model.

Y_{pre} and Y_{true} are predicted and true concentrations in µg mL^{-1} respectively. The RMSECV value was used as a diagnostic test for examining the errors in the predicted concentrations. It indicates both of the precision and accuracy of predictions.

The proposed CLS, PCR and PLS calibration models were evaluated by internal validation, recoveries were obtained in between 98.66-100.06% for BIM and 98.79-99.00% for TM. CLS, PCR and PLS methods were evaluated and comparative study of prediction capabilities of mentioned chemometric approaches were carried out.

Two methods were employed for evaluation where the first method was carried out by plotting the known concentration against the predicted concentration. A satisfactory correlation coefficient (r^2) value was obtained for each drug by the mentioned Chemometric approaches, and the second method was carried out by determining Root mean standard error of calibration (RMSEC) and Root mean standard error of prediction (RMSEP) by the following expression:

$$SEC(SEP)=\sqrt{\frac{\sum_{i=1}^{n}(C_i^{Added}-C_i^{Found})^2}{n-1}} \quad \text{.....(4)}$$

Here, C_i^{Added} represents the added concentration, C_i^{Found} denotes the determined concentration and n is total number of samples. The RMSECV, RMSEC and RMSEP values were obtained by optimizing the calibration matrix of absorption spectra for CLS, PCR and PLS are shown in Table 3 indicating good accuracy and precision. The values of RMSEC, RMSECV, RMSEP and PRESS were found to be minimum for PLS method hence, it could be concluded that PLS is the most suitable method among developed Chemometric methods.

Plots of actual Vs measured values for BIM and TM by (A) CLS (B) PLS and (C) PCR methods called Score plots (Figure 5) and plotting the concentration residuals against the predicted concentrations which were again used to carried out the residual plot (Figure 6). All the residuals distributed in between -2 to +2 value. Chemometric is the technique of separation of necessary informationfrom whole spectra at multiple wavelength, and removal or reducing the noise.

Table 3: Statistical parameters and Figure of Merits for Chemometric methods

Para meter	BIM			TM		
	CLS	PLS	PCR	CLS	PLS	PCR
RMSEC	0.067	0.067	0.06927	0.673	0.672	0.671
RMSECV	0.0850	0.08627	0.090	0.777	0.781	0.779
RMSEP	0.0559	0.0518	0.0584	0.215	0.2428	0.242
PRESS	0.0283	0.027	0.0293	0.4163	0.515	0.51464
r^2	0.996	0.996	0.995	1	1	1
Slope	1.0583	1.0496	1.0567	0.9864	0.9831	0.9829
Noise	0.003745	0.003829	0.003837	0.003745	0.003827	0.003837
Sensitivity	0.944912	0.9527	0.9946345	1.013788	1.01719	1.01739
LOD (µg/mL^{-1})	0.013081	0.0132	0.0133	0.012192	0.01241	0.012445
LOQ (µg/mL^{-1})	0.039638	0.04018	0.04054	0.036945	0.03764	0.03771

The figures in bold indicates that PLS model was found to be the best model amongst all models.

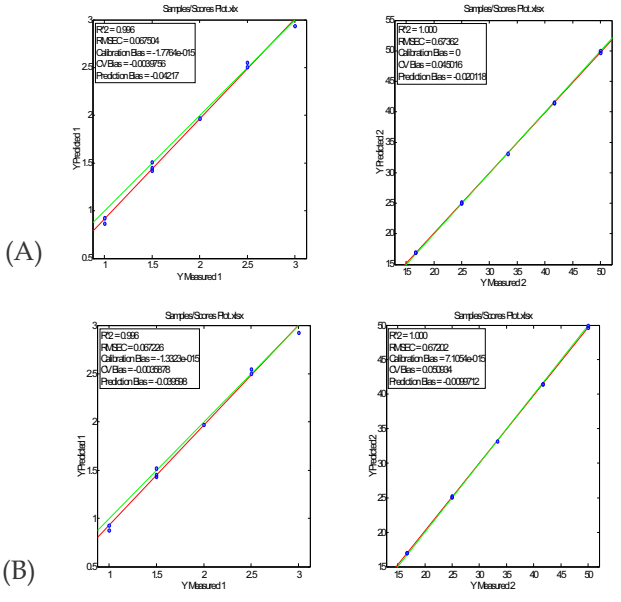

(C)

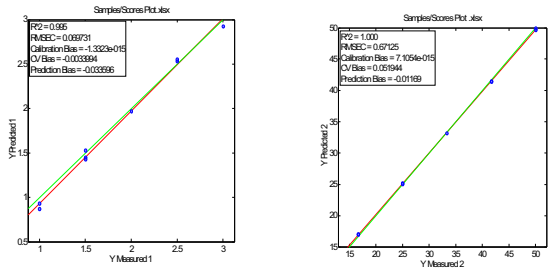

Figure 5 Plots of actual Vs. predicted values for BIM and TM by (A) CLS (B) PLS and (C) PCR methods.

Validation of Chemometric Methods

Analytical figure of merits (FOM) are very important to quantify the quality of a given methodology or for method comparison. In multivariate calibration, several FOM have been reported e.g. sensitivity (SEN), Limit of detection (LOD) and Limit of quantitation (LOQ). Results of FOM are shown in Table 3.

Analysis of Marketed Formulation

The developed methods were applied for analyzing the BIM and TM in marketed formulation and study was repeated five times. The results obtained are shown in Table 4.

Table 4: Assay of Marketed Formulation (Careprost Plus) by proposed methods

BIMATORPOST			
	Label Claim (%)	Amount found (%)	Mean ± RSD(%)
CLS	100	98.8	98.8 ± 0.2317
PLS	100	98.66	98.66 ± 0.33
PCR	100	100.06	100.06 ± 0.36
TIMOLOL MALEATE			
	Label Claim (%)	Amount found (%)	Mean ± RSD(%)
CLS	100	99	99 ± 1.78
PLS	100	98.83	98.83 ± 1.77
PCR	100	98.79	98.79 ± 1.76

The results obtained were complying with the label claim. The statistical comparison of the developed methods were made by using one way ANOVA to determine the variance between the recovery data for the marketed formulation and the method developed. For formulation the F-calculated obtained is less than F-critical. This indicates that there is no significant difference between the above all three developed methods.

(A)

(B)

(C)

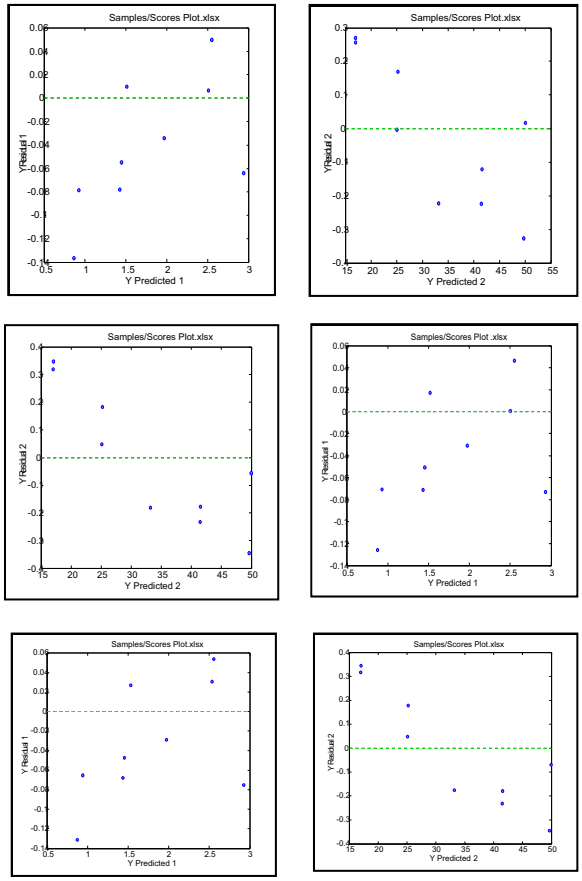

Figure 6 Plots of Concentration Residual vs. Predicted Concentration for BIM and TM by (A) CLS (B) PLS and (C) PCR methods.

CONCLUSIONS

This study is mainly done for check the interference of excipients and additives for two drugs. Three different Chemometric methods (CLS, PLS, PCR) were developed and validated as per IUPAC guideline. The developed method was applied successfully for simultaneous estimation of BIM and TM in an ophthalmic formulation. The values of RMSEC, RMSECV, RMSEP and PRESS were found to be minimum for PLS method hence, it was concluded that PLS is the most suitable method among developed all Chemometric methods. CLS, PLS, PCR were compared statistically by applying ANOVA test shows that there is no observed any significant difference between all developed methods. The developed methods are beneficial in terms of ease of performing and reduced cost of the analysis for routine analysis, quality control of mixture and commercial preparation containing these two drugs.

ACKNOWLEDGEMENTS

The authors express their sincere thanks to Sun pharmaceuticals Pvt. Ltd. Authors are thankful to the

Mr. Nisarg Patel and Ms. Mittal Patel for their support in learning of software. The authors also express their gratitude towards Ramanbhai Patel College of Pharmacy for providing necessary facilities to carry out the project work.

References:

1. https://www.drugbank.ca/drugs/DB00905 (07/14/2017)
2. https://www.drugbank.ca/drugs/DB00373 (07/14/2017)
3. Indian Pharmacopoeia, Government of India, Ministry of Health and Family Welfare, the Indian Pharmacopoeial Commission, Ghaziabad 2010, Volume 3, Page No.2229.
4. Azzouz T, Puigdomenech A, Aragay M, Tauler R. (2003) 'Comparison between different data pre-treatment methods in the analysis of forage samples using near-infrared diffuse reflectance spectroscopy and partial least-squares multivariate calibration method.' *Analytica Chemica Acta,* Vol. 484 PP. 121-134.
5. Patel NS, Nandurbarkar VP, Patel AJ, Patel SG. (2014) 'Absorption Correction and Chemometric Method for estimation of Celecoxib and Diacerin in bulk and Capsule dosage form.' *Spectrochimica Acta Part A: Molecular and Bimolecular Spectroscopy.* Vol. 125 pp.46-52.
6. Bebawy L I. (2002) 'Application of TLC-densitometry, first-derivative UV-spectrophotometry and ratio derivative spectrophotometry for the determination of Dorzolamide Hydrochloride and Timolol Maleate.' *Journal of pharmaceutical and biomedical analysis.* Vol. 27(5) pp. 737-746.
7. Olivieri AC, Faber NM, Ferré J, Boqué R, Kalivas JH, Mark H. (2006) 'Uncertainty estimation and figures of merit for multivariate calibration (IUPAC Technical Report).' *Pure and applied chemistry*.Vol. 78(3) pp.633-461.
8. Haaland DM, Thomas EV.(1998) 'Partial least-squares methods for spectral analyses. 1. Relation to other quantitative calibration methods and the extraction of qualitative info'mation.' *Analytical Chememistry.* Vol. 60(11), pp.1193-1202.
9. Steves M. Short, Robert P. Cogdill, and Carl A. Anderson.(2007). 'Determination of Figures of Merit for Near-Infrared and Raman Spectrometry by Net Analyte Signal Analysis for a 4-Component Solid Dosage System.' *AAPS pharmaceutical science and technology.* Vol. 8 (4) Article 96, pp. E1–E11.
10. Kulkarni SP, Amin PD. (2000) 'Stability indicating HPTLC determination of Timolol Maleate as bulk drug and in pharmaceutical preparations. *Journal of pharmaceutical and biomedical analysis.*'vol. 23(6), pp.983-987.
11. Maguregui M, Jimenez R, Alonso R, Akesolo U. (2002) 'Quantitative determination of Oxprenolol and Timolol in urine by capillary zone electrophoresis.' *Journal of Chromatography A.* vol. 949(1), pp.91-97.
12. Sharma N, Rao SS, Reddy AM. (2012) 'A Novel and Rapid Validated Stability-Indicating UPLC Method of Related Substances for Dorzolamide Hydrochloride and Timolol Maleate in Ophthalmic Dosage Form.' *Journal of Chromatographic Science.vol.* 50 (9), pp. 745-755.
13. Kumar SS, Natraj K, Khan A, Kumar BK, Rao JV. (2011) 'Development and Validation of RP-HPLC Method for Estimation of Bimatoprost in Pharmaceutical Dosage Forms.' *Journal of Pharmacy Research* Vol. 4(10) pp. 1-2.
14. Nasir F, Iqbal Z, Khan A, Ahmad L, Shah Y, Khan AZ, et al.(2011) 'Simultaneous determination of Timolol Maleate, Rosuvastatin calcium and Diclofenac sodium in pharmaceuticals and physiological fluids using HPLC-UV.' *Journal of Chromatography B.* vol. 879(30), pp. 3434-343.
15. Gasco M, Gallarate M, Trotta M, Bauchiero L, Gremmo E, Chiappero O. (1989) 'Microemulsions as topical delivery vehicles: ocular administration of Timolol.' *Journal of pharmaceutical and biomedical analysis. Vol.* 7(4), pp. 433-439.
16. El-Laithy HM.(2009) ' Novel Transdermal delivery of Timolol Maleate using sugar esters: preclinical and clinical studies.' *European Journal of Pharmaceutics and Biopharmaceutics.* Vol. 72(1), pp. 239-245.
17. Lee V H, Li S Y, Sasaki H, Saettone M F, Chetoni P.(1994) 'Influence of drug release rate on systemic Timolol absorption from polymeric ocular inserts in the pigmented rabbit.' *Journal of Ocular Pharmacology & Therapeutics. Vol.* 10(2), pp. 421-429.
18. Rakić D, Antunović M. (2006) 'Preparation and testing of buffered eye drops containing pilocarpine chloride with Timolol Maleate.' *Vojnosanitetski pregled. Vol.* 63(10), pp. 873-877.

19. Sharif N, Ke T, Haggard K, Kelly C, Williams G, Graff G, et al.(2002) 'Bimatoprost Hydrolysis to 17-Phenyl PGF2alpha by Human and Rabbit Ocular Tissues and Agonist Activity of Bimatoprost and 17-Phenyl PGF2alpha.' *Investigative Ophtalmology and Visual Science.* Vol. 43(12), pp. 4080.
20. Shafiee A, Bowman LM, Hou E, Hosseini K.(2013),'Ocular pharmacokinetics of Bimatoprost formulated in DuraSite compared to Bimatoprost 0.03% ophthalmic solution in pigmented rabbit eyes.' *Clinical ophthalmology* (Auckland, NZ). Vol. 7, pp. 1549.
21. Marwada KR, Patel JB, Patel NS, Patel BD, Borkhatariya DV, Patel AJ.(2014), 'Ultraviolet spectrophotometry (dual wavelength and chemometric) and high performance liquid chromatography for simultaneous estimation of meropenem and sulbactam sodium in pharmaceutical dosage form.' *Spectrochimica Acta Part A: Molecular and Biomolecular Spectroscopy.* Vol. 124, pp. 292-299.
22. Rajput S J, George R K, Deepti B R. (2008) "Chemometric Simultaneous estimation of Clopidogrel Bisulphate and Aspirin from Combined Dosage Form.' *Indian Journal of Pharmaceutical Sciences,* vol. 70(4),Jul-Aug, pp. 450-454.
23. Damiani PC, Moschetti AC, Rovetto AJ, Benavente F, Olivieri AC.(2005) 'Design and optimization of a Chemometrics-assisted spectrophotometric method for the simultaneous determination of Levodopa and Carbidopa in pharmaceutical products.' *Analytica Chimica Acta.*, Vol. 543(1), pp. 192-198.
24. Ferraro MC, Castellano PM, Kaufman TS. (2004) 'Chemometric determination of amiloride hydrochloride, atenolol, hydrochlorothiazide and timolol maleate in synthetic mixtures and pharmaceutical formulations'. *Journal of Pharmaceutical and Biomedical Anaysis.* Vol. 34(2), pp. 305-314.
25. Martens H, Naes T, Multivariate Calibration plot, Wiley, New York, 1992, 3rd Edition, 116-158.
26. Mc Kay B, Hoogenraad M, Damen E, Smith A.(203) 'Advances in multivariate analysis in pharmaceutical process development.' *Current opinion in drug discovery & development.* Vol. 6(6), pp. 966-77.
27. Faber N.M. (1999), 'Notes on two competitng definitions of multivariate sensitivity.' *Analytica Chimica Acta*, vol . 381, pp. 103-110.
28. Kumar N, Bansal A, Sarma G, Rawal RK.(2014), 'Chemometrics tools used in analytical chemistry: An overview.' *Talanta.*, vol. 123, pp. 186-199.
29. Wise BM, Gallagher NB.(1996), 'The process chemometrics approach to process monitoring and fault detection.' *Journal of Process Control.* Vol. 6(6), pp. 329-48.
30. Kokot S, Grigg M, Panayiotou H, Phuong TD. (1998), Data interpretation by some common chemometrics methods. *Electroanalysis.* Vol. 10(16), pp. 1081-1088.
31. Esbensen KH, Hjelmen KH, Kvaal K. (1996) 'The AMT approach in chemometrics—first forays.' *Journal of Chemometrics*. Vol. 10(5 6), pp. 569-90.
32. Olivieri AC, Faber NM, Ferré J, Boqué R, Kalivas JH, Mark H. Uncertainty estimation and figures of merit for multivariate calibration (IUPAC Technical Report). Pure and applied chemistry. 2006;78(3):633-61.

Research Article

A facile synthesis of Iron Sulfide thin films by Chemical Bath Deposition Method

Abey M Abraham[1], Jaimini V Patel1, C K. Sumesh[1]*

[1]Department of physical Sciences, P. D. Patel Institute of Applied Sciences, CHARUSAT, Changa, India

Received: 18/05/2018
Revised: 10/08/2018
Accepted: 13/08/2018

Correspondence to:
*C. K. Sumesh:
cksumesh.cv@charusat.ac.in

Abstract:

The study on iron chalcogenides are of particular interest because of their interesting magnetic, semiconducting, and structural properties. In this study, we investigated the facile chemical bath deposition of the monophasic FeS thin films. Layer by layer and continuous deposition method of synthesis of thin film to form a homogenous and uniform film has been employed. The XRD structural analysis confirmed the formation of FeS films with a tetragonal (mackinawite) structure. Optical band gap analysis revealed that the as-synthesised FeS thin films possess light harvesting capacity in the visible region of the solar spectrum.

Keywords: Metal chalcogenides, FeS Thin film, CBD method

INTRODUCTION

The wide growing demands of thin film solar cell and photovoltaic applications are demanding cost effective, inexpensive, non-toxic and earth abundant materials as an alternative to conventional materials (Ramasamy, 2012). Most of the materials widespreadly used for thin film based applications, namely cadmium, lead, indium and selenium are either toxic or non-abundant. The fast growing exploitation of non-renewable energy as solar energy applications therefore demands environmental friendly materials. Thin film solar cells based on copper, tin and iron have geared significant progress in the last few years either in metal oxides or sulfides (Zhang,2004); (Liu,2017); (Chen,2016); (Rondiya,2017); (Ge,2016). The hybrids and heterostructures based on these materials absorb the most of the visible solar spectrum. These materials are also proved to be a powerful candidate in thermoelectric, magnetic semiconductors, superconductors and sensors. Iron and copper chalcogenides are of particular interest because of their interesting magnetic, semiconducting, and structural properties. From the large family of iron sulfide phases, iron sulfide (FeS) is showing great interest because of its electronic, magnetic, and optical properties with applications that include solar cells and lithium ion batteries. They are also found potential applications in the biomedical applications, including protein immobilization and separation, magnetic targeting and drug delivery, cancer hyperthermia, magnetic resonance imaging (MRI) and many more. Xu *et al.* demonstrated interconnected porous FeS/C composite using FeS nanoparticles embedded in carbon nanosheets for its use in anode for LIBs. A new nanocomposite formulation using FeS and graphene oxide anode for lithium-ion batteries is proposed by Fei *et al.* via facile direct-precipitation approach. (Huang,2016); (Lu,2013); (Wei,2015); (Xu,206); (Fei,2013). Iron sulfides nanoparticles are considered to be advanced inorganic material with non-conventional applications, such as high-energy density batteries, precursors for the synthesis of superconductors and materials for photoelectrolysis. Therefore, the study of nonmaterial and thin film based on iron sulfide (FeS) with particle size and morphological changes is of great interest in the field of materials science. Various deposition and synthesis techniques have been experimented to deposit thin

films of iron sulfide (FeS) including chemical vapor deposition, electro-deposition, hydrothermal method, sputtering and chemical bath deposition (CBD) (Dutta, 2012); (Kim, 2011) (Fei, 2013); (Beal, 2012); (Min, 2009); (Sines,2012). The CBD is always found to be the simple, low temperature and cost effective method to deposit high quality thin films of FeS. The formation of different phases of FeS is always related to many factors, including temperature, solution pH, and aging time. Herein, we report a reproducible method for the deposition of nanocrystalline monophase of FeS thin films and are expected to be a general method for the preparation of other metal sulfide.

MATERIALS AND METHODS

Experimental Details

Materials

All the reagents used in the experiment, iron chloride tetra-hydrate ($FeCl_2$), thioacetamide (CH_3CSNH_2) and urea ($CO(NH_2)_2$) were purchased from Sigma Aldrich and used without purifying it further. HCl was used to manage the pH of the solution and Distilled water was used as solvent in all experimental procedure.

Synthesis of FeS Thin Films

The monophasic FeS thin films were grown onto glass substrates of dimension ($2 \times 5\ cm^2$) from the acidic bath as shown in figure 1 a. The required molarity of the solution is 0.15M iron chloride tetra-hydrate ($FeCl_2$), 1M urea and 2M thioacetamide. For that 180 ml of distilled water is kept in a beaker on a heat bath. When the temperature of the distilled water is raised above 50° C, 1.7292gm $FeCl_2$ is added and vigorously stirred using a magnetic stirrer which is attached to the heating unit. When $FeCl_2$ is dissolved completely in water, 3.6gm of urea and 9.0gm of thioacetamide was added to the solution under stirring. When all the reagents were dissolved completely, almost transparent solution is formed (figure 1b). The temperature is maintained at 85± 5°centigrade. Then 0.5M HCl is added drop by drop to the solution to adjust the pH to 3. After 10 min of reaction at fixed temperature under stirring, the color of solution

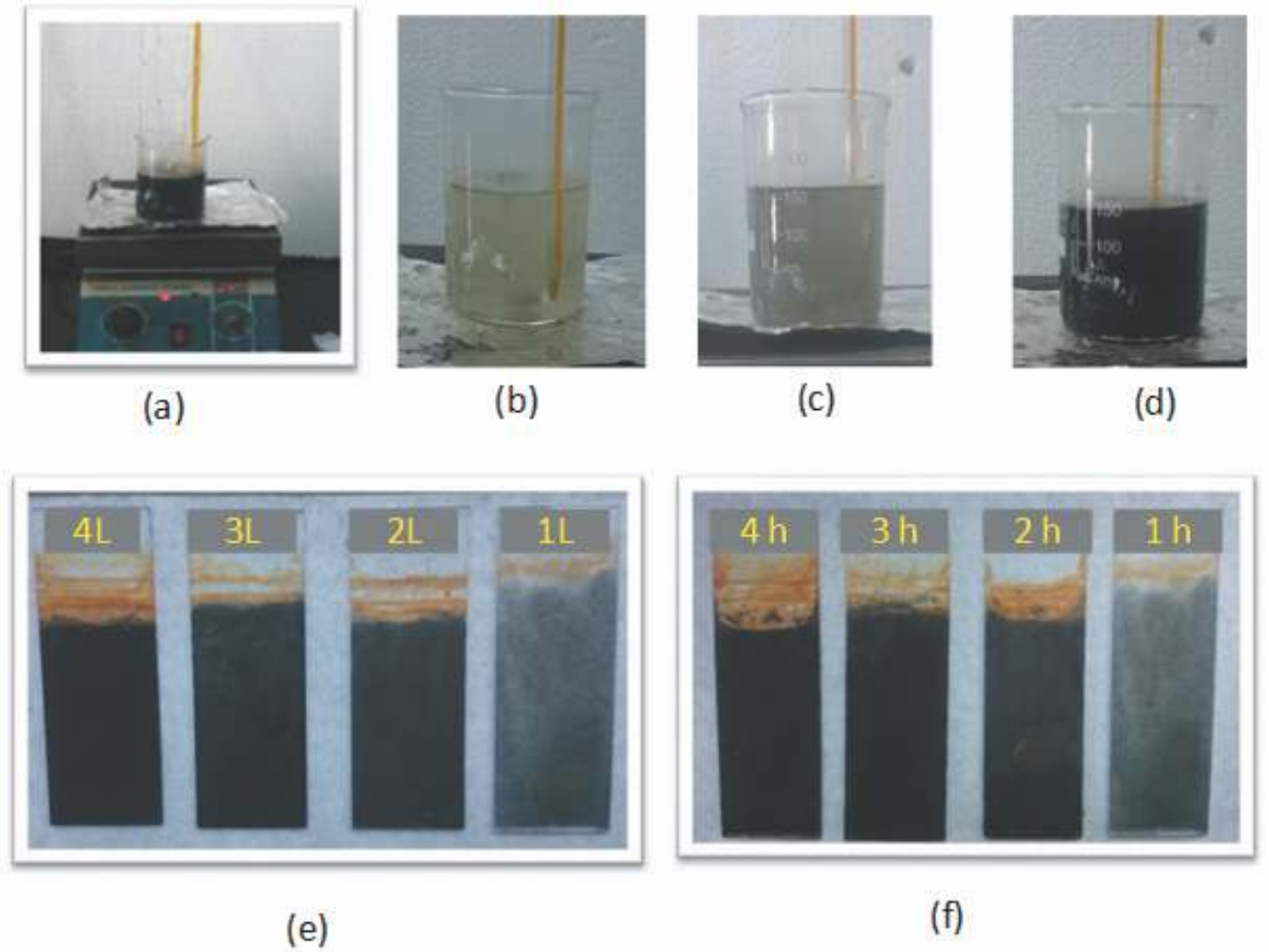

Fig. 1. (a) Experimental set up for chemical bath deposition of films, (b-d) progress of the reaction and confirmation of homogeneous bath, (e) layer by layer deposition and (f) continuous bath deposition.

changes to grey (figure 1c). Glass substrates were then immersed vertically in the chemical bath. After 20 min the solution turns to thick black contrast (figure 1d). The speed of stirring is reduced to very slow. A continues deposition method and layer by layer deposition method was employed for obtaining uniform films of FeS. To check the time dependent effect on the deposition of film, glass slides were removed from the reaction mixture after an interval of 1 hour. For the layer by layer deposition, the samples were removed at regular intervals, washed, dried and immersed back into the reaction mixture. The process was continued till the formation of uniform film. The images of typical such FeS films deposited is shown in figure 1(e) and (f).

All the films were washed with methanol and acetone to remove surface contaminants and chemical residues and post annealed at 70^0C for 1 hour before testing for any characterizations.

Peel test was performed for all the prepared samples using a commercially available adhesive tape for analyzing the adhesion between films and their substrates (Hull, 1987). The crystal structure and phase constitution of FeS thin film was characterized by X-ray diffraction (XRD) (D2 phaser BRUKER, $\lambda_{Cu\text{-}K\alpha}$=0.15418 nm). The UV absorption spectra of the sample were performed on a UV-VIS spectrophotometer (Shimadzu UV 3600, Japan) to check the optical band gap of the films. Hot probe analysis was used to test the conductivity of the sample. van der Pauw method of electrical resistivity measurement was done for selected samples.

RESULTS AND DISCUSSION

A thin film formed by precipitation using a controlled chemical reaction is employed in chemical bath deposition (CBD). During the reaction the slow release of the sulfur ion and iron ions and condensation of these ions on the substrate surface takes place to form homogeneous FeS films (Brien,1998). In a controlled hydrolysis reaction of iron salt ($FeCl_2$) and thioacetamide (CH_3CSNH_2) salt in the acidic media, Fe^{2+} and S^{2-} ions re released. The role of urea in the reaction mixture is to act as a chelating agent. Hydroxide ions via hydrolysis released in the mixture provide ammonia for the formation of complex ion with Fe^{2+}. These complex ions react with S^{2-} ions to form FeS. The reaction mechanism is explained briefly by following equations (Akhtar, 2015).

$$FeCl_2 \rightarrow Fe^{2+} + 2Cl^- \quad (1)$$

$$CH_3SCNH_2 + H_2O \leftrightarrow S^{2-} + CH_3SCONH_2 + 2H^+ \quad (2)$$

$$CO(NH_2)_2 + H_2O \leftrightarrow S^{2-} + 2NH_3 + CO_2 \quad (3)$$

$$Fe^{2+} + HO + 5NH_3 \leftrightarrow [Fe(NH_3)4]^{2+} \quad (4)$$

$$[Fe(NH_3)_4]^{2+} + S^{2-} \leftrightarrow FeS + 4NH_3 \quad (5)$$

$$[Fe(NH_3)_5]^{2+} + CH_3SCCNH_2 + H_2O \rightarrow FeS + 4NH_3 + CH_3SCONH_2 + 2H^+ \quad (6)$$

The XRD pattern shown in figure 2 of the typical FeS thin film is in good agreement with that of iron sulfide ((PDF No. 86-0389). It should be noted that the strongest peak oriented along (001) in the pattern can be well indexed as the mackinawite phase (P4/nmm space group) of FeS. The presence of single and intense peak reveals the growth of FeS crystallites along c-axis. Thus, it is suggested that nanocrystalline FeS is formed as the broadness of the peaks, intensity and positions are well matched with previously reported data for nanocrystalline mackinawite (Xing, 2015); (Hajja, 2013); (Lennie, 1995). The formation of monophasic mackinawite phase of FeS is further confirmed from the diffraction as the pattern does not show any extra peaks. The crystalline size of the particle and micro strain has been calculated from the X-Ray diffraction pattern using scherer's formula:

$$t = \frac{kl}{b\cos q} \quad (7)$$

$$e = \frac{b2q\cos q}{4} \quad (8)$$

where t is the grain size, ε is the micro strain, k is a constant taken to be 0.9, β is the full width half maximum(FWHM) and λ is the wave length of X-Rays. The obtained particle size and micro strain values are tabulated in table 1.

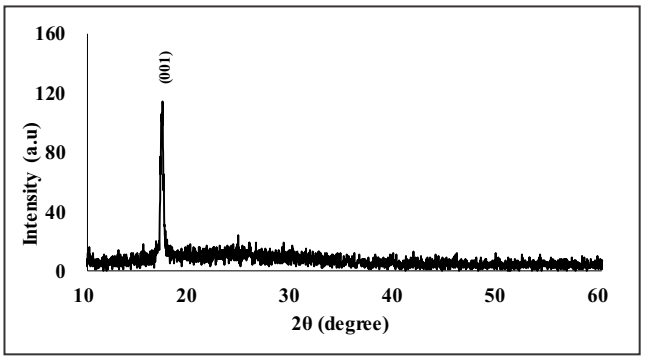

Fig. 2. Typical p-XRD pattern of FeS thin film deposited on a glass substrate

It is inferred that the crystallite size of the particle is increasing with increase the deposition time and number of layers. This data, verifies that the crystalline size of particles in thin films increases with the increase of the film thickness synthesized by acidic bath method. It is also found that the quality of the film

Table 1. Calculated values of grain size and micro strain from the XRD diffraction data

FeS Thin films	Duration / Layer	FWHM (Degree)	Grain Size (nm)	Micro strain
Layer by layer deposition	1 Layer	0.475	17.68	0.0134
	2 Layer	0.298	28.18	0.0084
	3 Layer	0.223	37.67	0.0063
	4 Layer	0.150	56.00	0.0042
Continuous depostion	1 Hour	0.475	17.68	0.0134
	2 Hour	0.253	33.20	0.0071
	3 Hour	0.161	52.18	0.0045
	4 Hour	0.128	65.63	0.0036

improves and shows crystallinity of the film as deposition time increases.

The absorption fitting method of calculating the band gap was employed (figure 3) and the values are tabulated in table 2. The band gap range of the films

Table 2. Optical band gap calculated from the absorption spectra

FeS Thin films	Duration / Layer	Band gap (eV)
Layer by layer deposition	1 Layer	1.98
	2 Layer	1.86
	3 Layer	1.86
	4 Layer	1.94
Continuous depostion	1 Hour	2.00
	2 Hour	1.82
	3 Hour	1.86
	4 Hour	2.06

revealed that the deposited films of FeS falls in the visible range region of the solar spectrum (Ghobadi, 2013).

Standard hot probe analysis was carried out to understand the carrier type of FeS thin films. A couple of cold probe and hot probe are attached to the semiconductor surface. The hot probe is connected to the positive terminal of the multimeter while the cold probe is connected to the negative terminal. If the

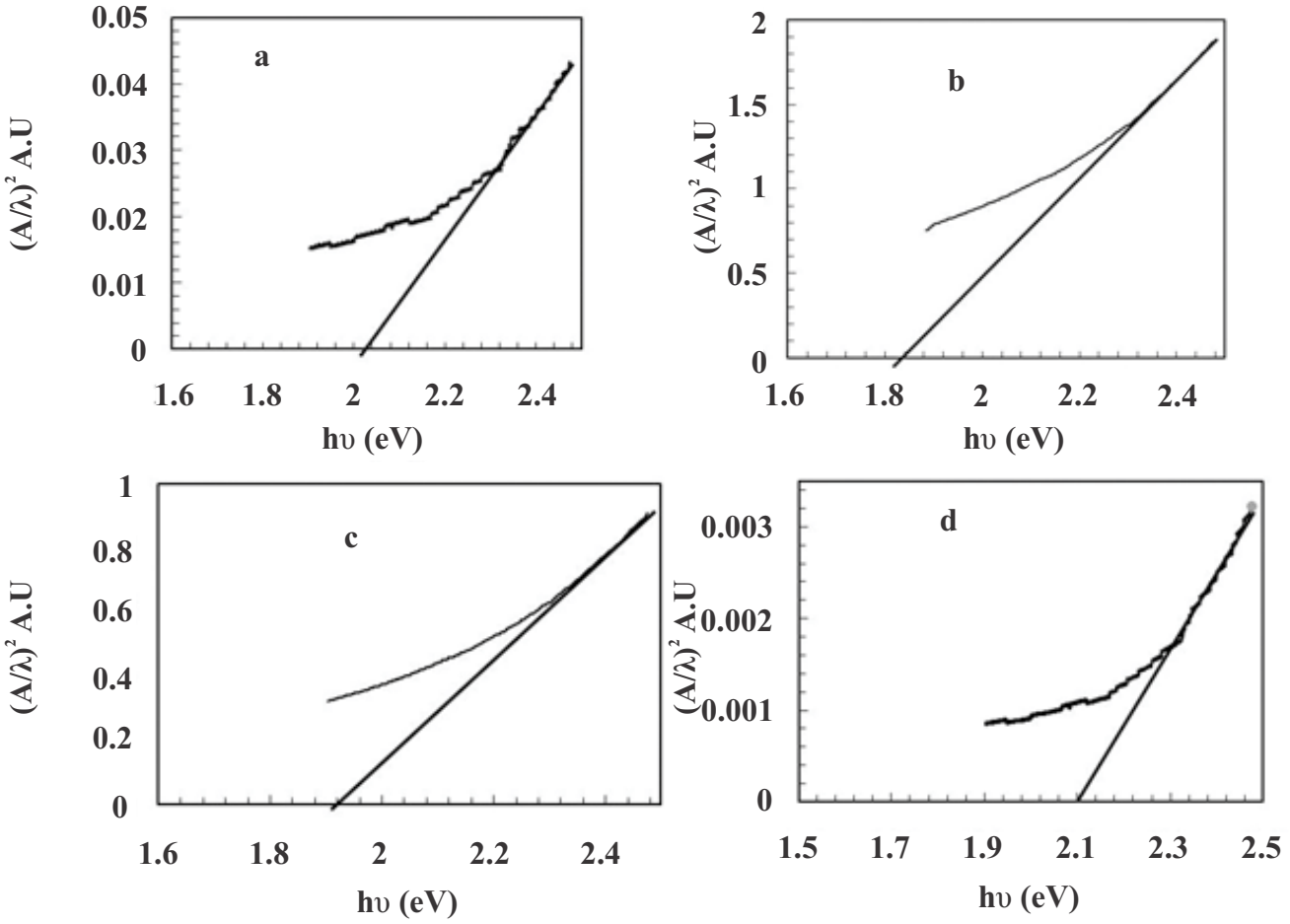

Fig. 3. Typical Band gap calculation from absorption fitting method of FeS thin films (a) 1hour, (b) 2 hour, (c) 3 hour and (d) 4 hour

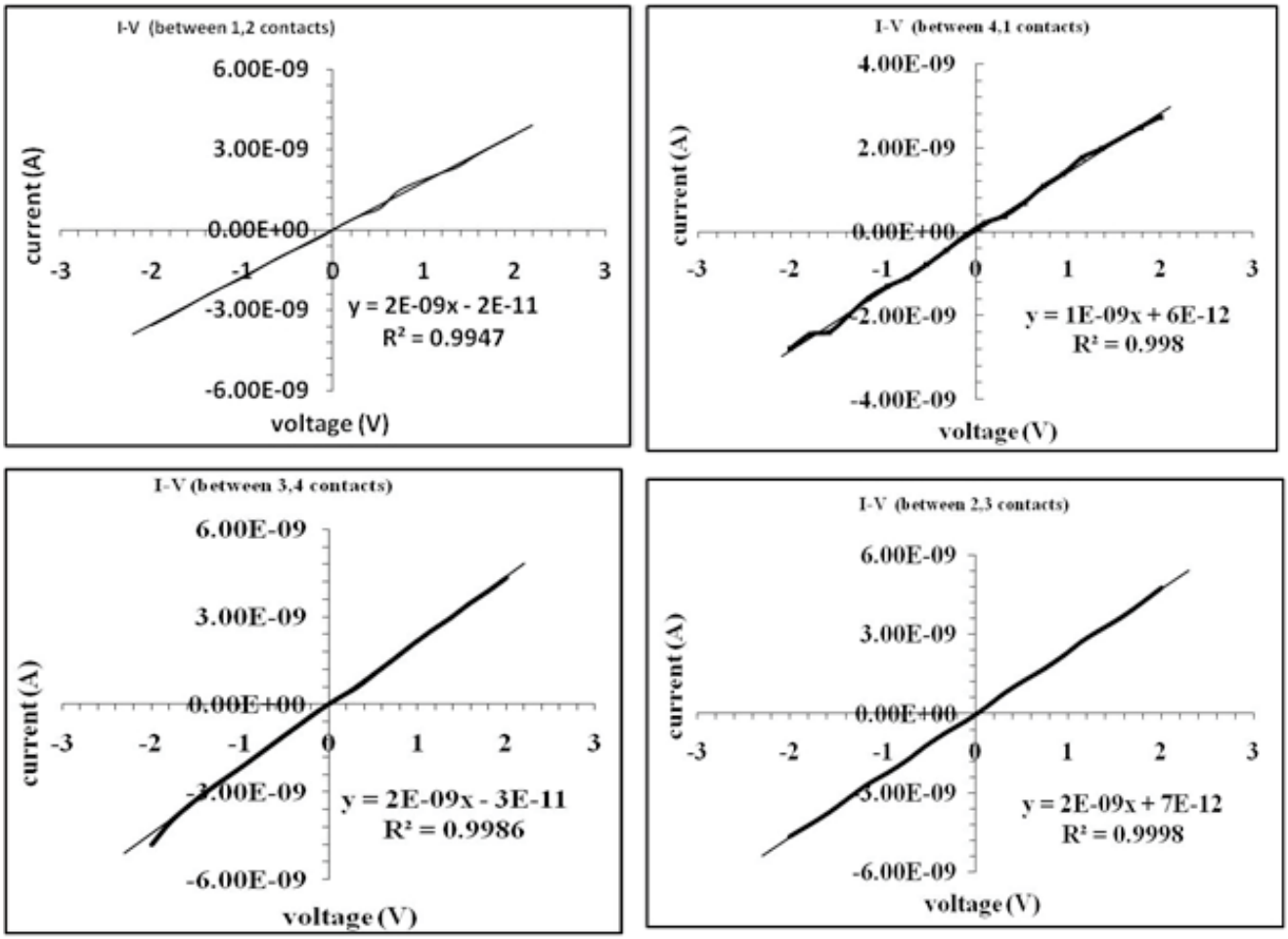

Fig.4. I-V analysis via e van der Pauw connections of as-deposited FeS thin films

semiconductor is n-type, then positive voltage is obtained across the meter. By this method, it is verified that the formed FeS is a n-type semiconductor.

The van der Pauw method of calculation of resistivity was employed to check the electrical conductivity measurements. The following conditions that must be satisfied to use electrical analysis: (a) The sample must have a flat shape of uniform thickness, (b) The sample must not have any isolated holes, (c) The sample must be homogeneous and isotropic, (d) All four contacts must be located at the edges of the sample, and (e). The area of contact of any individual contact should be at least an order of magnitude smaller than the area of the entire sample. The as synthesized FeS films were tested for electrical conductivity measurements.

The contacts were named (1,2) (2,3) (3,4) (4,1) and current, voltage analysis was done for all the four set of contacts as shown in the figure 4. The linearity of the graphs shows that the contacts made are good ohmic contacts and shows uniform conductivity across all the terminals. The average resistance across two points is calculated as ~ 1.75×10^9 ohms.

CONCLUSION

In summary, we have synthesized FeS thin films by chemical bath deposition method. Tape test was passed for the adhesion FeS films on glass substrate. Structural analysis verified that the formed FeS thin film is of Mackinawite structure. The crystalline size of the particle increases with the increase of deposit hours and as the increase of the number of layers. The strain size is decreasing correspondingly as the increase of crystalline size. Optical analysis shows the absorption of FeS is in the visible region of the optical spectra. The as-deposited FeS thin film is found to be n-type semiconductor in nature. Electrical conductivity analysis of the film shows high resistivity nature of the film.

REFERENCES

1. Karthik,R. Mohammad, A.M., Neerish R., and Paul O. (2013) 'Routes to Nanostructured Inorganic Materials with Potential for Solar Energy Applications', *Chem. Mater.*, 25 (18), pp 3551–3569
2. Lizhi, Z., Jimmy, C. Y., Maosong, M., Ling, W., Quan, L., and Kwan, W.K. (2004) 'A General Solution-Phase Approach to Oriented

Nanostructured Films of Metal Chalcogenides on Metal Foils: The Case of Nickel Sulfide' *J. Am. Chem. Soc.,* 126 (26) pp 8116–8117

3. Yang, L., Maixian, L.,and Mark, T. S. (2017) 'Plasmonic Copper Sulfide-Based Materials: A Brief Introduction to Their Synthesis, Doping, Alloying, and Applications' *J. Phys. Chem. C*, 121 (25) pp 13435–13447
4. Lihui, C., Masanori, S., Mitsutaka, H., Takashi, N., Ryota, S., Hiroki, K., and Toshiharu ,T. (2016) 'Tin Ion Directed Morphology Evolution of Copper Sulfide Nanoparticles and Tuning of Their Plasmonic Properties via Phase Conversion' *Langmuir*, 32 (30), pp 7582–7587
5. Sachin, R., Nitin, W., Yogesh, J., Sandesh, J. Santosh, H., and Mukul, K. (2017) 'Structural, Electronic, and Optical Properties of Cu2NiSnS4: A Combined Experimental and Theoretical Study toward Photovoltaic Applications' *Chem. Mater*., 29 (7), pp 3133–3142
6. Jie, G. Yue, Y., and Yanfa, Y. (2016) 'Earth-Abundant Orthorhombic BaCu2Sn(SexS1–x)4 (x ≈ 0.83) Thin Film for Solar Energy Conversion, *ACS Energy Lett.,* 1 (3), pp 583–588
7. Amit, K. D., Swarup, K.M., Divesh. N. S., Anup, M. Papu, B., Parimal, P. and Bibhutosh,A. (2012) 'Synthesis of FeS and FeSe Nanoparticles from a Single Source Precursor: A Study of Their Photocatalytic Activity, Peroxidase-Like Behavior, and Electrochemical Sensing of H2O2'ACS *Appl. Mater. Interfaces,* 4 (4), pp 1919–1927
8. Jing, H., Yuancheng, L., Anamaria, O. Qiong, L., Peng, G. Liya, W., Lily, Y. and Hui, M. (2016) 'Magnetic Nanoparticle Facilitated Drug Delivery for Cancer Therapy with Targeted and Image-Guided Approaches' *Adv Funct Mater.* 26(22), pp 3818–3836
9. Wensheng, L. Yuhua, S., Anjian ,X., and Weiqiang, Z. (2013) 'Preparation and Protein Immobilization of Magnetic Dialdehyde Starch Nanoparticles, *J. Phys. Chem. B,* 117 (14), pp 3720–3725
10. Xiang, W., Weihan ,L., Jin, S., Lin, G.u, and Yan, Y. (2015) 'FeS@C on Carbon Cloth as Flexible Electrode for Both Lithium and Sodium Storage' *ACS Appl. Mater. Interfaces,* 7 (50), pp 27804–27809
11. Yuanxian, X., Wenyue ,L.,Fan, Z., Xiaolong, Z., Wenjun, Z., Chun,S.L. and Yongbing, T. (2016) 'In situ incorporation of FeS nanoparticles/carbon nanosheets composite with an interconnected porous structure as a high-performance anode for lithium ion batteries' *J. Mater. Chem. A*,4, pp 3697-3703
12. Ling, F., Qianglu, L., Bin, Y., Gen, C., Pu, X., Yuling, L., Yun, X., Shuguang, D., Sergei,S., and Hongmei, L. (2013) 'Reduced Graphene Oxide Wrapped FeS Nanocomposite for Lithium-Ion Battery Anode with Improved Performance' *ACS Appl. Mater. Interfaces,* 5 (11), pp 5330–5335
13. Eun-Ju, K., Jae-Hwan, K., Abdul, M. A., and Yoon-Seok, C.(2011) 'Facile Synthesis and Characterization of Fe/FeS Nanoparticles for Environmental Applications' *ACS Appl. Mater. Interfaces,* 3 (5), pp 1457–1462
14. YuLin, M., Lin, H., YouCun, C., YuanGuang ,Z., YingGuo, Z.(2009) 'Simple method to synthesis iron sulfide self-assembled microstructure and magnetic properties' *Materials Chemistry and Physics* 114 (2009) pp 518–521
15. Sines, T., Dimitri, D.V.,Rajiv,M.,Popczuna, J. and Raymond, E.S.(2012) 'Synthesis of tetragonal mackinawite-type FeS nanosheets by solvothermal crystallization' *Journal of Solid State Chemistry*, 196 pp 17-20
16. Hull, T.R.,Colligon, J.S. and Hill, A.E. (1987) 'Measurement of thin film adhesion' *Vacuum* 37, pp 327-330
17. Paul, O. and John, M. (1998) 'Developing an understanding of the processes controlling the chemical bath deposition of ZnS and CdS' *J. Mater. Chem.*, 8 pp 2309-2314
18. Chengcheng, X., Dan, Z., Ke, C., Shumin, Z.,Xin, W., Haiying, Q., Jiabin, L., Yinzhu,J. and Liang, M. (2015) 'In situ growth of FeS microsheet networks with enhanced electrochemical performance for lithium-ion batteries' *J. Mater. Chem. A,* 3 pp 8742-8749
19. Mendili, Y.E., Abdelouas, A., Hajja, H. E.and Bardeaub, J.F. (2013) 'Phase transitions of iron sulphides formed by steel microbial corrosion' *RSC Adv.,* 3 pp, 26343–26351
20. Lennie, A. R., Redfern, S.A.T., Schof1eld, P. F, and Vaughan, D. J. (1995) 'Synthesis and Rietveld crystal structure refinement of mackinawite, tetragonal FeS' *Mineralogical Magazine*, 59, pp 677-683
21. Muhammad, S.A., Asma, A., Mohammad, A. M. (2015) 'Synthesis of mackinawite FeS thin films from acidic chemical baths' *Materials Science in Semiconductor Processing* 32 pp 1–5
22. Nader, G., 'Band gap determination using absorption spectrum fitting procedure', (2013) *International Nano Letters*, 3:2 PP 1-4

Research Article

Screening of significant medium components for enhanced elicitor production from Fusarium oxysporum cubense using Plackett-Burman Design

Janki N. Thakker[1]*, Pinakin C. Dhandhukia[2], M. Kumari[3], I. L. Kothari[3]

[1] Department of Biotechnology, PD Patel Institute of Applied Science, CHARUSAT University, Changa-388421, Gujarat, India

[2]Department of MIcrobiology, SPTM college of arts and Science, Veer Narmad South Gujarat University, Athwa Gate, Surat

[3]Lab#103, BRD School of Biosciences, Sardar Patel Maidan, Vadtal Road, Satellite Campus, Post Box No. 39, Sardar Patel University, Vallabh Vidyanagar-388120, (Gujarat), India.

Received: 30/03/2017
Revised: 08/07/2017
Accepted: 04/08/2017

Correspondence to:
*Janki N. Thakker:
jankithakker.bt@charusat.ac.in

Abstract:

The Plackett-Burman design, a statistical screening method, was used to screen eleven media such as glucose, sucrose, fructose, sorbitol, glycerol, malt extract, yeast extract, urea, NaNO3, NH4NO3 and (NH4)2SO4 for biomass production of Fusarium oxysporum f.sp . cubense (Foc), a causative agent of Panama disease of bananas. Malt extract, yeast extract and fructose have been found to have a significant positive effect on the production of elicitors, while glycerol, NaNO3, NH4NO3 and (NH4)2SO4 exhibited a significant negative effect on the production of the elicitor. In addition, a 3-fold increase in dry mycelial weight (DMW), which served as a source of elicitor, was achieved in the medium combination 3 in only six days compared to the biomass of Foc achieved in 21 days in potato dextrose broth. Therefore, medium components with significant positive and negative effects were identified that could be increased or decreased, respectively for higher elicitor production and further optimization.

Keywords: Elicitor, Fusarium oxysporum f.sp. cubense, media component, Dry mycelial weight

INTRODUCTION

World production of banana in 2016 was about 103 million tons, among which about 16.8 million tons was contributed by India as the largest banana producer. Many commercial varieties of banana succumb to a destructive pathogen *Fusarium oxysporum* f.sp. *cubense* (Foc) causing Panama disease (fusarial wilt). For countering the wilt caused by Foc, several reports support the use of pathogen derived elicitor or synthetic elicitors, mimicking the process of vaccination, to induce complex defense against pathogen (Lakshmanan and Selvaraj, 1986; Mandeel and Baker 1991; Kothari et al. 2008; Bektas and Eulgem 2015). Upon subsequent infection by pathogen in these primed plants resulted in more rapidly activated and robust defense responses (Bektas and Eulgem 2015). Although this concept is very aged, its molecular basis is still only partly understood. Recently, Khan et al. (2016) reported that they characterized the role of *Magnaporthe oryzae* hypersensitive protein 2 (MoHrip2) as an elicitor protein from blast pathogen *M. oryzae*. MoHrip2-treated rice seedlings exhibited induced rice resistance to blast. However, the majority of the mode of action is still unknown. In our previous study, the effectiveness of crude extract prepared from biomass of pathogenic Foc (elicitor) was investigated for the control of Panama disease in tissue cultured banana plantlets (Thakker et al. 2007). Defense related

enzymes induced upon application of elicitors were purified, and their direct antifungal activity was also reported (Thakker et al. 2009). Growth of Foc is slow on conventional growth medium like potato dextrose broth convoyed by a low biomass production (Patel et al. 2004) demands the development of a new medium to support rapid growth with a commendable biomass production.

Present study focuses on the screening of medium components for mass production of the biomass which can be used to prepare elicitor using statistical experiment design. Media composition as well as the growth conditions influence the culture growth, therefore, a fermentation improvement program begins with measurement of product yield as a response to test variables. Changing one independent variable at a time (OVAT) while keeping others at fixed concentration used conventionally or applying statistical designs is used to screen large number of variables. The rapid, and reliable results, shortlisting of significant nutrients, comprehend the interactions among the nutrients at various concentrations, and reduction in number of experiments which saves time, cost, chemicals, and manpower are the advantages offered by statistical methods over conventional methods (Srinivas et al. 1994; El-sersy and Abou-Elela, 2006). The Plackett-Burman design is an efficient way to screen a large number of variables rapidly to identify the most important variables (Deshmukh and Puranik, 2010). The crude biomass of the Foc was sucessfully tested as an elicitor in *in vitro* (Thakker et al. 2007) and *in vivo* (Thakker et al. 2011). Therefore, the aim of the present study was to evaluate the media components significantly affecting the biomass production of Foc using Plackett-Burman design.

MATERIALS AND METHODS

Microorganism

Previously isolated culture of Foc from infected banana plant was maintained on potato dextrose agar (PDA) as described by Thakker et al. (2009).

Chemicals and Solvents

All the dehydrated media components and solvents (99.9%) were purchased from Hi-Media (Mumbai, India) and Qualigens (Mumbai, India) respectively.

Cultural technique

The basal medium which contained (g L^{-1}) KH_2PO_4, 2.0; KCl, 0.3; $ZnSO_4$ $7H_2O$, 0.03; $CuSO_4$ $7H_2O$, 0.003; and Na_2MoO_4 $2H_2O$, 0.003 was used as base throughout the study. The levels and concentrations of other medium components viz glucose, sucrose, fructose, sorbitol, glycerol, malt extract, yeast extract, urea, $NaNO_3$, NH_4NO_3, $(NH_4)_2SO_4$, and their combination were as per given in Table 1, and 2, respectively. The nutrient components required to be screened were added to the base as per required concentration. The pH was maintained 5.5 throughout the experiment. Using a sterile cork borer of eight mm diameter, an agar plug was cut from three days old fungal mat on PDA. One plug was used for inoculation of 100 ml broth in 250 ml Erlenmeyer flask and incubated for six days at 27°C in static condition.

Table 1. Medium components, their variables design codes and respective concentration coded by high (+) and low (-) used in Plackett-Burman design

Variable	Medium Components	+ Value (g L^{-1})	- Value (g L^{-1})
X1	Glucose	20	2
X2	Sucrose	20	2
X3	Fructose	20	2
X4	Sorbitol	20	2
X5	Glycerol	20	2
X6	Malt Extract	20	2
X7	Yeast Extract	10	1
X8	Urea	10	1
X9	$NaNO_3$	10	1
X10	$(NH_4)_2SO_4$	10	1
X11	NH_4NO_3	10	1

Plackett-Burman experimental design

Each independent variable was tested at two level of concentrations represented by high (+), and low (-), for all eleven medium components selected for the study. Each variable with a code, variable name and their respective concentrations corresponding to high and low level values are shown in Table 1. The design space was formed with a two level design with only minima, and maxima of input variables. Eleven input parameters resulted in twelve experiments with design v+1 where, v is a number of variables. The resulting twelve experimental cases are shown in Table 2 with the number of positive signs for high concentration, and negative signs for low concentration of the respective variable. Each column contains the same number of positive and negative characters. Each row then represents a test batch and each column represents an independent variable. The effect of each variable was determined by Eq (1):

$$E_{(xi)}=(\mathrm{S}DMW_i^{+}-DMW_i^{-})/N \quad (1)$$

Where $E_{(xi)}$ is the concentration effect of the tested variable. $DMWi^{+}$ and $DMWi^{-}$ are DMW test productions where the measured variable (*xi*) was present at high and low concentrations; N is the number of trials divided by two. Experimental error was determined by calculating variance between six times replicated variable as Eq (2):

$$V_{eff}=\mathrm{S}(E_{spr})^2/n \quad (2)$$

Where *Veff* is the varience of the concentration effect, *Espr* is the concentration effect for the replicated variable with a single point and n is the number of replicats of variable.

The standard error (SE) of the concentration effect was calculated by square root of the variance of the effect, and the significance level (p-value) of each concentration effect was determined using the student's t-test (Eq 3):

$$t(xi)=E(xi)/SE \quad (3)$$

Where, $E_{(xi)}$ is the effect of variable *xi* (Ahuja et al. 2004; Shi and Zhu, 2006).

Measurement of DMW

The fungal growth was determined by DMW measurement. After 6 days of growth, the mycelia mat was separated from the broth by filtration through a pre-weighed filter paper and dried in an oven at 60 ° C until three consecutive constant values were obtained.

Statistical analysis of data

The DMW yields obtained in the experiments were calculated to determine the variability of significance using the Microsoft Excel regression coefficient and the statistical t-values for equal unpaired samples.

RESULTS AND DISCUSSION

Choosing the right carbon source, nitrogen source and other nutrients is one of the most important stage for developing an efficient and economical fermentation process. Plackett-Burman is recommended if more than five factors are to be investigated (Reddy et al. 1999).

These designs are very useful for the economic detection of large effects of variables, provided that all interactions are negligible compared to a few important main individual effect of variables (Siva Kiran et al. 2010). The two-level Plackett-Burman design was selected because it only screens the variable in the experiment "v + 1" (Plackett and Burman, 1946; Bie et al. 2005).

A systematic experiment was performed by setting the Plackett-Burman independent variables (Plackett and Burman, 1946) at two levels, and the corresponding dry mycelial mass (DMW) was measured in each batch, followed by a statistical analysis to interpret significant media components. Such approach is a useful screening process used to identify the contribution of each media component to a system response that allows reducing the number of variables to be taken into account (Liu et al. 2003). These experimental designs are available in multiples of four and are advantageous over multifactor design which are difficult and include a large number of experiments to screen the variables (2^v where v is the total number of variables). Higher order linear full factorial and quadratic Box-Behnken constructs would require 66 and 52 experimental batches for same number of variable that would be prohibitively uneconomical (Naveena et al. 2005). The aim of this study was to explore the main effects of eleven independent variables in an economical way to increase the production of biomass of Foc. Due to the orthogonal nature of the Plackett-Burman design, it only gives the net effect of every variable that is not preplexed by the interaction between the variables (Dhandhukia and Thakkar, 2007).

Table 1 shows the independent variables and the corresponding high and low concentrations of eleven factors used in the optimization study marked +1 and -1. When adjusting diffrent level, caution is required because a small difference may not have any effect and a large difference for the sensitive component may mask other components (Ahuja et al., 2004). In this study, higher levels of ingredients were selected to correspond to ten times their lower levels (Table 1). The various mono- and disaccharides used in the study were reported as the main source of carbon for various fungi. Various sources of nitrogen in the form of ammonia and nitrate ions were included in the study together with urea. The yeast extract was included as a complex source that provides carbon, nitrogen and a rich source of vitamins (Dhandhukia and Thakkar, 2007). Malt extract contains up to 55% maltose sugar per weight basis as well as provides nitrogen source along with many essential vitamins (Almeida et al. 2005).

Twelve run Plackett-Burman design constructs with two concentration levels for each variable were monitored for screening medium components for their ability to support the DMW production shown in Table 2. The X1-X11 variables represent respective medium components and the replicated variable is denoted by an asterisk. The total output of each batch for

cumulative biomass production followed the order of biomass production as, 3> 2> 9> 6> 7> 1> 8> 5> 12> 11> 10. The highest produced biomass was 15.27 gL^{-1} at run 3 and the lowest biomass production was 1.52 gL^{-1} at run 10 (Table 2).

Table 2. Plackett-Burman design with 12 runs generated by fractional rotation of the full factorial pattern and DMW measured as response where X1 to X11 are independent variables

Run	Components											DMW ($g\ L^{-1}$)
	X 1	X 2	X 3	X 4	X 5	X 6	X 7	X 8	X 9	X 10	X 11	
1	+	+	-	+	+	+	-	-	-	+	-	3.75
2*	-	+	+	-	+	+	+	-	-	-	+	10.29
3	+	-	+	+	-	+	+	+	-	-	-	15.26
4	-	+	-	+	+	-	+	+	+	-	-	8.51
5	-	-	+	-	+	+	-	+	+	+	-	2.86
6	-	-	-	+	-	+	+	-	+	+	+	7.02
7	+	-	-	-	+	-	+	+	-	+	+	5.36
8	+	+	-	-	-	+	-	+	+	-	+	3.10
9	+	+	+	-	-	-	+	-	+	+	-	9.02
10	-	+	+	+	-	-	-	+	-	+	+	1.52
11	+	-	+	+	+	-	-	-	+	-	+	1.78
12	-	-	-	-	-	-	-	-	-	-	-	2.32

Table 3. Statistical parameters measured in terms of *t*-value, probability, confidence level and ranking of variables for DMW production for each variable tested

Medium Component	E*xi* Absolute	SE	$t_{(xi)}$	Confidence (%)	Ranking
Glucose	11.54**	0.64	48.23	99.99	8
Sucrose	3.13**	0.64	42.90	99.99	11
Fructose	21.35**	0.64	19.97	95.99	6
Sorbitol	9.79**	0.64	67.14	99.99	9
Glycerol	40.0**	0.64	56.08	99.99	2
Malt extract	27.51**	0.64	47.55	99.99	3
Yeast extract	80.24**	0.64	43.19	99.99	1
Urea	4.87	0.64	3.27	99.97	10
$NaNO_3$	12.47	0.64	3.83	82.4	7
NH_4NO_3	23.46	0.64	0.17	16.53	5
$(NH_4)_2SO_4$	25.28*	0.64	4.66	99.14	4

**p<0.0001, *p<0.05 level of significance

Table 3 shows the effect of each medium component on DMW production, as well as the standard error, t(*xi*), p, the confidence level, and the order of each component. The components were tested at a confidence level of 95% based on their effects. The component with positive effect with confidence level of more than 95% was interpreted to be required at a higher concentration than the indicated high value (+). However, the significantly negative effect showed that the component was effective in DMW production, but the required amount was lower than the indicated low(-) concentration in plackett-Burman design (Dhandhukia and Thakkar, 2007). All factors in this study had an effect on DMW production with a confidence level of 95% or higher, and were considered significant for DMW by Foc (Table 3). The main effects of components in the DMW production medium are shown in Fig. 1

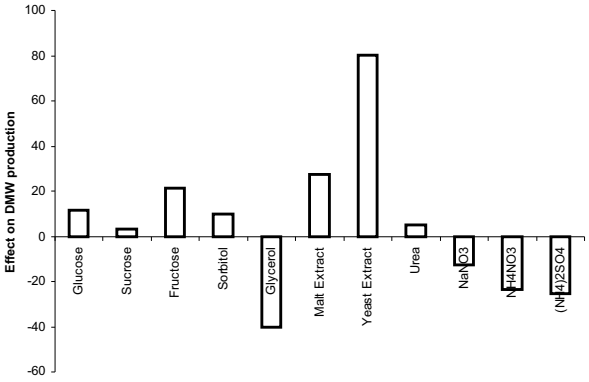

Fig. 1. Main effect of media components on DMW production. The components with positive value increase growth and negative value decrease the growth of Foc.

The yeast extract had the maximum positive effect on DMW production, followed by malt extract, fructose, glucose, sorbitol, urea, and sucrose. The effect of glycerol and other NO_3 salts were negative, indicating that these components are required in the DMW production medium but at a lower concentration than the established low level in the study, or can be omitted from further selection. Contarary to our findings, Gheorghe et al. (2015) reported, the most suitable source of nitrogen for growth of *F. oxysporum f. Sp. glycines*, the pathogen of *Glycine max*, were sodium nitrate, ammonium nitrate, ammonium sulfate, asparagine and peptone. This suggests that different forms of a particular species of *F. oxysporum* have specific requirements.

Yeast extract and malt extract were better components of the medium than any other carbon source tested. Supplementation of one or more "B" group vitamins either as separate or in the form of yeast

extract improved the production of DMW. Yeast extract serves as a source of nitrogen as well as a source of vitamin, but is an expensive element for designing economic media (Dhandhukia and Thakkar, 2007). The results of the Plackett-Burman design indicate that yeast extract is required for growth and should be delivered at a high concentration. Malt extract contains 55% carbohydrates such as maltose (Almeida et al., 2005), it also contains an easily available source of nitrogen, vitamins and minerals that can cause a positive effect on growth. Fructose also had a positive effect on growth.

The ammonical and nitric form of the nitrogen source has a negative effect on the growth of the Foc. In addition, Foc prefers nitrogen from complex sources such as malt extract and yeast extract. Excessive growth can also be due to the presence of vitamins in sufficient quantity together with the readily available essential amino acids present in the yeast extract and malt extract (Almeida et al., 2005).

In previous studies, potato dextrose medium was used to produce elicitors. The maximum achieved DMW of Foc was 5.2 g L^{-1} after 21 days at 27 °C in a static condition (Patel et al., 2004). However, in this study, a three-fold increase in growth was achieved only on a sixth day at 27 °C in a static condition. This suggests that achieving the right combination of medium components by identifying the most significant components, higher biomass of Foc can be achieved in a shorter time. Ahuja et al. (2004) reported the use of the Plackett-Burman design to achieve the exponential growth of aggregated shipworm bacteria. Liu and Wang (2007) have successfully used a statistical approach to biomass optimization and the production of extracellular polysaccharides of *Agaricus blazei*. Similarly, Plackett-Burman design was adopted to determine the media components, ie, magnesium sulphate and ferric ammonium citrate, significantly influencing the antibacterial activity of *Synechocystis aquatilis* (Deshmukh and Puranik 2010). The present study reports several important nutrients useful for increasing the yield of DMW and also identified nutrients that should be used in a lower concentration.

CONCLUSIONS

In contrast to the classical method for optimization of medium components, statistical technique was implemented, where the levels of variables were changed simultaneously to determine their individual impact on biomass production. This study showed that the Plackett-Burman design is a powerful tool in optimizing the composition of the medium used for production of rapid and enhanced biomass of Foc that can be used as an elicitor to combat panama disease.

ACKNOWLEDGEMENT

Authors express their gratitude to Department of Biotechnology, New Delhi for financial support.

REFERENCES

1. Ahuja, S.K., Ferreira, G.M. and Moreira, A.R. (2004) 'Application of Plackett-Burman design and Response Surface Methodology to achieve exponential growth for aggregated shipworm bacterium', *Biotechnology and Bioengineering* Vol. 85, March, pp. 666-675.
2. Almeida, R.B., Garbe, L.A., Nagel. R., Wackerbauer, K. and Tressl, R. (2005) 'Regio– and Stereoselectivity of Malt Lipoxygenases LOX1 and LOX2', *The Journal of Institute of Brewing and Distilling,* Vol. 111, July, 265–274.
3. Bie, X., Lu, Z., Lu, F. and Zeng, X. (2005) 'Screening the main factors affecting extraction of the antimicrobial substance from *Bacillus* sp. fmbJ using the Plackett–Burman method', *World Journal of Microbiology and Biotechnology*, Vol. 21, October, pp. 925–928.
4. Bektas, Y. and Eulgem, T. (2015) ' Synthetic plant defense elicitors', *Frontiers in Plant Science*, Vol. 5, January, pp. 1-17.
5. Deshmukh, D.V. and Puranik, P.R. (2010) 'Application of Plackett-Burman design to evaluate media components affecting antibacterial activity of alkaliphilic Cyanobacteria isolated from Lonar Lake', *Turkish Journal of Biochemistry*, Vol. 35, June, pp. 114–120.
6. Dhandhukia, P.C. and Thakkar, V.R. (2007) 'Significant medium components for enhanced production of jasmonic acid by *Lasiodiplodia theobromae* using Plackett-Burman Design', *Current Trends in Biotechnology and Pharmacy*, Vol. 1, June, pp. 79-86.
7. El-Sersy, N.A. and Abou-Elela, G.M. (2006) 'Antagonistic effect of marine *Nocardia brasiliensis* against the fish pathogen *Vibrio damsela*: Application of Plackett-Burman experimental design to evaluate factors affecting the production of the antibacterial

agent', *International Journal of Oceans and Oceanography*, Vol. 1, January, pp. 141-150.

8. Gheorghe, B.A., Stelica, C., Relu, Z.C. and Maria, O. (2015) 'The biological growth parameters of the *Fusarium oxysporum* f. sp. *glycines* fungus', *Romanian Biotechnological Letters*, Vol. 20 No. 6, pp.10922-10928.
9. Khan, N.U., Liu, M., Yang, X. and Qiu, D. (2016) 'Fungal Elicitor MoHrip2 Induces Disease Resistance in Rice Leaves, Triggering Stress-Related Pathways', *PLOS One*, Vol. 11 No.6, June pp. e0158112. doi:10.1371/journal.pone.0158112
10. Kothari, I.L., Thakker, J.N. and Patel, M. (2008) 'Chp 5 Elicitor Biotechnology' In Setia, R.C., Nayyar, H. and Setia, N.I. (ed.) 'Corp Improvement: Strategies and applications' IK International Publishing House Pvt Ltd, New Delhi, India pp. 64-77.
11. Lakshmanan, P. and Selvaraj, P. (1986) 'An effective method for the control of Panama disease of banana: Shanmugam, N. (Ed.) Seminar Proceedings on 'Management of soil-borne disease of crop plants', Tamilnadu Agricultural University, Coimbtore, India pp. 20.
12. Liu, C., Liu, Y., Liao, W., Wen. Z. and Chen, S. (2003) 'Application of statistically-based experimental designs for the optimization of nisin production from whey', *Biotechology Letters*, Vol. 25, June, pp. 877–882.
13. Liu, G.Q. and Wang, X.L. (2007) 'Optimization of critical medium components using response surface methodology for biomass and extracellular polysaccharide production by *Agaricus blazei*', *Applied Microbiology and Biotechnology*, Vol. 74, February, pp. 78–83.
14. Mandeel, Q. and Baker, R. (1991) 'Mechanisms involved in Biological control of Fusarium wilt of cucumber with strains of nonpathogenic *Fusarium oxysporum*', *Phytopathology*, Vol. 81, December, pp. 462-469
15. Naveena, B.J., Altaf, M., Bhadriah, K. and Reddy, G. (2005) 'Selection of medium components by Plackett-Burman design for the production of L (+) lactic acid by *Lactobacillus amylophilus* GV6 in SSF using wheat bran', *Bioresource Technology*, Vol. 96, March, pp. 485-490.
16. Patel, M., Kothari, I.L. and Mohan, J.S.S. (2004) 'Plant defence induced in *in vitro* propagated banana (*Musa paradisiaca*) plantlets by Fusarium derived Elicitors', *Indian Journal of Experimental Biology*, Vol. 42, July, pp. 728-731.
17. Plackett, R.L. and Burman, J.P. (1946) 'The design of optimum multifactorial experiments', *Biometrica*, Vol. 3, June, pp. 305–325.
18. Reddy, P.R.M., Reddy, G. and Seenayya, G. (1999) 'Production of thrermostable β–amylase and pullulanase by *Clostridium thermosulfurogenes* SV2 in solid-state fermentation: Screening of nutrients using Plackett-Burman design', *Bioprocess Engineering*, Vol. 21, August, pp. 175-179.
19. Shi, F. and Zhu, Y. (2006) 'Application of statistically-based experimental designs in medium optimization for spore production of *Bacillus subtilis* from distillery effluent', *BioControl*, Vol. 52, December, pp. 845-853.
20. Siva Kiran, R.R., Konduri, R., Rao, G.H. and Madhu, G.M. (2010) 'Statistical optimization of endo-polygalacturonase production by overproducing mutants of *Aspergillus niger* in solid-state fermentation', *Journal of Biochemical Technology*, Vol. 2, January, pp. 154-157.
21. Srinivas, M.R.S., Naginchand, K. and Lonsane, B.K. (1994) 'Use of Plackett–Burman design for rapid screening of several nitrogen sources, growth/product promoters, minerals and enzyme inducers for the production of alpha-galactosidase by *Aspergillus niger* MRSS 234 in solid state fermentation', *Bioprocess Engineering*, Vol. 10, March, pp. 139–144.
22. Stroble, R.J. and Sullivan, G.R. (1998) 'Ch 6. Experimental design for improvement of fermentations', In, Demain, A.L. and Davies, J.E. (Ed.), A Manual of Industrial Microbiology and Biotechnology 2nd edition, ASM Press, Washington DC, USA, pp. 80-93.
23. Thakker, J.N., Patel, N. and Kothari, I.L. (2007) '*Fusarium oxysporum* Derived Elicitors Induced Enzymological Changes in Banana Leaves against Fusarium Wilt Disease',

Journal of Mycology and Plant Pathology, Vol. 37, July, pp. 510-513.

24. Thakker, J.N., Shah, K. and Kothari, I.L. (2009) 'Elicitation, partial purification and antifungal activity of β 1, 3- glucanase from banana plants', *Journal of Pure Applied Science PRĂJNĂ*, Vol. 17, December, pp. 10-16.

25. Thakker, J.N., Patel, P. and Dhandhukia, P.C. (2011) 'Induction of defense related enzymes in susceptible variety of bananas: Role of Fusarium derived elicitors', *Archives of Phytopathology and Plant Protection*, Vol. 44 No. 20, July, pp. 1976-1984.

Research Article

Impact Assessment of Reactive Power Capabilities of Distributed Generating Units in Radial Distribution Network

Pankita Mehta[1], Praghnesh Bhatt[1]*, Vivek Pandya[2]

[1]C S Patel Institute of Technology, CHARUSAT, Changa, India
[3] School of Technology, Pandit Din Dayal Petroleum University, Gandhinagar, India

Received: 12/01/2017
Revised: 00-00-0000
Accepted: 14/05/2017

Correspondence to:
*Praghnesh Bhatt:
pragneshbhatt.ee@charusat.ac.in

Abstract:

Power generation by renewable energy source has been promoted worldwide due to several reasons such as constrained resources for fossil fuel and greater environment concern. Hence, increasing amounts of Distributed Generation (DG) are being connected to radial distribution networks (RDN). The solar photovoltaic (PV), wind turbine generators, fuel cells and small micro turbine have been used for distributed generation system which have different active and reactive power generation capabilities. Hence, they have different impacts on system performance such as voltage profile, losses and voltage stability. The optimal location of DGs, their sizing and reactive power generation capabilities plays a vital role to enhance the performance of RDN. In this paper, optimal location and sizing of DGs has been ascertained with the use of Golden Section Search (GSS) method considering the objectives of minimizing the active power losses in RDN. Moreover, the impact of varying degree of DG penetration with different reactive power generation capabilities have been analyzed to exactly assess their impact on voltage profile, losses and voltage stability. The obtained results have provided the insight for selection of the optimal location of DG and utilization of reactive power generation capabilities of DG units to allow their more penetration in RDN.

Keywords: Distributed Generation, Reactive Power, Voltage Profile, Power Loss

I. INTRODUCTION

The policies for the power generation by renewable energy sources have been encouraged worldwide as they turned to be a crucial to provide clean, sustainable and eco-friendly environment (Ackerman, 2001). The Distributed Generation (DG) requires the generation capacity in the range of 5 kW to 5 MW and generally employs PV cell, wind turbine generator, small hydro plants or fuel cells. DGs are one of the most cost-effective and an economical solution to solve the problems of radial distribution network (RDN) such as voltage profile, loss minimization and stability (Walling, 2008). Several system problems such as voltage, relay coordination and protection, OLTC operations and islanding are discussed in (Walling, 2008) with the penetration of DGs in RDN.

(Georgilakis, 2013) presented a state of the art on several models and methods for optimal placement and sizing of DG, analysis methods and sketched the guidelines for future research trends in this field.The comprehensive literature review on the challenges and possible solutions with the DGs and capacitor placement in RDN has been addressed in (Mehta, 2015) with the focus on problems such as optimal placement and sizing of DGs, voltage stability enhancement and loss minimization. The strategy for optimal placement of DGs in RDN for voltage stability enhancement is proposed in (Mehta, (2015) with modal analysis and continuation power flow. The best location of DG and sizing of DG for voltage stability enhancement is

proposed in (Al Abri, 2013) by mixed-integer nonlinear programming where bus voltages, line capacity and DG penetration level are set as constraints.

Keane (2011) addressed the voltage rise issues with penetration levels of DG and enhanced utilization of voltage control resources has been explored. (Ochoa, 2011) presented the benefits of reactive power capabilities of DG units by examining the possibilities for minimizing the reactive support by adopting enhanced pre-defined fixed power factors. Optimal sizing and optimal placement of generators for modified IEEE 6 bus, IEEE 14 bus and IEEE 30 bus systems has been solved in (Ghosh, 2010) with Newton-Raphson iterative method with the objective to minimize both cost and loss factors. Considering load growth in future and voltage regulation as a constraint, (Mistry, 2014) has addressed mulitple DG placement with the use of PSO with constriction factor approach.

Different types of DGs placement has been proposed by (Kansal, 2013) for minimizing the power distribution loss by maintaining optimal power factor for DG supplying, both real and reactive power using 33-nodes and 69-nodes RDN. More recently a backtracking search optimization algorithm (BSOA) is addressed by El-Fergany (2015) with the objective to reduce the network real loss and enhance the voltage profile where fuzzy rules are used with loss sensitivity factors and bus voltages to determine initial DG's locations.

In literature, many efforts have been reported in area of optimal location and sizing of DG to improve the performance of RDN. But there are limited papers on DG placement which has addressed the impact of reactive power generation capability of DGs while determining its placement. Hence, in this paper, the objectives of the work are set as below:

- To determine the optimal location of DG and its size by considering minimization of active power losses
- To propose different indices to assess the performance of RDN
- To increase the penetration of DG by its utilizing its reactive power capability
- To compare the voltage profile, active and reactive power losses and voltage stability indices for base case and with varying reactive power support from DG

ACTIVE AND REACTIVE POWER CAPABILITIES OF DGs

DG technologies are classified based on their capability of injecting real and/or reactive power in the system. Accordingly, DG technologies are grouped in the following manner (Mehta, 2015).

Type 1: DG capable of controlling active power (P) and reactive power (Q)

DG units that are based on synchronous machine for small hydro, geothermal, and combined cycles fall in Type 1 category. Recently developed variable speed wind turbine generators such as Double Fed Induction Generator (DFIG) and Permanent Magnet Synchronous Generator (PMSG) also possess the similar characteristic. They generate active power as well as they are capable to generate or absorb the reactive power. They can be operated in either voltage control mode or power factor control mode. In voltage control mode, they are supposed to keep its terminal voltage constant at its specified voltage value. But it can do so only if it has sufficient reactive power generation capability. Once its maximum reactive power limit is reached, it will be unable to keep its voltage at specified value. In power factor mode, the DG will deliver the fixed amount of reactive power based on its set target of power factor. In this mode, terminal voltage is not guaranteed to be at specified level. DG in Type 1 category can reduces the import of power from the source, as a result associated active and reactive power losses gets reduced in lines and thus improves the voltage profile. It is evident that any loss reduction is beneficial to distribution utilities, which is generally the entity with an interest to minimize the loss.

Type 2: DG capable of injecting active power (P) only

Photovoltaic (PV), micro turbines, fuel cells, which are integrated to the main grid with the help of converters/inverters are the examples of Type 2 category. These types of DG units may require reactive power for their operations if they are integrated to main grid with the help of line commutated converters. On the other hand, with the advancement in power electronics, they are capable to supply reactive power to the system when interfaced through the self-commutated converters. In this work, it is assumed that DG units in this category neither absorbs nor delivers reactive power to system and operates with unity power factor only.

Type 3: DG capable of injecting reactive power (Q) only

The DG units equipped with synchronous compensator are considered as Type 3 category. It will not generate any active power (P) but only supplies

reactive power (Q) in a system when operating with over excitation.

Type 4: DG capable of injecting active power (P), but consuming reactive power (Q)

Fixed speed squirrel cage induction generator (SQIG) used for wind turbine generating (WTG) system falls under this category. SQIG in super-synchronous mode is capable of injecting real power in the system whereas it demands reactive power from the system. Generally, the reactive power demand of induction generator is compensated by capacitor banks or static var system (SVC) at its terminal. The operation of induction generator at higher wind speed raises the active power generation with simultaneous increase in reactive power consumption. As a result the induction generator will further depress the system voltage if the capacitors banks or SVC at its terminal are unable to compensate this increased reactive power demand. Hence, the problem of voltage stability is further aggravated.

Thus, it is worthwhile to note that the type of DG technology adopted will have a significant bearing on the performance of distribution network. The installation of synchronous machine-based DG units that are close to the loads can lead to beneficial impact on system voltage stability margin; on other end, the case with an induction generator may have detrimental impact on the system stability margin. Therefore, it is an utmost requirement to analyse the effect of different types of DG technologies on the voltage stability to enjoy the system wide benefits.

DETERMINATION OF OPTIMAL LOCATION AND SIZING OF DG

In this work, the one of the objectives are to determine optimal location and size of DG to achieve minimum voltage deviation as well as active power losses. The DG is placed on each bus individually and its size is varied from 0% to 100% in step size of 1% of load power. For finding out the optimal size and location of DG, Golden Section Search (GSS) method is used (Gozel, 2008). The complete flow chart of the GSS method is shown in Fig. 1.

To minimize $\left| \left(P_{dg} \right) = P_{loss} \right.$ (1)

$|V_i| \le 1+0.05pu \; i=1,2,...,n$

Subject to $0 \le P_{dg} \le \sum P_{load}$ (2)

In Fig. 1, i bus number; n total number of buses; optsize(i) optimum size of DG at bus i,; optploss(i) total power losses with optimum size of DG at bus i,; DG_U upper bound of the search interval of DG; DG_L lower bound of the interval; D interval at each iteration step; S_1 and S_2 points within the interval where $S_1<S_2$

The different performance measurement indices are defined and listed in Table 1 to assess the impact of DG on losses and voltage profile.

Table 1. Indices for the performance measurement of test system

Active Power Loss Indices	$APLI=\frac{P_{Loss}-P^{DG}_{Loss}}{P_{Loss}} 100\%$
Reactive Power Loss Indices	$QPLI=\frac{Q_{Loss}-Q^{DG}_{Loss}}{Q_{Loss}} 100\%$
Aggregate Voltage Deviation Index	$AVDI=\sum_{i=1}^{n}(V_i^{DG}-V_i^{basecase})^2$

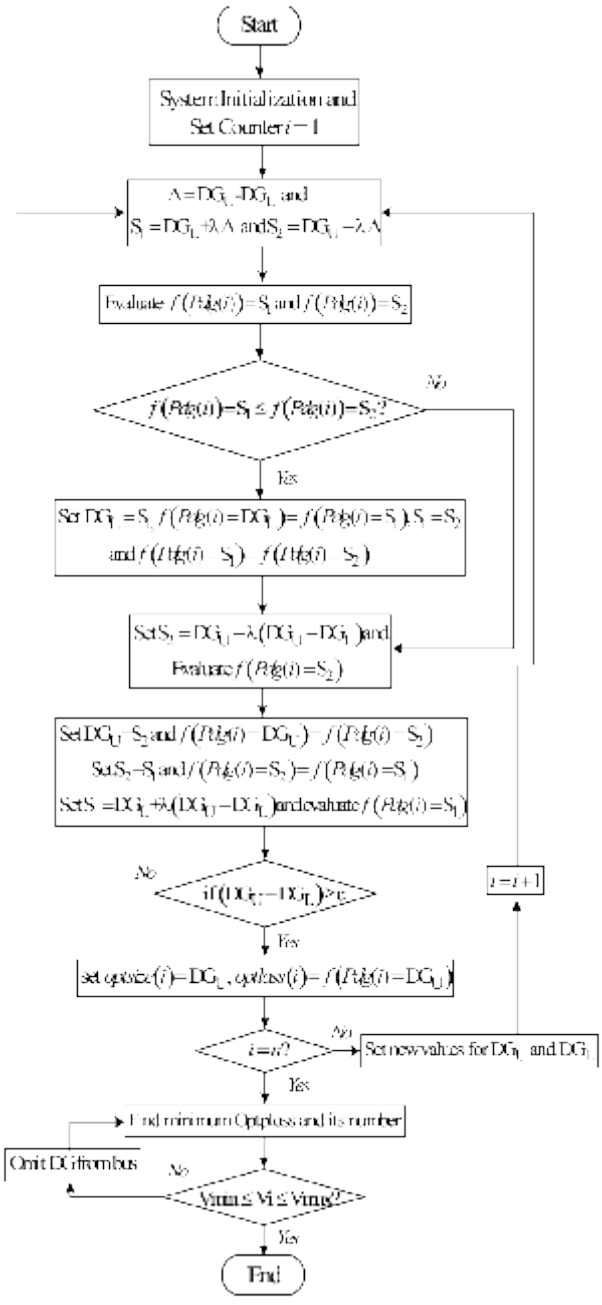

Fig. 1 Algorithm of Golden Section Search for determination of optimal DG location

RESULTS AND DISCUSSION

The test system of 33-nodes RDN is used for the analysis. The schematic of the test system and required data are given in (Mehta, 2015). The system has 3,715 kW active power and 2,300 kvar reactive power.

Determination of Optimal Location of DGs

The optimal location and size of DG has been determined by the method outlined in Fig. 1. In Fig. 2 (a), the optimal size of DG on each individual bus is presented whereas Fig. 2 (b) gives active power losses in a system after its placement on that bus. It can be noticed from Fig. 2 (b) that DG placed at node 6 results in minimum losses whereas DG placed at nodes 26-30 are the other buses which give comparatively higher losses. But sizing requirement of DG at node 6 is greater as compared to DG at node 29. Hence, grater reduction in DG sizing has been given more priority and it is decided to place DG at node 29 for the subsequent analysis.

Voltage Profile Improvement with Different Modes of Reactive Power Generation by DGs

Fig. 3 shows the voltage profile comparison for base case and with the placement of DG at node 29. In this comparison, DG penetration level of 30% has been considered. It means that DG generates power equal to 30% of total load demand of the system. Fig. 3 also represents the voltage profile obtained after considering the DG with different reactive power capability mode. With 30% penetration, DG is assumed to generate 1,200 kW power. The corresponding generations of reactive power by DG in different modes are listed in Table 2.

In Fig. 3, it can be clearly noticed that the test system without any DG source results in the highest voltage deviation. All node voltages get improved with the placement of DG at node 29 irrespective of the mode of its reactive power generation. Fig. 3 gives deep insight related to impact assessment of reactive power capability. It can be observed that with DG operating with 0.9 leading and 0.9 lagging are on two extreme boundaries. With 0.9 lagging PF, DG is supposed to deliver 0.5811 Mvar to the system which can supplement the reactive power demand of the RDN, thus have maximum impact on voltage profile improvement. On the other hand, DG with 0.9 leading PF is supposed to absorb 0.5811 Mvar from the RDN which ultimately distress the system, hence the voltage profile has become worsen even in comparison to DG with Unity PF operation. But this profile is better when it is compared to base case. Active power support in unity PF mode from DG results in lower power drawl from sub-station as compared to base case. Thus it results in lesser current and lesser reactive power losses and it results in voltage profile improvement.

Table 2 DG Penetration level and corresponding active and reactive power generation

	Level	PF Control	P_{DG} (MW)	Q_{DG} (MVAR)
Base Case	Zero	--	0	0
DG at Node 29	30 %	Unity	1.2	0
	60 %		2.4	0
	90 %		3.6	0
	30 %	0.95 Lag	1.2	0.3944
	60 %		2.4	0.5811
	90 %		3.6	1.18
	30 %	0.90 Lag	1.2	0.5811
	60 %		2.4	1.1623
	90 %		3.6	1.7435
	30 %	0.95 Lead	1.2	- 0.3944
	60 %		2.4	- 0.5811
	90 %		3.6	- 1.18
	30 %	0.90 Lead	1.2	- 0.5811
	60 %		2.4	- 1.1623
	90 %		3.6	- 1.74356

Impact of Penetration Level of DGs

The Penetration levels of DGs in RDN have significant impacts on its performance. The optimal level of penetration can definitely improve the voltage profile of all nodes in RDN and can also reduce active and reactive power losses. But it has been observed that penetration level of DG beyond certain level may deteriorate the performance of DG. Fig. 4 clearly depicts the impact of varying DG penetration level by considering base case, 30%, 60% and 90% comparison. It can be observed that as the DG penetration level increases, bus voltage values are continuously increases. DG penetration level up to 60 % gives promising improvement and tries to maintain the bus voltages within the strict band across their nominal values. The careful observation of Fig. 4 (a)-(e) reveal that DG reactive power generation capability play a vital role to maintain the bus voltages with varying DG penetration level.

The DG operating with 0.9 lagging PF affects severely with DG penetration level and many of the bus voltages magnitudes have crossed their maximum values. The bus voltages higher than their maximum

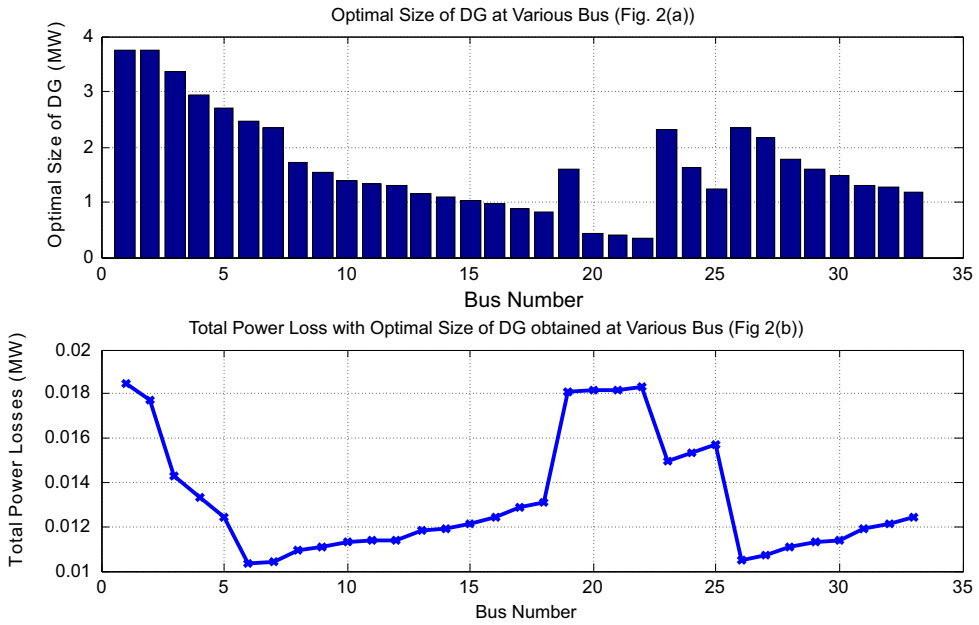

Fig.2. Optimal Size of DG at each bus and its corresponding active power losses

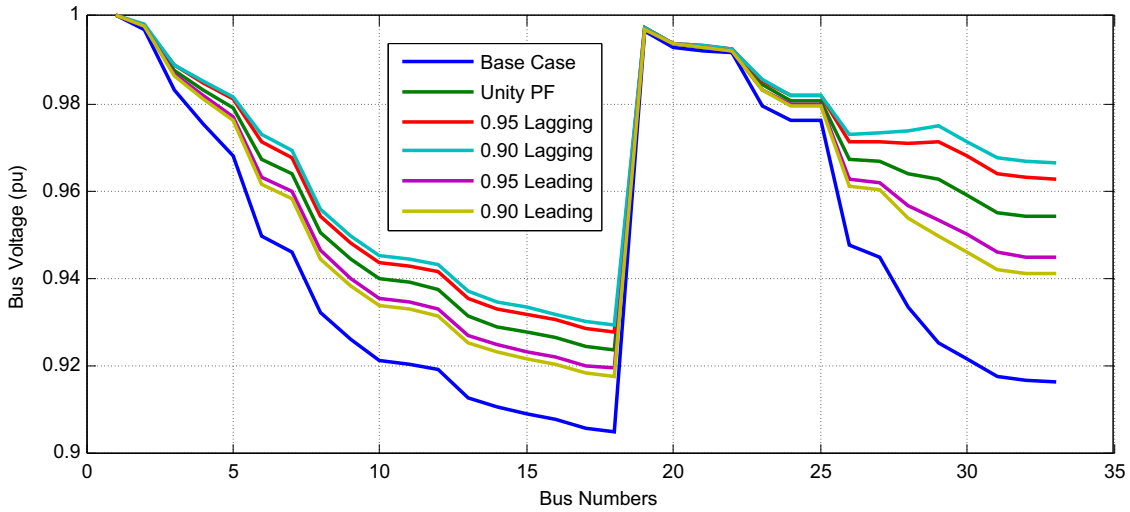

Fig. 3 Bus Voltage profile of 33-nodes RDN without and with DG in different reactive power generation mode

allowable values may damage the equipment connected at distribution level, hence larger DG penetration with lagging PF cannot be allowed in RDN. On the other hand, bus voltage values remain in a strict band of voltage regulation limit of ± 0.05 pu even with 90% DG penetration level. This is the most important and useful observable while planning for DG penetration in RDN. The system operator may go for the higher and higher power generation from DG sources if they have DGs capable of reactive power control. DGs with Type 1, Type 2 and Type 3 discussed in earlier section are the most suitable DG resources to explore the maximum benefits as the system operator can operate them as per the requirement.

Active and Reactive Power Losses with DG Placement and AVDI

Fig. 5 shows the variation in active and reactive power losses with the placement of DG at bus 29. In this case study, only 30 % DG penetration has been presented but similar results are observed with higher penetration level. From Fig. 5 (a), it can be noticed that placement of DG reduces the active power losses for all the cases, but the operation of DG in lagging PF mode is the most effective in active power loss reduction. On the other hand, DG in unity PF mode is the best options for minimizing reactive power loss as it does not allow further exchange of reactive power across the feeder

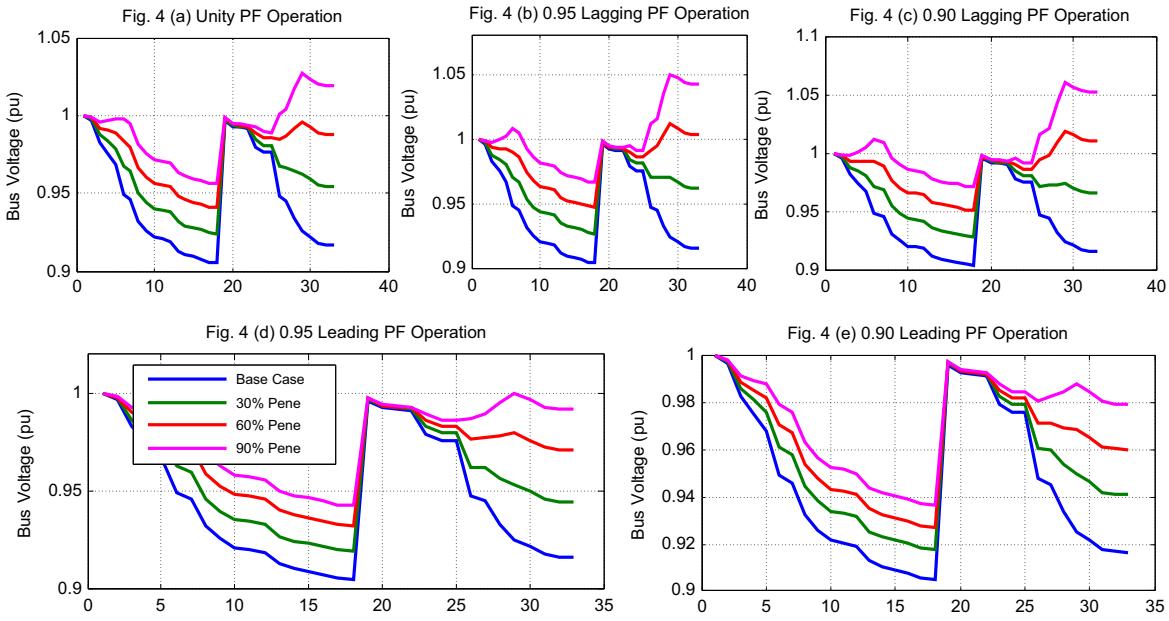

Fig. 4 Comparative voltage profile with different penetration level and PF operation mode

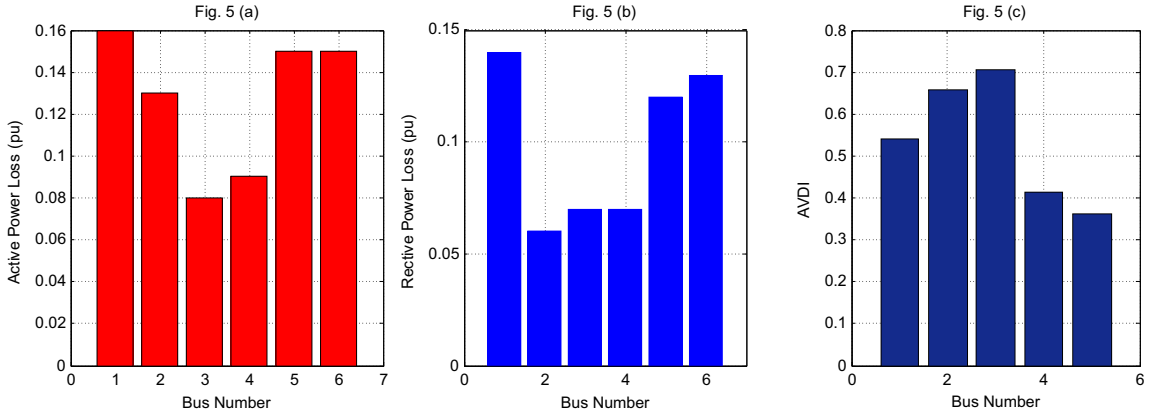

Fig. 5 Performance Indices for 33-Nodes RDN with different PF operation mode at 30% penetration level

sections. DG with leading PF results in highest reactive power loss as it force the DG to absorb the reactive power, thus creates highest losses as shown in Fig. 5 (b). But doing so it can greatly restricts the bus voltages to go beyond its nominal value of 1 pu which can be observed from Fig. 4 (d)-(e). Fig. 5 (c) represents the AVDI which is the highest for DG in 0.9 lagging PF operation as expected.

CONCLUSIONS

The proper selection of DG and its sizing results in better voltage profile across all the buses, reduction in active and reactive power losses and enhanced stability. The proper utilization of DG reactive power generation capacity allows more penetration of DG. The higher penetration of DG creates the voltage rise issue and thus limits its further penetration. The operation of DG in leading PF mode helps to absorb excess reactive power from the network, thus restores all the bus voltage magnitude within the limits. On the other hand, the losses in the system slightly increase in leading PF mode which can be taken care by proposing the multi objective optimization method in order to achieve multiple benefits of DG in RDN.

REFERENCES

1. Ackermann, T., Andersson, G., and Soder, L., (2001),' Distributed generation: a definition1', *Electric Power Systems Research*, vol. 57, issue 3, , April, pp. 195-204.
2. Mehta, P., Bhatt, P., and Pandya, V., (2016), 'Challenges and Solutions for Improvement in Radial Distribution Network: A Review', *International Conference on Women in Science and Technology: Creating Sustainable Career ICWSTCSC- 2016, Indian Journal of Technical Education* with ISSN 0971 – 3034, 28-30th January, pp. 170.
3. Georgilakis, P. S. and Hatziargyriou, N. D., (2013), 'Optimal Distributed Generation Placement in Power Distribution Networks: Models, Methods, and Future Research,' in *IEEE Transactions on Power Systems*, vol. 28, no. 3, August, pp. 3420-3428.
4. Mehta, P., Bhatt, P., and Pandya, V., (2015), 'Optimal Selection of Distributed Generating Units and its

Placement for Voltage Stability Enhancement and Energy Loss Minimization', *International Journal of Ain Shams Engineering*, *Elsevier online publication*, December.

5. Walling, R. A., Saint, R., Dugan, R. C., Burke, J. and Kojovic, L. A., (2008), 'Summary of Distributed Resources Impact on Power Delivery Systems,' in *IEEE Transactions on Power Delivery*, vol. 23, no. 3, July, pp. 1636-1644.
6. Al Abri, R. S., El-Saadany, E. F. and Atwa, Y. M., (2013), 'Optimal Placement and Sizing Method to Improve the Voltage Stability Margin in a Distribution System Using Distributed Generation', in *IEEE Transactions on Power Systems*, vol. 28, no. 1, February, pp. 326-334.
7. Keane, A., Ochoa, L. F., Vittal, E., Dent, C. J. and Harrison, G. P., (2011), 'Enhanced Utilization of Voltage Control Resources With Distributed Generation," in *IEEE Transactions on Power Systems*, vol. 26, no. 1, February, pp. 252-260.
8. Ochoa, L. F., Keane, A., and Harrison, G. P., (2011), 'Minimizing the Reactive Support for Distributed Generation: Enhanced Passive Operation and Smart Distribution Networks', in *IEEE Transactions on Power Systems*, vol. 26, no. 4, November, pp. 2134-2142.
9. Ghosh, Sudipta., Ghoshal, S.P. and Ghosh, Saradindu., (2010), 'Optimal sizing and placement of distributed generation in a network system', *International Journal of Electrical Power & Energy Systems*, ISSN 0142-0615, vol. 32, Issue 8, October, pp. 849-856.
10. Mistry, Khyati., Roy, Ranjit. (2014), 'Enhancement of loading capacity of distribution system through distributed generator placement considering techno-economic benefits with load growth', *International Journal of Electrical Power & Energy Systems*, vol. 54, January, pp. 505-515.
11. Kansal, Satish., Kumar, Vishal. and Tyagi, Barjeev., (2013), 'Optimal placement of different type of DG sources in distribution networks', *International Journal of Electrical Power & Energy Systems,* vol. 53, December, pp. 752-760.
12. El-Fergany, Attia. (2015), "Optimal allocation of multi-type distributed generators using backtracking search optimization algorithm", *International Journal of Electrical Power & Energy* Systems, vol. 64, January, pp. 1197-1205.
13. Gozel, T., Eminoglu, U., Hocaoglu, M., (2008), 'A tool for voltage stability and optimization (VS&OP) in radial distribution systems using MATLAB graphical user interface (GUI)', *Simulation Modelling Practice and Theory*, vol. 16, issue 5, May, pp. 505-518.

Research Article

Dissolution Enhancement of Quetiapine Fumarate by Liquisolid Compacts Technique

Dharmang Pandya[1]*, Rajesh Parikh[2], Balram Gajra[1], Gaytri Patel[1]

[1]Ramanbhai Patel College of Pharmacy, CHARUSAT University, Changa, Anand, Gujarat
[2]Gujarat Technological University,Chandkheda, Ahmedabad, Gujarat

Received: 27/01/2018
Revised: 09/05/2018
Accepted: 18/06/2018

Correspondence to:
*Dharmang Pandya:
dharmangpandya.ph@charusat.ac.in

Abstract:

The main objective of present investigation was to develop Liquisolid compacts (LSC) as novel solid oral dosage form of Quetiapine fumarate (QTPF) for its dissolution enhancement. QTPF is a BCS class – II drug, used in schizophrenia. The patents on LSC (US5968550 & US6423339B1) helped in method of preparation and its modification. For QTPF LSC, selection of non volatile liquid vehicle, carrier, coating material (adsorbent), super disintegrant were done. LSCs were developed by using Propylene Glycol (PG) and Capmul MCM30 as a combination of non volatile liquid vehicles, Avicel PH112 as a carrier, Aerosil 300 as an adsorbent (coating material) and Kyron T 314 as super disintegrant. The final batch was characterized by tests like flow property (angle of repose and carr's index), The prepared tablets were evaluated for drug content, weight variation, tablet hardness, friability, disintegration time, X Ray Diffraction (XRD) study, Fourier Transform Infrared Spectroscopy (FTIR) study, in vitro drug release study and dissolution efficiency study. Accelerated stability study was performed for 6 months (at 40^0C ± 2^0C temperature and 75% ± 5 Relative humidity (RH)). The results of all characterization tests were in acceptable range. Results of in vitro drug release study of QTPF final batch showed better improvement in dissolution rate as compared to marketed tablet (Seroquel 25) and pure drug. Stability study of the optimized batch for 6 months showed no significant change in drug content, physical appearance, hardness, % friability and in vitro drug release. This study concluded that LSC is proved as one of the suitable approach for developing stable solid oral dosage form of poorly water soluble drug like QTPF.

Keywords: Dissolution enhancement, LSC, QTPF, Schizophrenia.

INTRODUCTION

Dissolution is the core concept of any physical or chemical science including biopharmaceutical and pharmacokinetic considerations in therapy of any therapeutic agent. The dissolution behaviour of a drug is key determinant to its oral bioavailability being the rate-limiting step in absorption of drugs from the gastrointestinal tract. As a result, more than 40% of new candidates entering drug development pipeline fail because of non optimal biopharmaceutical properties. (Wong S.M. et al (2006)).

Over the years, various techniques have been employed to enhance the dissolution profile, the absorption efficiency and bioavailability of water insoluble drugs and/or liquid lipophilic medication. (Kapsi S G et al (2001)). Nowadays, many dissolution enhancement techniques can be used for solving this problem. (Gubbala L P et al. (2014)). The LSC (LSC) technique is the most promising and considered as commercially effective method for dissolution rate enhancement of poorly water soluble drugs. (Nokhodchi A et al (2005)).

As per the patents' review, it is known that LSC technique was first introduced by Spireas S and Bolton S M (1999) to incorporate water in soluble drugs into rapid release solid dosage forms. The principle of liquisolid system is to contain liquid medications (i.e., liquid drugs, drug solutions or suspensions) in powdered form and delivery of drug in a similar way to soft gelatin capsules containing liquids. The patents on LSC helped in method of preparation and its modification. LSC technique refers to the conversion of liquid medications into apparently dry, non-adherent, free flowing and compressible powder mixtures by blending the liquid medications with suitable excipients, which are generally termed as carriers and coating materials. (Spiridon Spireas (1998))

As per the flow mentioned in Fig.1, a liquid lipophilic drug can be converted into liquisolid system without being further modified. On the other hand, if a solid water-insoluble drug is formulated, it should be initially suspended in suitable non volatile solvent system to produce drug solution or drug suspension of desired concentration. (Spireas S et al. (1998)).

QTPF is a BCS class – II, second-generation 'atypical' antipsychotic agent for the treatment of schizophrenia and bipolar mania. QTPF, 2-[2- (4-dibenzo [b, f] [12, 13] thiazepin-1 1-yl-1-piperazinyl) ethoxy]-ethanol fumarate (2:1) (salt), is belonging to the class dibenzothiazepine derivate. It is extensively metabolized in the liver with sulfoxide metabolite and parent acid metabolite, by sulfoxidation and oxidation; both metabolites are pharmacologically inactive, leading to lower bioavailability (9%) (Potu A. R. et al. (2012)). The active pharmaceutical ingredient in a solid dosage form must undergo dissolution before it is available for absorption from the gastrointestinal tract. (Banakar UV (1991)). Oral route is the most commonly used and preferred route for the delivery of drugs, although several factors like pH of gastro intestinal tract, residence time, and solubility can affect drug absorption or availability by this route. For hydrophobic drugs, the dissolution process acts as the rate-controlling step and, which determines the rate and degree of absorption. So, Bioavailability of poorly water-soluble drugs is limited by their solubility and/or dissolution rate. (Porter C. J et al. (2001)). So the objective of the present work was to formulate the LSC of QTPF to improve the dissolution rate which will further lead to increase in bioavailability of drug.

MATERIALS AND METHODS

Materials

QTPF (pure drug) was received as a gift sample from Intas Pharmaceuticals Ltd., Ahmedabad, India. PG, Tween 80 from Merck Specialities Pvt. Ltd., Mumbai, Polyethylene Glycol (PEG) 400, PEG 600 from Loba Chemie Pvt. Ltd., Vadodara, Glycerine from S. D. Fine Chem Ltd., Mumbai, Capmul MCM30 from Abitec, Janesville, WI, Capryol 90, Labrafil from Gattefosse, France, Lauroglycol, Avicel PH101 & PH102, from FMC Biopolymer, Ireland, Avicel PH112 from FMC Biopolymer, Belgium, Lactose Monohydrate (LM) Dicalcium Phosphate (DCP), Aerosil 200, Aerosil 300, Aeroperl 300 from Evonik Industries AG, Germany, Kyron T 314 from Corel Pharma Chem, Ahmedabad were obtained. All other reagents used were also of analytical grade.

Methods

Selection of liquid vehicle

Solubility study of QTPF was carried out in some non-volatile liquid vehicles (i.e. PEG 400, PEG 600, Glycerin, Tween 80, Labrafil, Capryol 90, Capmul MCM30, Lauroglycol and PG) and their blends (mixture of more than one non volatile liquid vehicles), Saturated solutions were prepared by adding excess drug in to the selected liquid vehicles and placed in the rotating stirrer cum incubator (080402, Nova) for 24h at 37^0C. Then after, the solutions were filtered through 0.45µm Millipore filter, diluted with methanol and analysed by UV- spectrophotometer (UV 1800 Shimadzu, Japan) at a wavelength of 291nm against blank sample. Each sample was analyzed thrice to calculate the solubility of QTPF. Same study was performed in to the blend of selected liquid vehicles' ratio. (Sirisolla J. (2015)).

Selection of carrier

Binding capacity is defined as the capacity of powder excipients to hold liquid without change in their flow properties. (Friedrich H. et al. (2006)). To one g of carrier material, liquid blend (50:50, PG: Capmul MCM30) was added in increment of 0.5ml and uniformly mixed. After each addition, Carr's index was measured. Various carrier materials like Avicel PH101, Avicel PH102, Avicel PH112, DCP and LM were used.

Selection of coating material (adsorbent)

To blend of carrier material and liquid, 100mg of coating material was added and uniformly mixed. Carr's index was measured. Various coating materials like Aerosil 200, Aerosil 300, Aeroperl 300 were used. (Friedrich H. et al. (2006))

Method of LSC Preparation

In fig.2, method of LSC preparation is shown. drug was mixed in blend of selected liquid vehicles. Then

after, carrier material was added till saturation of carrier in the mixture. Then, selected coating material was added until flowable mixture achieved. Lastly, Kyron T 314 was added as super disintegrant to improve the powder blend's porosity. (Kumar Nagabandi et al (2011))

Evaluation of LSC

Pre compression studies of LSC

Pre-compression studies may play a key role in dose variations, to get a uniform filling of tablet dies and acceptable flow properties are required for the proposed liquisolid powder systems.

Flow property

Flow properties were studied by Angle of repose and Carr's Index. (Aulton, M. E. (2013)) The fixed height cone method was used to determine the angle of repose in triplicate and the average value was calculated for each powder:

$$\theta=\frac{h}{r} \quad ...Eq.1$$

Where,

θ = perpendicular angle,

h = height of material and

r = radius of the material.

Carr's Index (Compressibility index) of the powder blend was determined by Carr's compressibility index. The formula for Carr's index is as below:

$$\text{Carr's Index } \frac{\text{Tapped Density-Bulk Density}}{\text{Tapped Density}} \times 100 ...Eq.2$$

Method of LSC tablet preparation

Compression was done using a rotary tablet punching machine under constant pressure by a direct compression procedure. The blend of powder mixture was placed in to the die and compressed under a sufficient compression force using a 10 mm diameter, flat punches to keep the hardness of the conventional tablet at 3 to 5kg/cm^2. Die filling, uniform compression and machine operation were undertaken using a standardized manual process for dimensional uniformity. (Kumar Nagabandi V et al. (2011))

Post compression studies for the LSC tablet

a) Drug content

Twenty tablets were weighed and powdered. An amount of powder (QTPF 28.5mg equivalent to Quetiapine 25mg) was dissolved in 100 ml of Methanol, filtered properly. Then it was diluted with suitable solvent and analyzed for drug content at 291 nm using UV-Visible spectrophotometer (UV 1800 Shimadzu, Japan). (Das A. K. et al. (2013))

b) Weight variation

Weight variation was measured by weighing 20 Tablets and average weight was found. Percentage weight variation of the individual tablet should fall within specified limits in terms of percentage deviation from the mean. (Vraníková B et. al. (2015))

c) Tablet Hardness

Hardness of liquisolid tablets (the force in Newton required to crush the prepared tablet) was evaluated using a hardness tester (Toshiba). Ten randomly selected tablets of each batch were tested in both directions (transversely and lengthwise); mean values and standard deviations were calculated. (Vraníková B et al. (2015))

d) Friability

The friability of the tablets was determined using friabilator (Electrolab, Mumbai). This device subjects the tablets to the combined effect of abrasions and shock in a plastic chamber resolving at 25 rpm and dropping the tablets at a height of 6 inches in each revolution. Pre-weighed sample of tablets was placed in the friabilator and were subjected to 100 revolutions. Tablets were dedusted using a soft muslin cloth and reweighed. (Vraníková B et al. (2015)).

The friability is given by the formula:

$$\% \text{ Friability}=\frac{\text{Loss of mass}}{\text{Initial mass}} \times 100 ...Eq.3$$

e) Disintegration time

The disintegration test was performed at 37 ^{0}C ± 2 ^{0}C temperature in distilled water using six tablets from each formulation by disintegration test apparatus (ED2L, Electrolab). The tablets were considered completely disintegrated when no residue remained in the basket. The presented values were the means and SDs of six determinations. (Vraníková B et al. (2015))

Characterization studies for LSC tablet

a) XRD study

XRD patterns were studied using X-ray diffractometer (D2 Phaser, Bruker AXS Inc. Germany). Samples were exposed to 1.540˚A Cu radiation wavelength and analyzed over the 2y range of 2–801. XRD patterns were determined for QTPF pure drug, formulation with drug and placebo. (Fahmy R. H et al. (2008))

b) FTIR study

The IR spectra for QTPF pure drug, formulation with drug and without drug were recorded using an FTIR spectrophotometer [NICOLET – 6700, Thermo Scientific, US]. The samples were scanned over the

frequency range 4000–400 cm-1. The resultant spectra were compared for any spectral changes. (Gubbi S. R et. al. (2010))

c) In vitro drug release study

Dissolution studies were performed for tablets prepared using LSC using dissolution apparatus (TDT-08L, Electrolab), pure drug and marketed product (Seroquel® 25mg – Astra Zeneca). The USP paddle method and dissolution medium were used for all in vitro dissolution studies. The stirring rate was 50 rpm, 900ml 0.1 N HCl was used as dissolution medium and maintained at 37˚C at appropriate intervals (0, 10, 20, 30, 45, 60, 90min). The samples were taken, filtered through a 0.45 µm filter and analyzed at 291nm by UV–visible spectroscopy (UV 1800 Shimadzu, Japan). The mean value of three determinations was used to calculate the drug release from each formulation. For the comparison of dissolution data in dissolution media for each formulation, percentages of drug dissolved were calculated. (Online available at http://www.accessdata.fda.gov/scripts/cder/dissolution/dsp) Similarity factor (f2) and difference factor (f1) were calculated as per the following equations. (Online available at http://www.fda.gov/cder/guidance .htm)

$$f2 = 50 \times \mathrm{Log}\{[(\frac{1}{n})\sum_{t=1}^{n}(Rt - Tt)^2]^{-0.5} \times 100 \quad \text{...Eq. 4}$$

$$f1 = \{[\sum_{t=1}^{n}(Rt - Tt|\}/\sum_{t=1}^{n} Rt]\} \times 100 \quad \text{...Eq. 5}$$

Where,

n is the number of time points,

R is the dissolution value of the reference at time t and T is the dissolution value of the test at time t.

d) Dissolution efficiency study

The dissolution efficiency (DE) of a pharmaceutical dosage form is defined as the area under the dissolution curve up to a certain time-t, is expressed as a percentage of the area of the release assay of the reference formulation and rectangle described by 100% dissolution in the same line. (Costa P. et al (2001))

The % dissolution efficiency was calculated as follows:

$$DE\ \% = \frac{\int_{t1}^{t2} y.dt}{y100 + (t2 - t1)} \times 100 \quad \text{...Eq.6}$$

Where,

y = time duration

y_{100} = time for 100% release

t_2 = Final time duration

t_1 = Initial time duration

f) Accelerated stability study

The Stability studies were performed as per ICH Q1A (R2) guideline. Sample (optimized formulation batch) was packed in aluminium strips and stored in stability chamber (Neutronics, India) at 40˚C 2 temperature & 75% 5 RH. Samples were withdrawn at time intervals of 1, 3 and 6 months and evaluated for physical appearance, drug content, hardness, % friability and *in vitro* dissolution. (Das A. K. et al (2013)).

RESULTS AND DISCUSSIONS

Selection of Non volatile liquid vehicle

Saturation Solubility Study was carried out to select suitable liquid vehicle for liquisolid system. The results of solubility studies of selected non volatile liquid vehicles described that drug's maximum solubility was observed in PG as shown in fig.3. Further in solubility, blends of vehicles were selected as given in Table 1. It showed that the blend of PG and Capmul MCM30 had more solubility of drug. Furthermore, the various ratios of the selected blend were utilized for the solubility studies and resulted maximum solubility of drug in 50:50 ratio of PG: Capmul MCM30 as shown in Table 2.

Selection of Carrier

Different carriers were studied for their binding capacity and flowability. As per the results of binding capacity mentioned in table 3, Avicel PH112 required very less amount of liquid blend for binding so maximum binding capacity was in it with good flowability. So Avicel PH112 was selected as carrier and used for further studies.

Selection of Coating material (Adsorbent)

As per the data shown in table 4, Aerosil 200, Aerosil 300, Aeroperl 300 were used as coating materials. From the results of flow property parameter like angle of repose and Carr's index, it was concluded that Aerosil 300 had better flowability than others so it was selected and used for further study.

Method of preparation of LSC tablets

For preparation of LSC, all the ingredients were used in specific quantities as mentioned in table 5.

Evaluation of LSC batches

Pre compression studies of the LSC

In pre compression studies, flow property tests like Angle of repose and Carr's Index were carried out. Angle of repose (θ) was found 32° ± 0.5 and Carr's index (%) was found 11.06 ± 0.02. These results showed good flow properties of prepared blend for tablet preparation.

Post compression studies for the LSC

Conventional tablets of QTPF were prepared by direct compression technique using PG: Capmul MCM30 (50:50 ratio) as a blend of liquid vehicles,

Avicel PH112 as carrier, Aerosil 300 as a coating material, Kyron T314 as disintegrating agent, Magnesium stearate as a binder. Prepared tablets of above said formulation were subjected to various evaluation tests such as drug content, weight variation, tablet hardness, friability, disintegration time. All the formulated tablets showed acceptable pharmacotechnical properties as compendia requirements of tablet shown in Table.6.

XRD study

Fig.4 shows the X-ray diffractogram of the pure drug and LSC optimized formulation. QTPF pure drug shows sharp peaks (highest intense peaks at 20° and 22° at 2θ) as compared to LSC (in which less sharp peaks at peaks 20° and 22° at 2θ drug) That shows that drug is partially converted into amorphous or solubilized form. The modification of crystallinity of the drug in optimized formulation may be due to the result of solubilisation by liquid vehicle which was absorbed into carrier material and adsorbed into coating material. The amorphization or solublization of QTPF may increase the dissolution rate.

FTIR study

FTIR spectroscopy was used to study the structural changes and possible interactions between pure drug and optimized formulation (as shown in Fig.5). The FTIR spectrum of QTPF pure drug showed its characteristic IR absorption peaks at 3741, 2872, 2315, 1963, 1734, 833 and 652 cm^{-1}. The characteristic peaks for optimized formulation were found at 3742, 2871, 2314, 1962, 1726, 828 and 657 cm^{-1}.These spectra observations indicated that there is no interaction between drug and excipients.

***In vitro* drug release study**

The dissolution profiles of the LSC tablets and marketed tablets of QTPF are shown in Fig.6. The percentage cumulative drug release (CDR) at different time intervals (0, 10, 20, 30, 45, 60, 90min) were calculated and total % CDR calculated. From the dissolution profiles, it can be concluded that LSC optimized formulation improved drug dissolution as compared to reference product and pure drug. It may be due to significantly increased surface area of the drug particles available for dissolution and amorphization through LSC technique. As shown in Fig.7, LSC showed prompt drug release (16.34%) compared to pure drug (9.24%) and reference product (15.24%). Similarity factor (f2) and difference factor (f1) were found 53 and 13 respectively for optimized LSC formulation with comparison of marketed product. Results indicated good similarity between formulated and marketed product.

Dissolution efficiency study

Further in comparison, 100 %DE was calculated from the area under each dissolution curve at time " ", measured using the trapezoidal rule, and as shown in Table 7, 8. They were expressed as percentage of the area of rectangle described by 100% dissolution at the same time which were also calculated. Regarding percentage DE, there was 1.66 time increment in %DE of optimized batch compared to conventional tablets.

$$\%DE_{\text{Optimized batch}} = \frac{1500 \times 100}{90 \times 100} = 16.66\%$$

$$\%DE_{\text{Reference product}} = \frac{1500 \times 100}{150 \times 100} = 10\%$$

$$\%DE = \frac{\text{DE Optimized batch}}{\text{DE Reference product}} = \frac{16.66}{10} = 1.66 \text{ times}$$

Dissolution efficiency of optimized batch and marketed preparation were found to be 16.66% and 10% respectively. So, optimized batch was found to be 1.66 times higher than marketed preparation in term of DE.

Stability study

In 6 months stability study, the final prepared formulation showed good results in parameters like physical appearance, %drug content, hardness, %friability, *in vitro* drug release. All parameters were checked periodically and found to be similar to the initial results as shown in Fig.7 and Table 9. There was not observed any remarkable change in any observed parameters' values for the period of 6 months.

CONCLUSION

From this research work, it can be concluded that LSC technique is a promising alternative for the formulation of water insoluble drug QTPF. Higher dissolution rate of drug from the formulation may give better bioavailability due to solubilisation of drug. Improved disintegration time may also contributed to enhancement in dissolution of drug in the formulation. By this study, it was also summarized that LSC can give stable solid oral dosage form of QTPF having better dissolution, which may enhance the bioavailibilty of the drug used in the treatment of schizophrenia.

ACKNOWLEDGEMENT

Authors are very thankful to Ramanbhai Patel College of Pharmacy, Charotar University of Science and Technology and P. D. Patel Institute of Applied Sciences, Charotar University of Science and Technology for providing the instruments' facilities and Intas Pharmaceuticals Ltd., Ahmedabad for providing QTPF (pure drug) as gift sample.

REFERENCES

1. Aulton, M. E. (2013). Powder flow - Pharmaceutics. The design and manufacture of medicines, 4th edn. Edinburgh: Churchill Livingstone, 187-199.
2. Banakar UV. (1991) Pharmaceutical dissolution testing. Taylor & Francis.
3. Costa P., & Lobo, J. M. S. (2001) 'Modeling and comparison of dissolution profiles', *European journal of pharmaceutical sciences*, Vol.23, pp. 123-133.
4. Das A. K., Bhanja & Srilakshmi, N. (2013) 'Formulation and evaluation of quetiapine immediate release film coated tablets', *Asian Journal of Pharmaceutical Clinical Research, Vol. 6*, pp. 109-114.
5. Fahmy R. H. & Kassem, M. A. (2008) 'Enhancement of famotidine dissolution rate through liquisolid tablets formulation: *in vitro* and *in vivo* evaluation', *European Journal of Pharmaceutics and Biopharmaceutics*, Vol.*69*, Issue.3, pp. 993-1003.
6. Friedrich, H., Fussnegger, B., Kolter, K., & Bodmeier, R. (2006) 'Dissolution rate improvement of poorly water-soluble drugs obtained by adsorbing solutions of drugs in hydrophilic solvents onto high surface area carriers', *European journal of pharmaceutics and biopharmaceutics*, Vol.*62, Issue.* 2, pp. 171-177.
7. Gubbala LP, Arutla S, Venkateshwarlu V. (2014) 'Preparation And Solid State Characterization Of Nanocrystals For Solubility Enhancement Of QTPF', *International Journal of Pharmacy and Pharmaceutical Sciences*, Vol.6, Issue.7, pp. 358-364.
8. Gubbi S. R., & Jarag, R. (2010) 'Formulation and characterization of atorvastatin calcium LSC', *Asian Journal of Pharmaceutical Sciences*, Vol.*5*, Issue.2, pp. 50-60.
9. Kapsi, S. G., & Ayres, J. W. (2001) 'Processing factors in development of solid solution formulation of itraconazole for enhancement of drug dissolution and bioavailability', *International journal of pharmaceutics*, Vol.229, Issue.1, pp.193-203.
10. Kumar Nagabandi, V., Ramarao, T., & Jayaveera, K. N. (2011) 'LSC: a novel approach to enhance bioavailability of poorly soluble drugs', *International journal of pharmacy and biological sciences*, pp. 89-102.
11. Nokhodchi, A., Javadzadeh, Y., Siahi-Shadbad, M. R., & Barzegar-Jalali, M. (2005) 'The effect of type and concentration of vehicles on the dissolution rate of a poorly soluble drug (indomethacin) from LSC', *Journal of Pharmacy and Pharmaceutical Sciences*, Vol.8, Issue.1, pp. 18-25.
12. Potu, A. R., Pujari, N., Burra, S., & Veerareddy, P. R. (2012) 'Formulation and evaluation of buccoadhesive QTPF tablets', *Brazilian Journal of Pharmaceutical Sciences*, Vol.48, Issue.2, pp. 335-345.
13. Porter, C. J., & Charman, W. N. (2001) 'Intestinal lymphatic drug transport: an update', *Advanced drug delivery reviews*, Vol.50, Issue.1, pp. 61-80.
14. Sirisolla, J. (2015) 'Solubility Enhancement of Meloxicam By Liquisolid Technique And Its Characterization', *International Journal of Pharmaceutical Sciences and Research*, Vol.6, Issue.2, pp. 835.
15. Spireas, S., & Bolton, S. M. (1999) *U.S. Patent No. 5,968,550*. Washington, DC: U.S. Patent and Trademark Office.
16. Spireas, S., Sadu, S., & Grover, R. (1998) 'In vitro release evaluation of hydrocortisone liquisolid tablets', *Journal of pharmaceutical sciences*, Vol.*87, Issue.*7, pp. 867-872.
17. Spiridon Spireas (1998) US6423339B1: Liquisolid systems and methods of preparing same.
18. ST Prajapati, HH Bulchandani, DM Patel, SK Dumaniya, CN Patel (2013) 'Formulation and evaluation of LSC for olmesartan medoxomil', *Journal of drug delivery*, August.
19. Vraníková B., Gajdziok, J., & Vetchý, D. (2015) 'Modern evaluation of liquisolid systems with varying amounts of liquid phase prepared using two different methods', *International Journal of BioMedical research.*
20. Website - FDA Guidance document available at http://www.accessdata.fda.gov/scripts/cder/dissolution/dsp (Accessed on: 4th May, 2018).
21. Website - FDA Guidance document available at http://www.fda.gov/cder/guidance.htm (Guidance for Industry - Dissolution Testing of Immediate Release Solid Oral Dosage Forms) (Accessed on: 4th May, 2018)
22. Wong, S. M., Kellaway, I. W., & Murdan, S. (2006) 'Enhancement of the dissolution rate and oral absorption of a poorly water soluble drug by formation of surfactant-containing microparticles', *International journal of pharmaceutics*, Vol.317, Issue.1, pp. 61-68.

Table.1 Solubility study of liquid vehicles' blend (n=3, mean ± S.D.)

Sr. No.	Liquid Vehicle Blend (50:50)		Solubility (mg/ml)
	I	II	
1	PG	PEG400	55.00 ± 0.47
2	PG	Capmul MCM30	59.00 ± 1.54
3	PG	PEG600	35.00 ± 5.14
4	PG	Capryol-90	12.00 ± 1.56
5	PG	Lauroglycol	38.00 ± 2.92

Table.2 Solubility study of liquid vehicles' blend ratio (n=3, mean ± S.D.)

Sr. No.	Ratio of Liquid Vehicle Blend (PG : Capmul MCM30)	Solubility(mg/ml)
1	50:50	59.00 ± 3.45
2	60:40	39.00 ± 4.64
3	70:30	28.00 ± 5.12
4	80:20	32.00 ± 2.84
5	90:10	37.00 ± 3.42

Table 3: Binding capacity of carriers

Batch No.	Carrier	Binding capacity* (ml/g)	Angle of repose (θ)	Remarks from Angle of repose	Carr's Index	Remarks from Carr's Index
1	Avicel PH101	4.54	39.25	Fair	13.24	Good
2	Avicel PH102	2.72	38.12	Fair	11.16	Good
3	Avicel PH112	5.95	38.24	fair	14.62	Good
4	LM	3.16	40.16	Fair	15.64	Good
5	DCP	2.77	41.82	Passable	17.04	Fair

*ml of liquid^/g of Carrier
[^PG : Capmul MCM30 (50:50)]

Table 4: Selection of Coating material

Batch No.	Coating material	Angle of repose (θ)	Remarks from Angle of repose	Carr's Index (%)	Remarks from Carr's Index
1	Aerosil 200	34.26°	Good	16.69	Fair
2	Aerosil 300	32.04°	Good	13.11	Excellent
3	Aeroperl 300	35.16°	Fair	17.12	Fair

Table 5: Composition of final optimized batch

Functionality of Ingredient	Name of the Ingredient	Weight per tablet
Drug	Quetiapine Fumarate	28.5mg
Liquid Vehicle	PG: Capmul MCM30 (50:50)	0.7ml
Carrier	Avicel PH112	390mg
Coating Material	Aerosil 300	40mg
Disintegrant	Kyron T 314	3%
Binder	Magnesium Stearate	2%
Glidant and Lubricant	Talc	1%

Table 6: Evaluation tests of final batch of LSC Tablet

Sr. No.	Post compression Parameter	Result (n=3, mean ± S.D.)	Remark
1	%Drug content	100% ± 1.05	Passed
2	%Weight variation	<7.5%	Passed
3	Hardness (kg/cm^2)	3.5 ± 0.26	Passed
4	%Friability	0.214 ± 0.03	Passed
5	Disintegration time (min)	2.36	Passed

Table 7: Cumulative dy*dt of Optimized batch for DE

Time (min)	% Release of drug (Y %)	Cumulative dy*dt
0	0	0
15	16.34	245.1
30	32.54	488.1
45	62.58	938.7
60	89.33	1339.95
75	94.56	1418.4
90	100	1500

Table 8: Cumulative dy*dt of Reference Product for DE

Time (min)	% Release of drug (Y %)	Cumulative dy*dt
0	0	0
15	15.24	228.6
30	27.46	411.9
45	58.16	872.4
60	76.32	1144.8
75	82.36	1235.4
90	88.12	1321.8
105	91.28	1369.2
120	96.34	1445.1
135	98.36	1475.4
150	100	1500

Table: 9 Stability study of final batch for 6 months (n=3, mean ± S.D.)

Duration	Physical appearance	% Drug content	Hardness	%Friability
0 Month	Off white and fair	100.00 ± 0.04	3.5 ± 0.26	0.214 ± 0.03
1 Month	Off white and fair	100.00 ± 0.05	3.5 ± 0.30	0.223 ± 0.25
3 Months	Off white and fair	100.00 ± 0.18	3.3 ± 0.36	0.216 ± 0.34
6 Months	Off white and fair	100.00 ±0.23	3.4 ± 0.25	0.232 ± 0.28

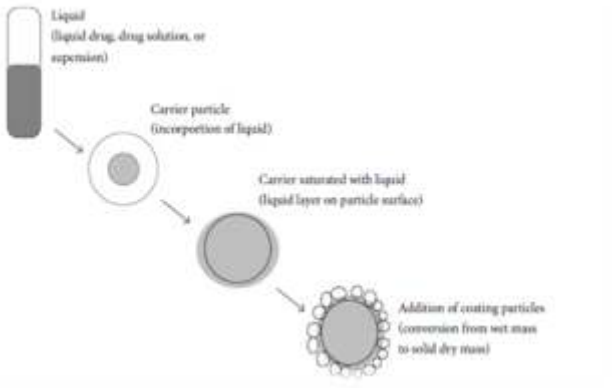

Fig.1: Concept of LSC' composition. (Spireas S et al. (1998))

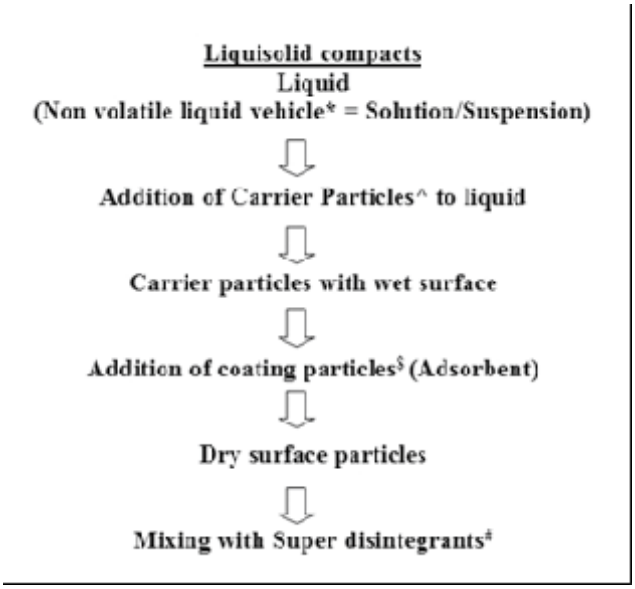

***Non volatile liquid vehicle:** PEG400, PEG600, PG, Glycerine, Tween 80, Labrafil, Capryol-90, Lauroglycol, Capmul MCM30.

^Carrier particles: Avicel PH101, Avicel PH102, Avicel PH112, LM, DCP

$Coating material: Aerosil 200, Aerosil 300, Aeroperl 300

#Superdisintegrants: Kyron T 314

Fig.2 Method of preparation for LSC

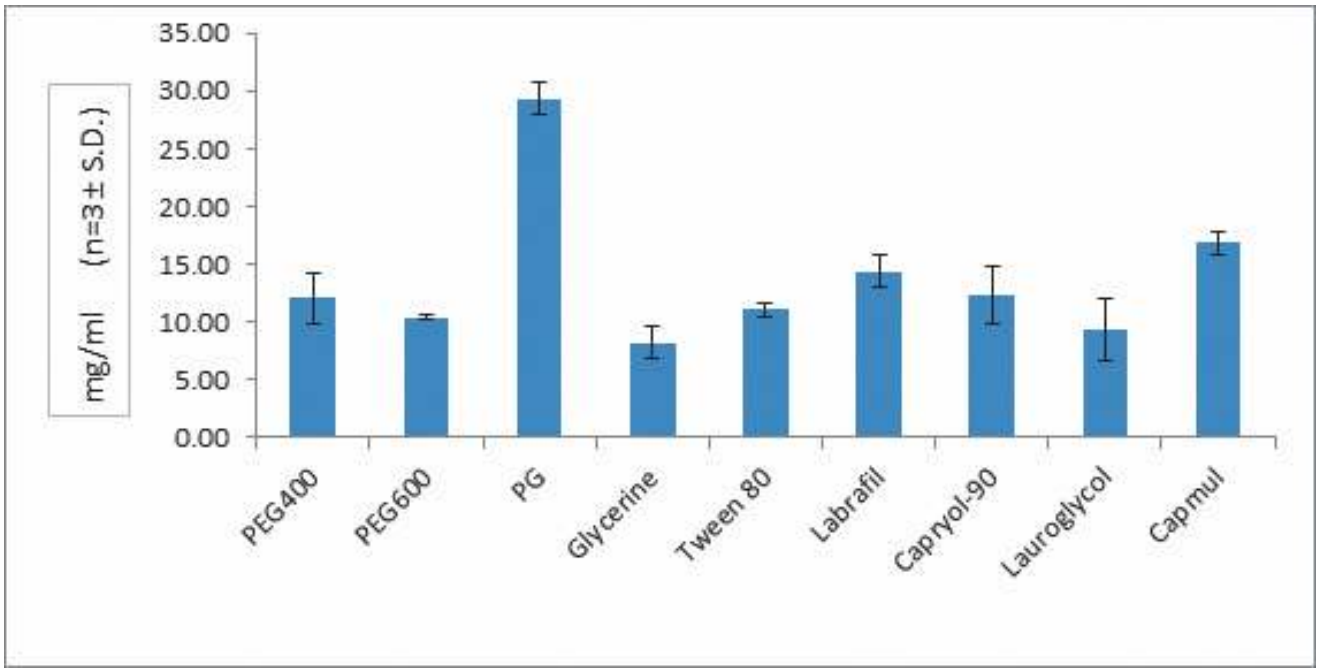

Fig.3: Solubility of liquid vehicles in QTPF (n=3, Mean ± S.D.)

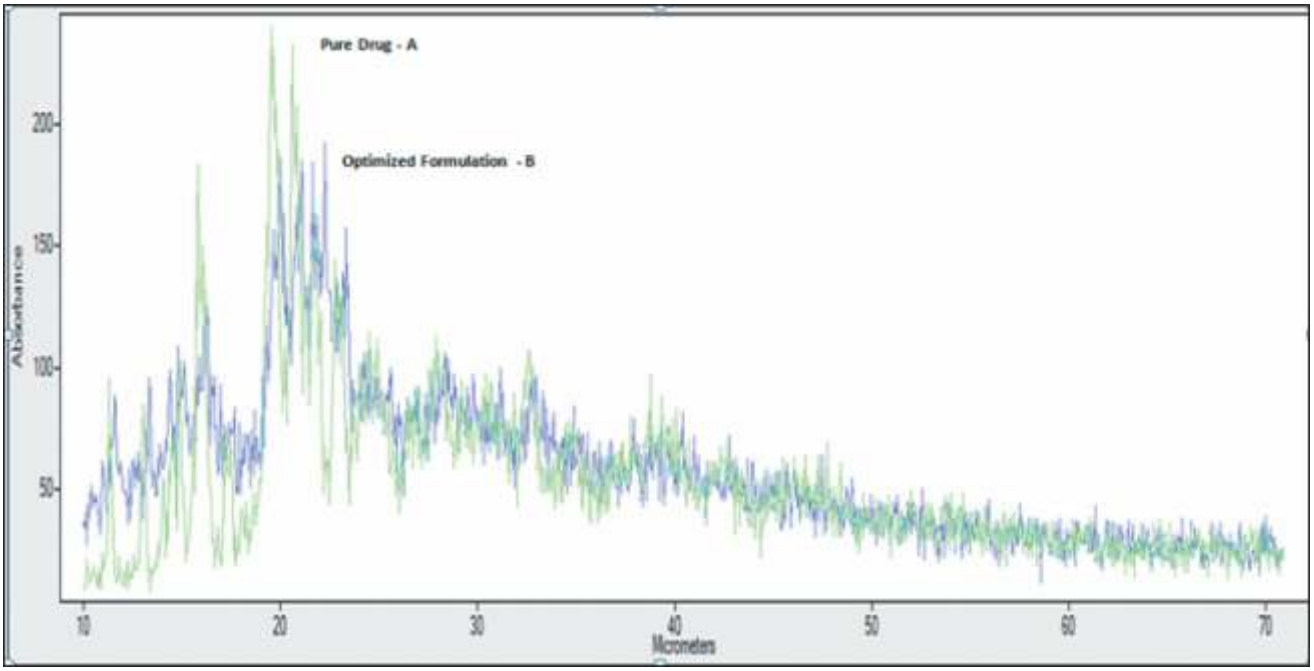

Fig.4 XRD of pure drug (A) and Optimized formulation (B)

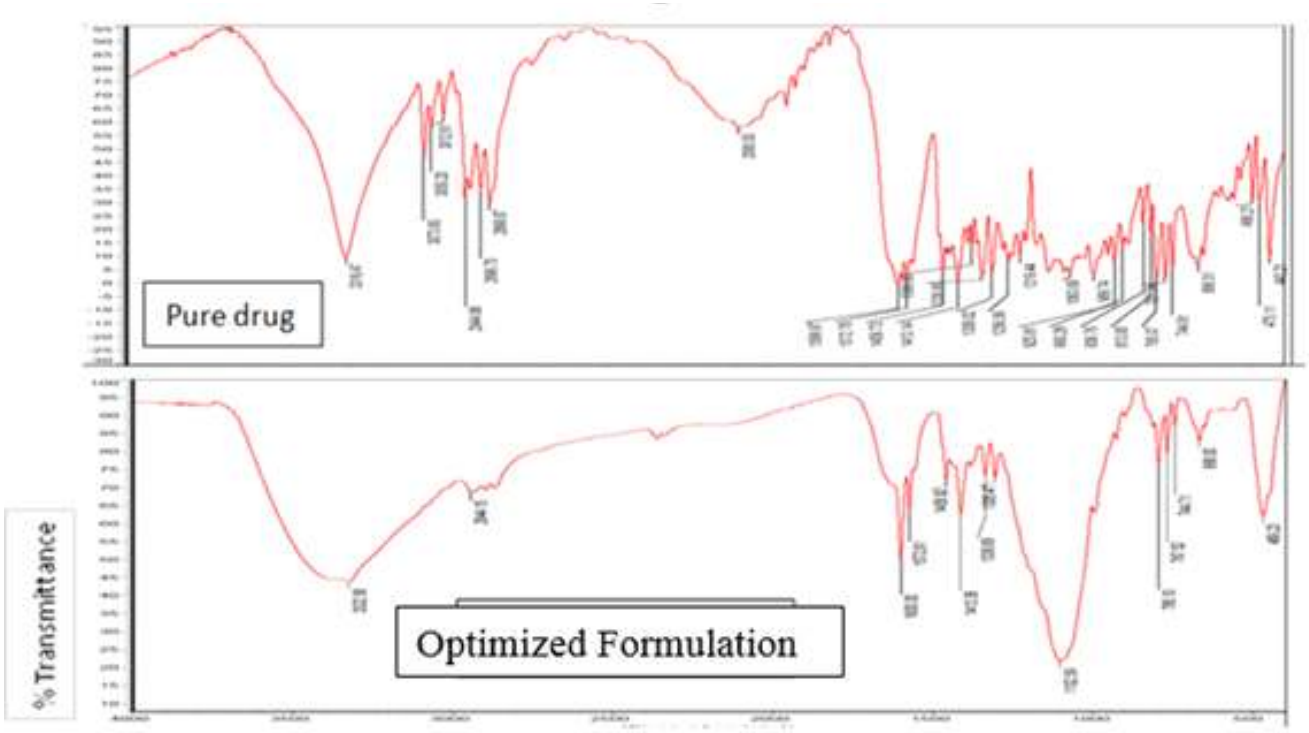

Fig.5: FTIR study comparison of Pure Drug (QTPF) and Optimized formulation

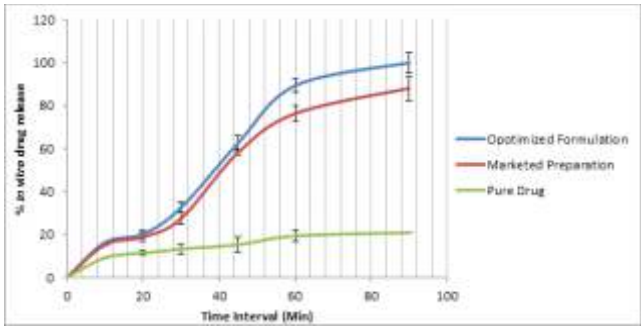

Fig.6 % In vitro drug release of pure drug, optimized formulation and Marketed preparation (n=3 ± S.D.)

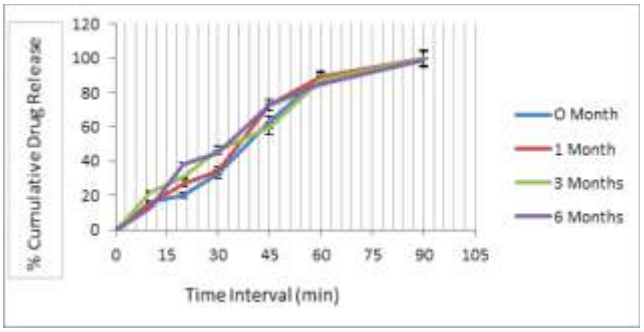

Fig.7 Drug dissolution of stability batches for 3months (n=3 ± S.D.)

Research Article

Comparative study of dry, wet and monolithic precast beam-column connections under progressive collapse mechanism

Parth Senjalia[1]*, V. R. Panchal[1], Dhaval D. Patel[1]

[1]Civil Engineering Department, CSPIT, CHARUSAT, Anand, India

Received: 17/06/2017
Revised: 07/02/2018
Accepted: 18/06/2018

Correspondence to:
*Parth Senjalia:
parth.senjalia@gmail.com

Abstract:

In any RCC & steel structures, connection plays a vital role, as they transfer forces from one element to another. The main objective of this study is to investigate the analytical behavior of precast beam-column connections under progressive collapse scenario. This paper comprises of one precast wet connection, one precast dry connection and one monolithic specimen. Reduced 1/3rd scaled precast beam-column connections were used for the analysis using ABAQUS software. Results are obtained in terms of load carrying capacity and vertical deflection. It is observed from the results that load carrying capacity of dry connection is higher than wet connection and monolithic connection.

Keywords: Finite Element Analysis, Abaqus, Monolithic Connection, Precast Wet Connection, Precast Dry Connection.

INTRODUCTION

The Finite Element Method (FEM) is a numerical method to obtain solutions of boundary value problems which consists of partial differential equations. FEM is also helpful in engineering and mathematical physics to solve complicated problems including complicated geometries, loadings and material properties. ABAQUS is one of the most broadly used FEA tool, used in structural, mechanical and aerospace engineering industries. ABAQUS is absolute software which provides simple and consistent interface for analysis and is also known for its quality, performance and ability to solve problems through numerical replication. Both linear and non-linear analysis can be performed using ABAQUS [1].

In Present Study, three 1/3rd scale specimens, consisting of two end columns, two beams and one middle removal column are used for analysis which is proposed from G+5 storey building [2]. All the connections are modeled using ABAQUS software. A C3D4, 4-Node tetrahedron type of element is used for concrete and T3D2, 2-Node 3D Truss element is used for reinforcement. Loading is applied in the form of displacement at the top of the middle column and analysis is carried out. Results are validated with Experimental results in terms of displacement and load carrying capacity.

FINITE ELEMENT ANALYSIS

Finite Element method is used to study non-linear behavior of beam-column connection and analysis is performed in ABAQUS/Standard.

Material Properties and Geometry

1. Concrete

Concrete is widely used material in construction industries. Concrete is made up of different ingredients like aggregates, cement, construction chemicals etc. so the property of concrete is varying in nature. Generally, concrete is strong in compression and weak in tension. Concrete part is defined as solid, homogeneous material for analysis. Solid concrete part

is discretized into small 3-D element. The modulus of elasticity is 27286 MPa and poison's ratio is 0.2. Both properties are assigned in linear properties. Concrete Damage Plasticity is used to define the non-linearity in concrete.

2. Steel

Reinforcement bar and stirrups are defined as truss element in analysis. Reinforcement bars are assumed as embedded element in concrete and also assumed as linearly elastic material. T3D2, 2 node linear 3-D Truss in space element is used in ABAQUS. The modulus of elasticity is 200 GPa and poison's ratio is 0.3.

Monolithic Connection

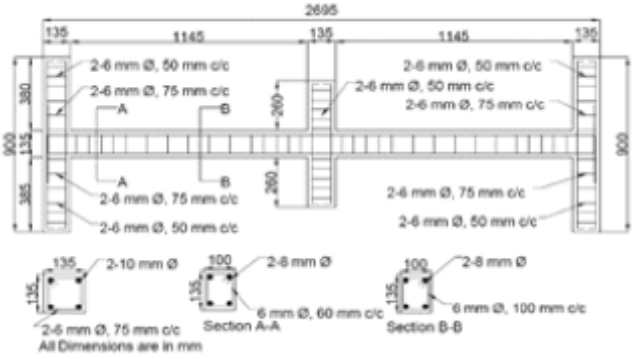

Figure 1 Detailing of Monolithic Connection

Figure 2 Experimental Test Setup for Monolithic Specimen

The reinforcement detailing of 1/3rd scale model is shown in Figure 1 and experimental test setup is shown in Figure 2 [2]. For the modeling of concrete section C3D4-linear Tetrahedron element is used and for reinforcement T3D2-Truss element is used. Embedded option from the Interaction module in ABAQUS is used for the interaction between steel and concrete. Model of monolithic connection and reinforcement cage is carried out in ABAQUS as shown in Figure 3.

Figure 3 Modeling of concrete section and Reinforcement

To Simulate Actual boundary condition of experimental work, both the end columns are pinned at top and load is applied in the form of displacement i.e. 0.2 mm at the bottom of the end columns. 100 mm displacement is given at the top surface of the middle column as shown in Figure 4.

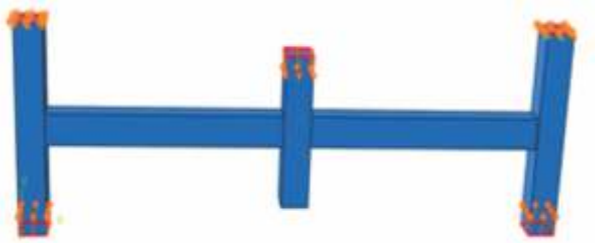

Figure 4 Loading and Boundary Condition for Monolithic Connection

Meshing of model

For meshing of monolithic connection, C3D8 Hexahedral element is used for concrete section and T3D2 Truss element is used for stirrups and steel bars. Figure 5 shows the details of meshing of monolithic frame.

Precast Wet Connection

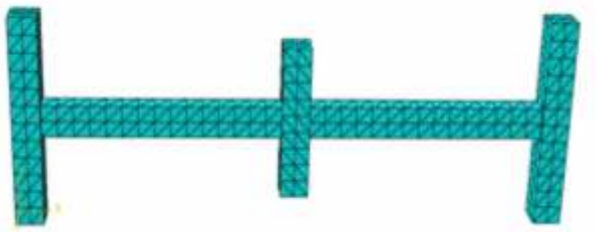

Figure 5 Hexahedral Meshing of Concrete Section

The reinforcement detailing of 1/3rd scale precast wet connection is shown in Figure 6.

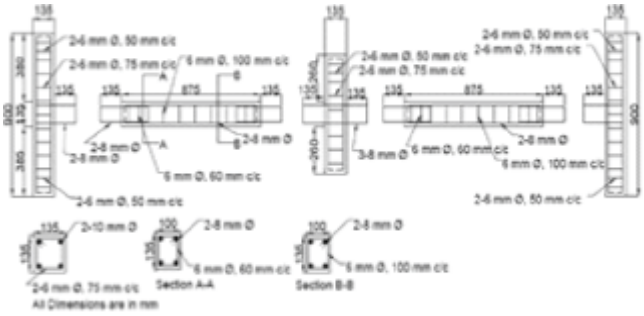

Figure 6 Reinforcement Detailing of Precast Wet Connection

Figure 7 Experimental Test Setup for Precast Wet Connection

Figure 7 shows the experimental test setup for precast wet connection [2]. The connection detailing of precast wet connection is shown in Figure 8. Model of precast wet connection and reinforcement cage is carried out in ABAQUS as shown in Figure 9.

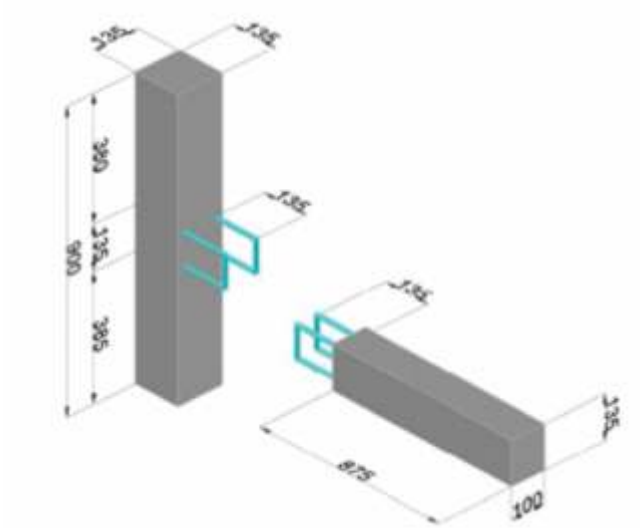

Figure 8 Connection Detailing of Precast Wet Connection

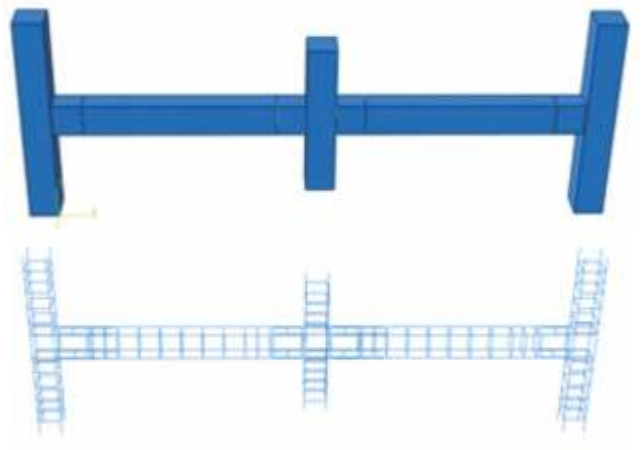

Figure 9 Modeling of Precast Wet connection and Reinforcement

Boundary conditions are applied according to experimental work as both the end columns are pinned at top and load is applied in the form of displacement i.e. 0.2 mm at the bottom of the end columns. 100 mm displacement is given at the top surface of the middle column as shown in Figure 10.

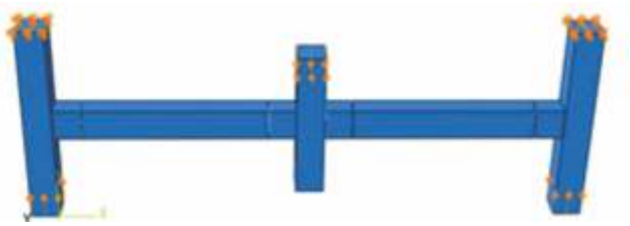

Figure 10 Loading and Boundary Condition for Precast Wet Connection

Meshing of model

Meshing used in precast wet connection is similar to that used in monolithic connection. Meshing of precast wet connection is shown in Figure 11.

Figure 11 Meshing of Precast Wet Connection

Precast Dry Connection

The reinforcement detailing of 1/3rd scale precast dry connection is shown in Figure 12.

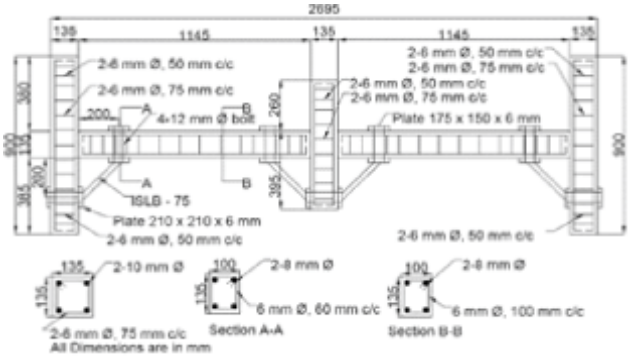

Figure 12 Reinforcement Detailing of Precast Dry Connection

Figure 13 Experimental test setup for Precast Dry Connection

Figure 13 shows the experimental test setup for precast dry connection [2]. The connection detailing of precast dry connection is shown in Figure 14. Model of precast dry connection and reinforcement cage is carried out in ABAQUS as shown in Figure 15.

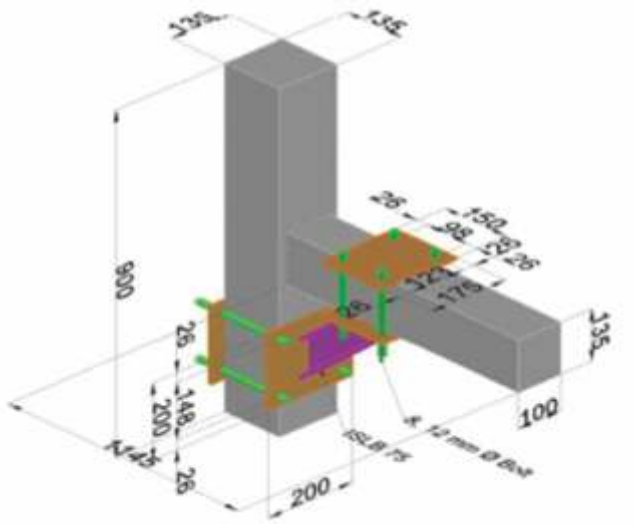

Figure 14 Connection Detailing of Precast Dry Connection

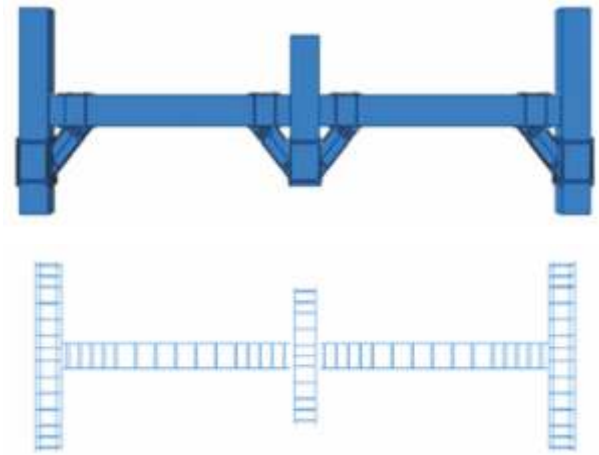

Figure 15 Modeling of Precast Dry Connection and Reinforcement

Boundary conditions are applied according to experimental work as both the end columns are pinned at top and load is applied in the form of displacement i.e. 0.2 mm at the bottom of the end columns. 100 mm displacement is given at the top surface of the middle column as shown in Figure 16.

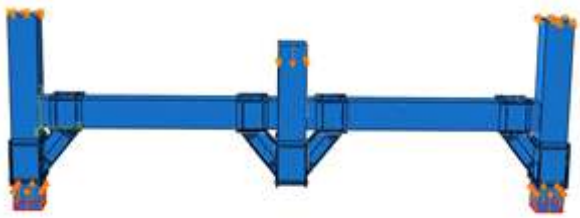

Figure 16 Loading and Boundary Conditions for Precast Dry Connection

Meshing of model

Meshing used in precast dry connection is similar to that used in monolithic connection. Meshing of precast dry connection is shown in Figure 17.

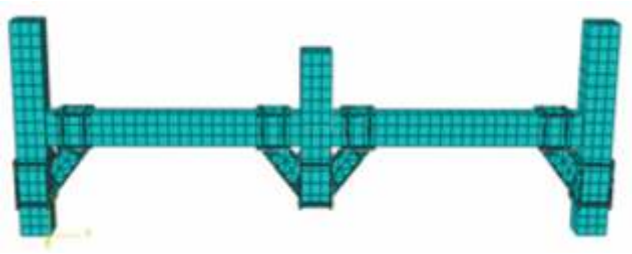

Figure 17 Meshing of Precast Dry Connection

RESULTS AND DISCUSSION

Non-Linear Analysis is performed and results are carried out in terms of Load-Deflection for all the connections. Load is carried out from the reaction of columns and deflection is measured from bottom surface of the middle column. Figure 18, Figure 20 and Figure 22 shows the analysis result of monolithic connection, precast wet connection and precast dry connection respectively. Figure 19, Figure 21 and Figure 23 shows the load v/s deflection curves of monolithic connection, precast wet connection and precast dry connection respectively. Table 1, Table 3 and Table 5 shows the final values of load and deflection of FEM results and Experimental result of monolithic connection, precast wet connection and precast dry connection respectively. Table 2, Table 4 and Table 6 shows percentage difference in results of monolithic connection, precast wet connection and precast dry connection respectively.

Result Comparison

In this section, results of monolithic connection, precast wet connection and precast dry connection are compared in terms of load deflection behavior and the curve shows quite similar results for both monolithic connection and precast wet connection but load carrying capacity and deflection of precast dry connection is higher than both monolithic connection and precast wet connection as shown in Figure 24.

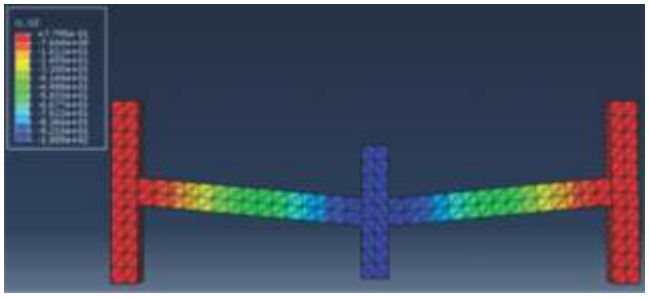

Figure 18 Analysis Result of Monolithic Connection

Table 1 Result Comparison of Monolithic Connection

Monolithic Connection			
EXPERIMENTAL		ANALYTICAL	
Load (kN)	Deflection (mm)	Load (kN)	Deflection (mm)
0	0	0	0
2	4.5	2	3.48
4	10.2	4	10.35
6	13.2	6	13.74
8	18.7	8	18.19
10	24.5	10	25.17
12	28.4	12	29.02
15	37.5	14	37.97
16	55.5	16	56.18
17	68.1	17.6	68.9
16	99.4	18	100.46

Table 2 Percentage Difference in Result of Monolithic Connection

	EXP	FEM	Difference
Load (kN)	17	18	5.88%
Deflection (mm)	99.4	100.46	1.06%

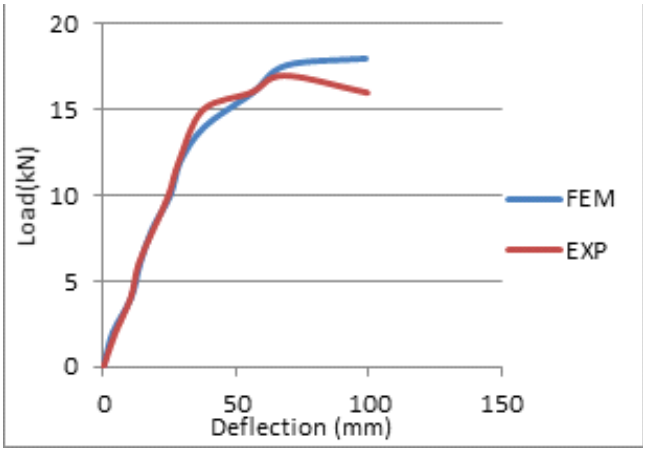

Figure 19 Load v/s Deflection of Monolithic Connection

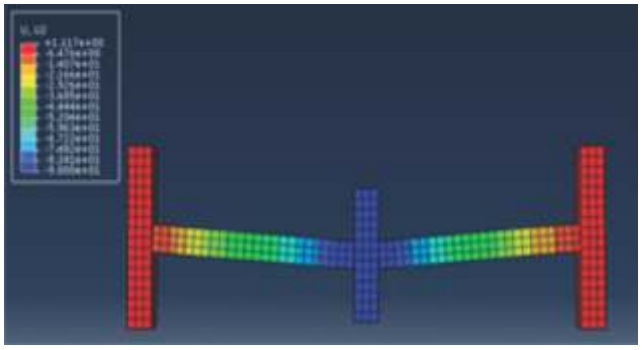

Figure 20 Analysis Result of Precast Wet Connection

Table 3 Result Comparison of Precast Wet Connection

Precast Wet Connection			
EXPERIMENTAL		ANALYTICAL	
Load (kN)	Deflection (mm)	Load (kN)	Deflection (mm)
0	0	0	0
2	1.02	0.77	1.125
4	3.16	4.08	3.23
6	6.4	7.85	6.55
8	10.5	9.04	10.71
10	14.1	10.58	13.56
12	18.9	12.66	18.52
14	22.7	14.39	22.99
13.5	87.7	17.884	89.99

Table 4 Percentage Difference in Result of Precast Wet Connection

	EXP	FEM	Difference
Load(kN)	14	17.8	27.14%
Deflection(mm)	87.7	89.99	2.61%

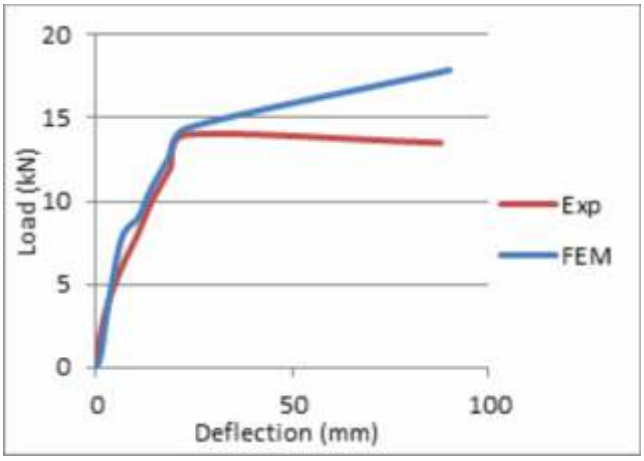

Figure 21 Load v/s Deflection of Precast Wet Connection

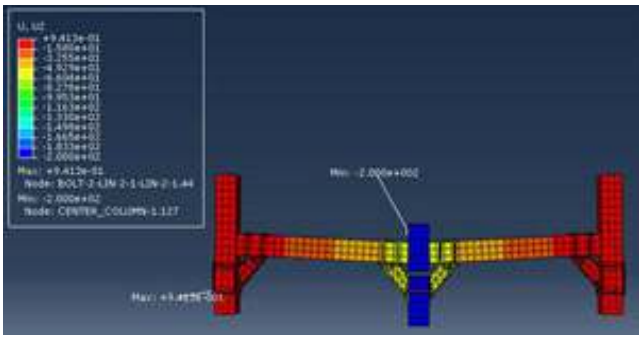

Figure 22 Analysis Result of Precast Dry Connection

Table 5 Result comparison of Precast Dry Connection

Precast Dry Connection			
EXPERIMENTAL		ANALYTICAL	
Load(kN)	Deflection (mm)	Load (kN)	Deflection (mm)
0	0	0	0
3	6.2	3.64	6.39
4	12.3	4.79	13.9
5	16.5	6.37	20.66
6	21.4	8.73	23.19
7	30	12.07	32.69
8	39.9	13.23	30.73
9	47.8	17.9	47.24
10	52.7	18.36	52.6
11	55.9	19.62	55.5
12	66.9	20.89	67.73
13	81.2	24.28	82.37
14	96.4	24.67	95.55
15	111.7	24	115.33
14.2	221.7	22.2	200

Table 6 Percentage Difference in Result of Precast Dry Connection

	EXP	FEM	Difference
Load(kN)	15	24	37.5%
Deflection(mm)	221.7	200	9.79%

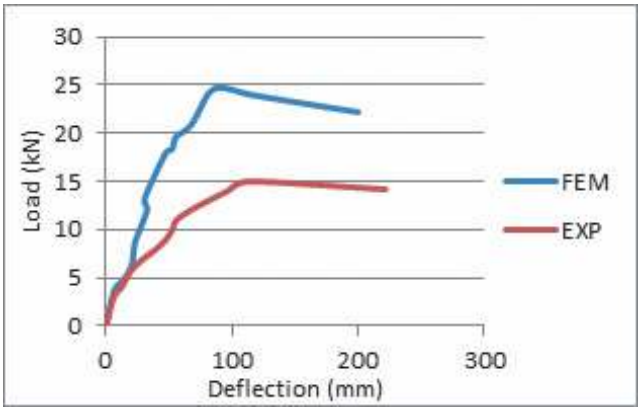

Figure 23 Load v/s Deflection of Precast Dry Connection

- Experimental results and analytical results are compared in terms of load and displacement at the bottom of middle column.
- The ultimate load carrying capacity of monolithic connection is 17 kN experimentally and 18 kN based on FE Analysis. So, the difference is 5.88%. Deflection of middle column from experimental result is 99.4 mm and 100.46 mm from FE Analysis. So, the difference is 1.06%.
- The ultimate load carrying capacity of precast wet connection is 14 kN experimentally and 17.8 kN based on FE Analysis. So, the difference is 27.14%. Deflection of middle column from experimental result is 87.7 mm and 89.99 mm from FE Analysis. So, the difference is 2.61%.
- The ultimate load carrying capacity of precast dry connection is 15 kN experimentally and 24 kN based on FE Analysis. So, the difference is 37.5%. Deflection of middle column from experimental result is 221.7 mm and 200 mm from FE Analysis. So, the difference is 9.79%.
- It is observed from FEM results that load carrying capacity and deflection of monolithic connection is faintly more than that of precast wet connection.
- It is observed from FEM results that load carrying capacity and deflection of precast dry connection is higher than that of monolithic connection and precast wet connection.

REFERENCES

1. Taher Nalawala (2016), "Nonlinear Finite Element Analysis of R.C. Beam-Column Joints". M.Tech Thesis, Nirma University.
2. Patel Dhaval (2015), "Behavior of Precast beam column connection under Progressive Collapse Scenario". M.Tech Thesis, Nirma University.
3. Magliulo, Ercolino, Cimmino, Capozzi, Man (2014) "FEM analysis of the strength of RC beams to column dowel connections under monotonic actions" *Journal of Construction and Building Material*, Vol. 69, pp 271-284.
4. Davari, Ramezani (2012) "FE Analysis of Precast concrete connections under incremental load" *Australian Journal of Basic and Applied science* Vol. 6, pp 341-350
5. T Obaidat, S Heyden (2010) "The effect of CFRP and CFRP/concrete interface models when modeling retrofitted RC beams with FEM" *Division of structural mechanics*, Vol. 92, pp 1391-1398.
6. Vaghei, Farzad, Hafez and Ali. (2014) "Evaluate Performance of Precast Concrete wall to wall Connection." *Journal of APCBEE Procedia*, Vol. 9, pp 285-290.
7. Chaudhari S.V., Chakrabarti M.A. (2012) "Modeling of concrete for nonlinear analysis Using Finite Element Code ABAQUS" *International Journal of Computer Applications*, Vol.44, pp 0975 – 8887.

Research Article

Effect of Parameter Variations on Sensorless Control of BLDC Motor Using Disturbance Torque Estimation

Mitesh B. Astik[1], Praghnesh Bhatt[2]*, Bhavesh R. Bhalja[3]

[1]Department of Electrical Engineering, A. D. Patel Institute of Technology, New Vallabh Vidyanagar, India
[2]Department of Electrical Engineering, C. S. Patel Institute of Technology, CHARUSAT, Changa, India
[3]Department of Electrical Engineering, Indian Institute of Technology, Roorkee, India

Received: 12/04/2017
Revised: 10/07/2018
Accepted: 27/04/2018

Correspondence to:
*Praghnesh Bhatt:
pragneshbhatt.ee@charusat.ac.in

Abstract:

The performance of a Brushless DC (BLDC) motor drive can be affected by disturbance torque which acts on the shaft of the motor. Hence, the information of the disturbance torque is important and necessary. The disturbance torque is estimated using disturbance torque observer. This disturbance estimated torque is the sum of proportional and the time integral of the estimation error of current. The speed of BLDC motor is estimated from the knowledge of estimated disturbance torque. A new controller scheme based on Modified Hybrid Fuzzy PI (MHFPI) controller is proposed to control the speed of BLDC motor. Simulations have been carried out for different disturbances such as step changes in the reference speed and load torque of the motor. Transient and steady state accuracy are determined in nominal conditions and the effects of motor parameters variations are analyzed. Comparison of the proposed scheme with the existing schemes clearly depicts that the effect of disturbance on actual and estimated responses are very less.

Keywords: : BLDC Motor, Disturbance Torque Estimation, MHFPI Controller, Observer Design, Sensorless Control.

INTRODUCTION

In an actual system, some external factors always exist which affect the system behavior. Disturbance torque acting on the motor shaft is one of the external factor which affect the behavior of the BLDC motor drive. Hence, the knowledge of the disturbance torque is important and necessary. But the disturbance torque cannot easily measured and hence, estimation is required. The estimation of disturbance torque has been proposed for DC motor, BLDC motor, PMSM motor and servo motor drive (Buja et. al. (1995); Park et. al. (2003); Akrad et. al. (2010); Chen and Cheng (2012)) respectively. Park et. al. (2003) proposed the load torque observer in which q-axis current of BLDC motor has been considered as compensating current. Rodriguez and Emadi (2006) have suggested digital control technique for BLDC motor drive using the speed and torque observation from the state observer. Bernat and Stepien (2011) have proposed LQR and feedback linearization method to design the optimal current driver.

Ghassemi and Vaez-Zade (2005) proposed a method for Direct Torque Control (DTC) of PM motors. The rotor position estimation error decreases the starting torque; consequently, it increases the time needed for start-up, especially in the DTC of PM Motors. So it is important that the rotor position estimation error be minimized. Asaei and Rostami (2008) presented an estimation method based on the stator current variations due to the saturation of the stator core. The error in estimated rotor position is around 6° during starting. Stirban et. al. (2012) proposed position and speed observer for sensorless control of PM BLDC motor from the estimation of line-to-line values of PM flux linkage. In this method, the speed error is very high and estimated rotor position error is around 3-4 electrical degree. Terzic and Jadric (2001) proposed an estimation method based on extended kalman filter for estimation of speed and rotor position of a BLDC motor. This method has very

large estimated rotor position error for below rated speed of the motor. Rostami and Asaei (2009) proposed a method for the estimation of initial rotor position for PM motors based on saturation effect. This method has the maximum estimated rotor position error is ±3.75°.

Nowadays, the Proportional Integral (PI) controller has been commonly used but they are not suitable for non-linear and particularly complex systems those have no exact mathematical models. Fuzzy logic is a controller which does not need a precise mathematical model of the system. Hence it can be used in place of PI controller. Shanmugasundram et. al. (2014) proposed design and implementation of the fuzzy controller to control the speed of BLDC motor in which the comparison between fuzzy and PID controller has been discussed. Arulmozhiyal (2012) proposed design and implementation of the fuzzy controller for BLDC motor using FPGA. In recent years, the hybrid fuzzy logic controller was proposed for induction motor, permanent magnet synchronous motor and BLDC Motor drive (Rubaai et. al. (2001); Zerikat and Chekroun (2007); Sant and Rajagopal (2009)) respectively.

In this paper, the disturbance torque is continuously estimated using classical observer. For accurate estimation of disturbance torque, two schemes are used in this paper i.e. disturbance torque as an unidentified input and as a state variable. The estimated disturbance torque is considered as the sum of proportional and time integral of the estimation error of current. This estimated disturbance torque is useful to estimate the speed of BLDC motor. The estimated rotor position is found from the estimated speed of the motor. Modified Hybrid Fuzzy PI (MHFPI) controller is used to control the speed of the motor. From the simulation results; the maximum estimated rotor position error observed in this paper is less than 1 electrical degree for nominal parameter and maximum 6 electrical degrees when 10% variations are applied to motor parameters.

MODELING OF BLDC MOTOR

The equation of the three phase voltages of BLDC motor can be expressed as Eq. (1) (Lee and Ahn (2009); Xia (2012)).

$$\begin{bmatrix} V_a \\ V_b \\ V_c \end{bmatrix} = \begin{bmatrix} R & 0 & 0 \\ 0 & R & 0 \\ 0 & 0 & R \end{bmatrix} \begin{bmatrix} i_a \\ i_b \\ i_c \end{bmatrix} + \begin{bmatrix} L & 0 & 0 \\ 0 & L & 0 \\ 0 & 0 & L \end{bmatrix} \frac{d}{dt} \begin{bmatrix} i_a \\ i_b \\ i_c \end{bmatrix} + \begin{bmatrix} e_a \\ e_b \\ e_c \end{bmatrix} \quad (1)$$

Where, V_a, V_b and V_c are stator phase voltages, i_a, i_b and i_c are the stator phase currents, R and L are the stator resistance and inductance per phase respectively, e_a, e_b and e_c are the back EMFs of each phase.

The relationship between motor speed (w) and back EMF (*e*) can be represented as shown in Eq. (2) (Park et. al. (2012).

$$\omega = \frac{e}{K_T} \quad (2)$$

Hence, Eq. (1) can be rewritten as shown in Eq. (3)

$$\begin{bmatrix} V_a \\ V_b \\ V_c \end{bmatrix} = \begin{bmatrix} R & 0 & 0 \\ 0 & R & 0 \\ 0 & 0 & R \end{bmatrix} \begin{bmatrix} i_a \\ i_b \\ i_c \end{bmatrix} + \begin{bmatrix} L & 0 & 0 \\ 0 & L & 0 \\ 0 & 0 & L \end{bmatrix} \frac{d}{dt} \begin{bmatrix} i_a \\ i_b \\ i_c \end{bmatrix} + K_T \begin{bmatrix} \omega_a \\ \omega_b \\ \omega_c \end{bmatrix} \quad (3)$$

The Mechanical equation of BLDC motor can be represented as Eq. (4).

$$T_e = J\frac{d\omega}{dt} + B\omega + T_L \quad (4)$$

Where, T_e is the electromagnetic torque, B and J are viscous friction coefficient and moment of inertia respectively and T_L is the load torque.

The relationship between torque and current is given by

$$T_e = K_T i \quad (5)$$

The line-to-line electrical and mechanical equations can be expressed by Eqs. (6) and (7) respectively

$$v_z = Ri_z + L\frac{di_z}{dt} + K_T\omega_z \quad (6)$$

$$K_T i_z = J\frac{d\omega_z}{dt} + B\omega_z + T_L \quad (7)$$

Where z is Line-to-line quantities of BLDC motor. The equations of brushless dc motor in terms of disturbance are given by

$$\dot{i}_z = -\frac{R}{L}i_z - \frac{K_T}{L}\omega_z + \frac{1}{L}v_z - \frac{1}{L}v_{dz} \quad (8)$$

Where,

$$v_{dz} = \Delta R i_z + \Delta L\dot{i}_z + \Delta K_T\omega_z \quad (10)$$

$$T_{dz} = T_L + \Delta J\dot{\omega}_z + \Delta B\omega_z - \Delta K_T i_z \quad (11)$$

Where, Δ is for the parameter variations, *dzv* and *dzT* are Line-to-line disturbance voltage and disturbance torque respectively. By rearranging the mechanical equation of the BLDC motor in Eq. (9), the disturbance torque can be written as

$$T_{dz} = K_T i_z - B\omega_z - J\dot{\omega}_z \tag{12}$$

This scheme requires a speed sensor which presents several disadvantages like an increase in machine size, reduction in reliability and more value of noise. In order to eliminate the speed sensor, the sensorless control method is proposed.

ESTIMATION OF SPEED AND DISTURBANCE TORQUE

In a sensorless BLDC motor drive, only currents and voltages can be measured. In this paper, the disturbance torque is estimated from the estimation error of current. For accurate estimation of disturbance torque, following two schemes are discussed in this section.

Disturbance Torque as an Unidentified input

The state variable model of the BLDC motor can be represented by

$$\begin{aligned} \dot{x} &= Ax + Bu + ET_{dz} \\ y &= cx \end{aligned} \tag{13}$$

Since the system expressed by Eq. (13) is completely observable; the full-order state observer can be designed by Eq. (14).

$$\dot{\hat{x}} = A\hat{x} + Bu + Kc\left(x - \hat{x}\right) \tag{14}$$

Where,

$$A = \begin{bmatrix} -\frac{R}{L} & -\frac{K_T}{L} \\ \frac{K_T}{J} & -\frac{B}{J} \end{bmatrix},\ B = \begin{bmatrix} \frac{1}{L} \\ 0 \end{bmatrix},\ c = \begin{bmatrix} 1 & 0 \end{bmatrix},\ E = \begin{bmatrix} 0 \\ \frac{1}{J} \end{bmatrix} \tag{15}$$

$$u = v_z,\ K = \begin{bmatrix} k_1 \\ k_2 \end{bmatrix},\ \left(x - \hat{x}\right) = \begin{bmatrix} e_{iz} \\ e_{wz} \end{bmatrix} = \begin{bmatrix} i_z - \hat{i}_z \\ \omega_z - \hat{\omega}_z \end{bmatrix}$$

Where K is the observer gain matrix. *ize* and *ze*ware the Line-to-line estimation error of current and speed respectively. From Eqs. (13-15)

$$\begin{bmatrix} \dot{e}_{iz} \\ \dot{e}_{wz} \end{bmatrix} = \begin{bmatrix} \dot{i}_z - \dot{\hat{i}}_z \\ \dot{\omega}_z - \dot{\hat{\omega}}_z \end{bmatrix} = \begin{bmatrix} -\left(\frac{R}{L} + k_1\right) & -\frac{K_T}{L} \\ \left(\frac{K_T}{J} - k_2\right) & -\frac{B}{J} \end{bmatrix} \begin{bmatrix} i_z - \hat{i}_z \\ \omega_z - \hat{\omega}_z \end{bmatrix} + \begin{bmatrix} 0 \\ \frac{1}{J} \end{bmatrix} T_{dz} \tag{16}$$

The estimation error of current tends to constant and hence the time derivative of estimation error i.e. 0=*ize*& for a nearly constant disturbance torque. Thus, estimation error of speed can be expressed in terms of estimation error of current and is given by Eq. (17).

$$e_{wz} = -\left(\frac{R + k_1 L}{K_T}\right) e_{iz} \tag{17}$$

To estimate the disturbance torque, consider the time derivative of speed error of Eq. (16) is to be zero and replace the value of speed error from Eq. (17) into Eq. (16). Thus the estimated disturbance torque can be represented by

$$\hat{T}_{dz} = \left[\left(K_T - k_2 J\right) + \left(\frac{B}{K_T}\right)\left(R + k_1 L\right)\right] e_{iz} \tag{18}$$

Assuming the viscous friction coefficient (B) is very less. Hence, Eq. (18) becomes

$$\hat{T}_{dz} = \left(K_T - k_2 J\right) e_{iz} \tag{19}$$

Disturbance Torque as a state variable

The state variable model of BLDC motor with disturbance torque as a state variable can be represented in Eq. (20).

$$\dot{x}_a = A_a x_a + B_a u \tag{20}$$

$$y_a = c_a x_a \tag{21}$$

As the pair *aA* and *ac* is observable, the motor states can be estimated by

$$\dot{\hat{x}}_a = A_a \hat{x}_a + B_a u + K_a c_a \left(x_a - \hat{x}_a\right) \tag{22}$$

where,

$$K_a = \begin{vmatrix} k_1 \\ k_2 \\ k_3 \end{vmatrix} \tag{23}$$

From Eqs. (22) and (23), the state of the motor can be estimated in the simplified form and can be written as

$$\begin{bmatrix} \dot{i}_z \\ \dot{\omega}_z \\ \dot{T}_{dz} \end{bmatrix} = \begin{bmatrix} -\frac{R}{L} & -\frac{K_T}{L} & 0 \\ \frac{K_T}{J} & -\frac{B}{J} & -\frac{1}{J} \\ 0 & 0 & 0 \end{bmatrix} \begin{bmatrix} \hat{i}_z \\ \hat{\omega}_z \\ \hat{T}_{dz} \end{bmatrix} + \begin{bmatrix} \frac{1}{L} \\ 0 \\ 0 \end{bmatrix} v_z + \begin{vmatrix} k_1 \\ k_2 \\ k_3 \end{vmatrix} \begin{bmatrix} 1 & 0 & 0 \end{bmatrix} \begin{bmatrix} i_z - \hat{i}_z \\ \omega_z - \hat{\omega}_z \\ T_{dz} - \hat{T}_{dz} \end{bmatrix} \tag{24}$$

From Eq. (24), the estimated disturbance torque can be represented by

$$\hat{T}_{dz} = k_3 \int e_{iz} dt \tag{25}$$

From Eqs. (19) and (25), the total estimated disturbance torque can be expressed as

$$\hat{T}_{dz} = (K_T - k_2 J) e_{iz} + k_3 \int e_{iz} dt \tag{26}$$

From Eq. (26), the disturbance estimated torque is the sum of proportional and the time integral of the estimation error of current.

The resultant disturbance estimated torque is given by

$$\hat{T}_d = \frac{\hat{T}_{d\,ab} + \hat{T}_{d\,bc} + \hat{T}_{d\,ca}}{3} \tag{27}$$

Fig. 1 shows the block diagram of disturbance torque and speed estimation of BLDC motor.

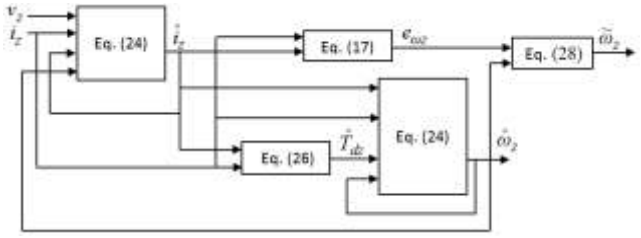

Fig. 1 Block diagram of speed and disturbance torque estimation

Actual speed of the motor (*z*w~) is found out by addition of speed delivered by the observer (*z*wˆ) and estimation error of speed (*ze*w) and can be represented as Eq. (28)

$$\tilde{w}_z = \hat{w}_z + e_{wz} \tag{28}$$

The final estimated speed of BLDC motor ()*m*wˆ is found by considering the absolute and maximum value of all the three line-to-line actual speed of the motor as shown in Fig. 2.

The disturbance current which is obtained from the disturbance torque estimation can be expressed by Eq. (29)

$$i_d = \frac{\hat{T}_d}{K_T} \tag{29}$$

The reference current *is** for the hysteresis current controller can be expressed as Eq. (30) which is the addition of the current *ci* from the MHFPI controller and disturbance current *id*.

$$i_s^* = i_c + i_d \tag{30}$$

Fig. 2 shows the overall block diagram of the proposed sensorless BLDC motor drive. The line-to-line voltage is calculated using DC-link voltage and commutation signals. The speed and disturbance torque are estimated from the observer as mentioned in this section. The estimated position of the rotor is found from the estimated speed of the motor. The estimated speed is fed to the error detector which finds the difference between the estimated and desired value of the speed. The output of the error detector is fed to the modified hybrid fuzzy PI speed controller which decides the current set value depending upon the gain values of the controller. The torque reference divided by the torque constant K_T would give current I_c. The reference current I_s^* for the hysteresis current controller is expressed from Eq. (30). The gate signals for inverter are generated using commutation signals and comparing the actual and reference current using the hysteresis current controller. These gate signals decide exact voltage to be applied across the BLDC motor. The gain of the hysteresis band controller using in this paper is 0.01 for better current control. For a better disturbance torque and speed estimation, the values of the observer gains 1*k*, 2*k* and 3*k*set in this paper are 5076, -192757 and 1688669 respectively. Ackerman's method is used to calculate the observer gains which is mentioned in Mandal (2006).

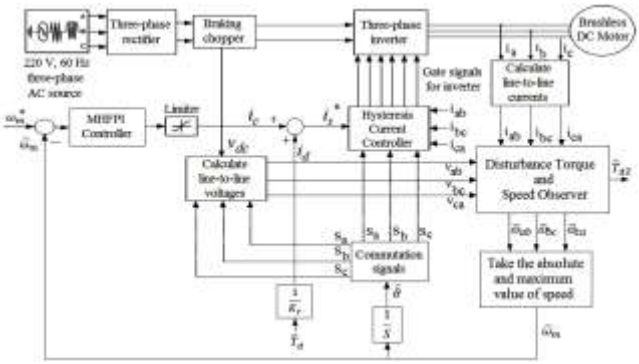

Fig. 2 Overall block Diagram of the proposed sensorless BLDC motor drive

MODIFIED HYBRID FUZZY PI CONTROLLER

The fuzzy logic controller has two inputs i.e. the error and change of error which are defined by

$$w_e(n) = w_m^*(n) - \hat{w}_m(n) \tag{31}$$

$$\Delta w_e(n) = w_e(n) - w_e(n-1) \tag{32}$$

Where, $w_m(n)^*$ and $w_m(n)$ are the reference speed and estimated speed of the motor respectively. $w_e(n)$ & $\Delta w_e(n)$ are the error and change of error in speed respectively. Indexes n and (n-1) indicate the present and the previous state respectively. $\Delta u(n)$ is output f fuzzy controller. Membership function of the FLC

input $we(n)$ is normalized between [-15, 15], $\Delta we(n)$ is normalized between [-1e^6, 1e^6] and the output $\Delta u(n)$ is normalized between [-25, 25]. The linguistic labels used to describe the fuzzy sets were "Negative Big" (NB), "Negative Medium" (NM), "Negative Small" (NS), "Zero" (Z), "Positive Small" (PS), "Positive Medium" (PM) and "Positive Big" (PB). The rule base structure used in this paper is Mamdani type. The set of decision rules used in this paper is shown in Table 1.

Table 1.Table of fuzzy rules

$\Delta we(n)$ / $we(n)$	NB	NM	NS	Z	PS	PM	PB
NB	NB	NB	NB	NB	NM	NS	Z
NM	NB	NB	NB	NM	NS	Z	PS
NS	NB	NB	NM	NS	Z	PS	PM
Z	NB	NM	NS	Z	PS	PM	PB
PS	NM	NS	Z	PS	PM	PB	PB
PM	NS	Z	PS	PM	PB	PB	PB
PB	Z	PS	PM	PB	PB	PB	PB

Parallel Fuzzy PI (PFPI) controller is the addition of PI and fuzzy controller. The combination of PI and PFPI controller are used as an MHFPI controller. The objective of this controller is to produce the better response than the conventional controllers. Two switching functions for the MHFPI controller have been considered. An approach for the switching control of this controller is such that for most of the time PI controller is activated and use of the PFPI controller only when the system behavior is oscillatory or tends to overshoot. The selection between the PI and PFPI controller is based on the following condition:

If the error signal $we(n)$ is strictly greater than zero and its previous value $we(n-1)$ was strictly less than or equal to zero, the PI controller will work. If the previous value of error signal is strictly greater than zero, PFPI controller will work.

$$U_{MHFPI} = \begin{cases} U_{PI}, \text{ for } w_e(n-1) \le 0 \ \& \ w_e(n) > 0 \\ U_{PFPI}, \text{ for } w_e(n-1) > 0 \ \& \ \text{all } w_e(n) \end{cases} \quad (33)$$

SIMULATION RESULTS AND DISCUSSIONS

The parameters of BLDC motor used in MATLAB/Simulink environment are given in Table 2.

Various simulations have been performed on BLDC motor to validate the effect of MHFPI controller and disturbance torque observer on its dynamic performance. The effect of variations in rotor reference speed and load torque along with the parameter variations have been evaluated in the proposed work.

Table 2. BLDC motor parameters

Parameters	Ratings
Stator resistance (R)	0.2 (Ω)
Stator inductance (L)	8.5 (mH)
Rotor inertia (J)	0.089 (kg-m^2)
Friction (B)	0.005 (Nm-s)
Number of poles (P)	4
Rated speed (ω_s)	300 (rpm)
Torque Constant (k_T)	1.4 (Nm/A_peak)
Flux linkage established by magnets (λ_p)	0.175 (volt-s)
Motor Output Power	3 HP

The following cases are considered for the validation of the proposed method.

Step Changes in Reference Speed Keeping Load Torque Zero

The variations in current, speed, torque, speed difference between actual and estimated speed, rotor position and difference in rotor position are shown in Fig. 3 for the step changes in speed from 0 rpm to 50 rpm at t=0 s, 50 rpm to 300 rpm at t= 0.15 s and 300 rpm to 50 rpm at t=0.5 s. From Fig. 3(a), it is observed that only two winding currents are conducted at any time and third winding current is zero. The variations in actual and estimated speed can be observed in Fig. 3(b), which indicate that the actual and estimated speed always keep tracking for every step changes in rotor reference speed. From Fig. 3(c), it can be seen that the actual torque successfully tracks the reference torque at all instants even during the step changes in the rotor reference speed. The maximum speed difference between actual and estimated speed is observed from Fig. 3(d) is 5 rpm during starting and 1 rpm during steady state. From Fig. 3(e) and 3(f), it is observed that the actual rotor position successfully tracks the estimated rotor position and the maximum difference between the two rotor positions is around 0.07 electrical degree.

The variations in moment of inertia and stator resistance are applied in BLDC motor along with the step changes in reference speed. The effect of these variations are observed in terms of speed difference

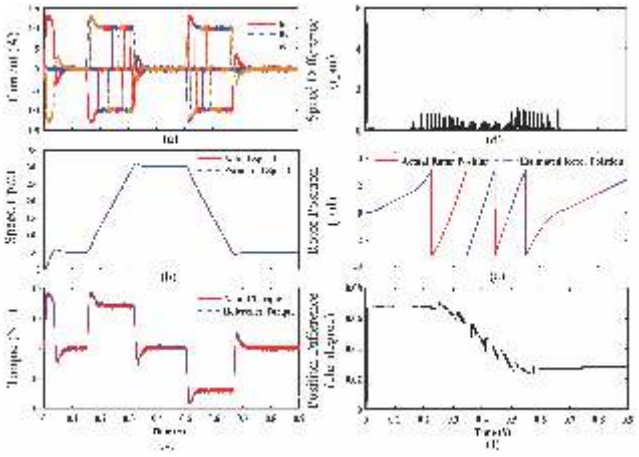

Fig. 3 Dynamic responses of stator current, speed, torque, speed difference, rotor position and position difference for the step changes in reference speed keeping load torque (T_L) = 0 Nm

and rotor position difference as shown in Fig. 4 and 5 respectively. It can be seen from Fig. 4(a) and 5(a) that the effect of variation in J on speed difference and position difference are almost same as they were obtained in Fig. 3(d) and 3(f) respectively. From Fig. 4(b), it can be observed that the maximum speed difference during starting is 5 rpm and transient and steady state speed difference are around 3 rpm and 1

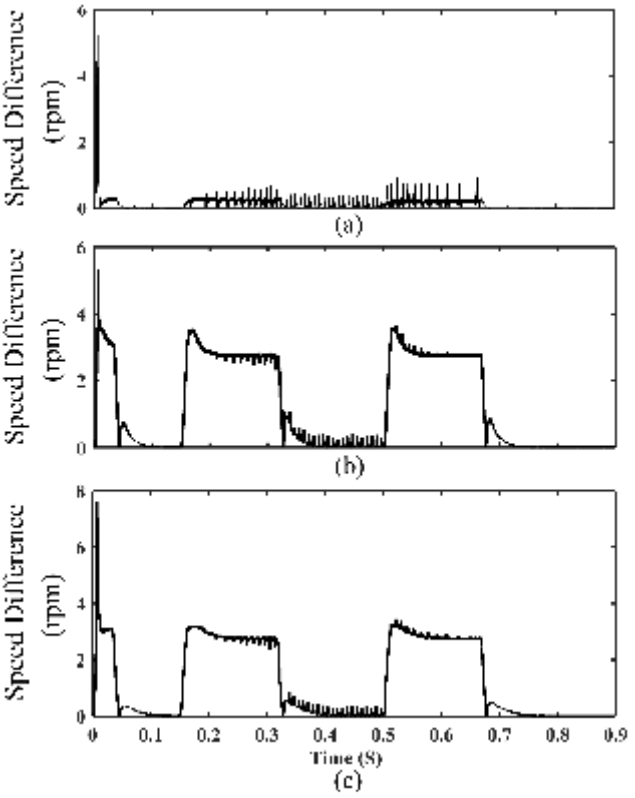

Fig. 4 Speed difference for the variations in (a) J= +10% (b) R= +10% and (c) R= +10% and J= +10% for the step changes in reference speed

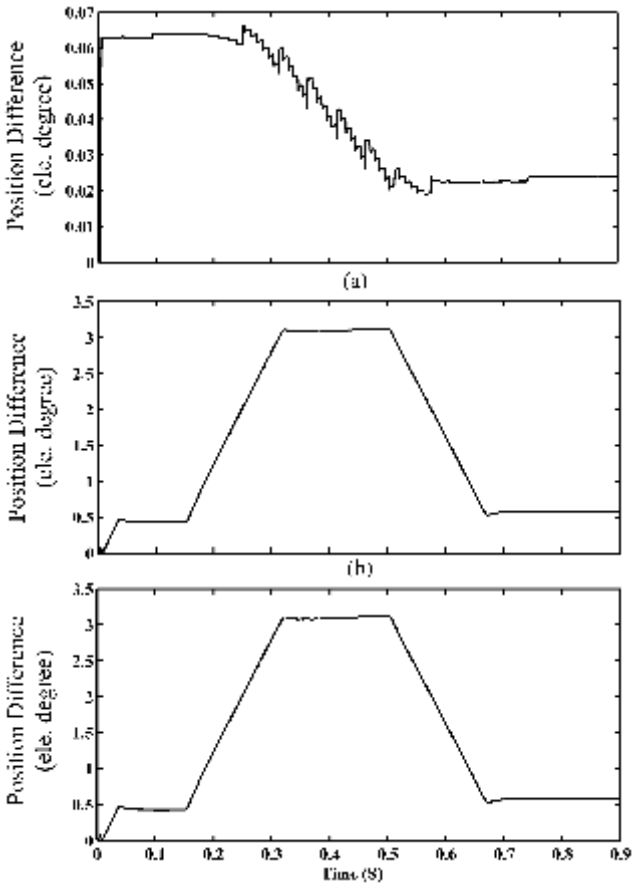

Fig. 5 Position Difference for the variations in (a) J= +10% (b) R= +10% and (c) R= +10% and J= +10% for the step changes in reference speed

rpm respectively when +10% variation is applied in stator resistance. It can be seen from Fig. 4(c) that the starting speed difference is increased when the variations are applied in R and J by +10% each. The steady state response is almost same as it was obtained in Fig. 4(b). From Fig. 5 (b), it can be observed that the maximum position difference is around 3 electrical degrees for +10% variation is applied in resistance. The same response is observed in Fig. 5(c) when the variation applied in R and J by +10% each.

Step Changes in Load Torque at Reference Speed

The variations in current, speed, torque, speed difference between actual and estimated speed, rotor position and difference in rotor position are shown in Fig. 6 for the step changes in load torque at constant reference speed. As shown in Fig. 6, the BLDC motor starts at 0 s and gradually attains 300 rpm within 0.2 s and remains 300 rpm up to 0.3 s. With the change in load torque from steady state torque to 10 Nm at 0.3 s, an increase in stator currents is observed as shown in Fig. 6(a). At 0.5 s, the load torque is set to -10 Nm with the associated changes in stator currents. The similar responses are found for the further change in load

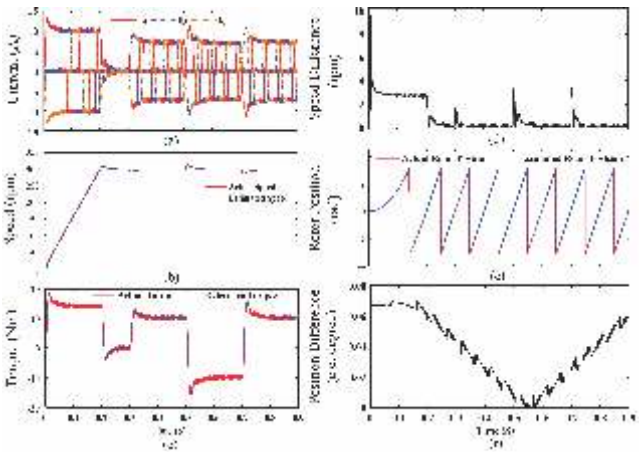

Fig. 6 Dynamic responses of current, speed, torque, speed difference, rotor position and position difference for the step changes in load torque (TL) keeping reference speed at 300 rpm

torque at 0.7 s. The momentary change in rotor speed can be seen from the Fig. 6(b) with the change in load torque. The actual torque successfully tracks the reference torque at all instants even during the step changes in the load torque which can be observed from Fig. 6(c). It can be seen from Fig. 6(d) that starting speed difference is around 9 rpm. Maximum steady state speed difference can be observed around 4 rpm when

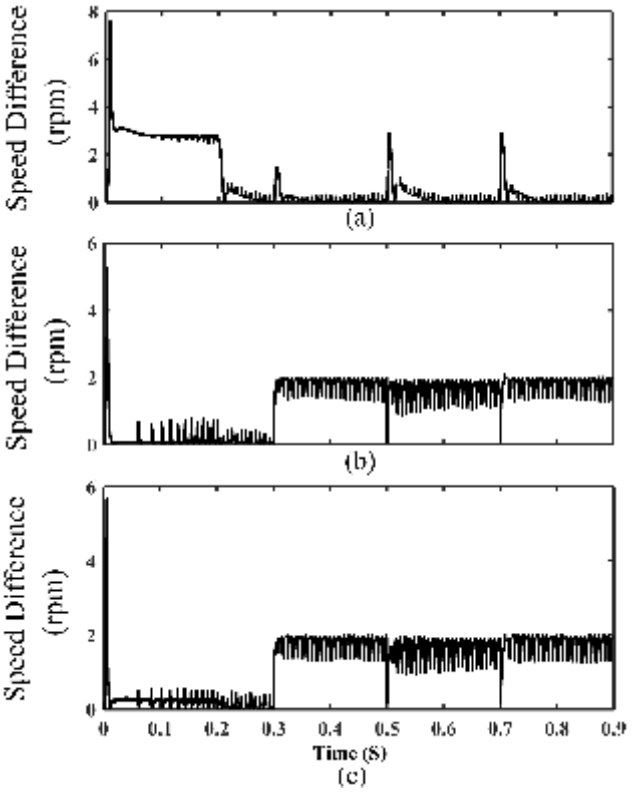

Fig. 7 Speed difference for the variations in (a) J= +10% (b) R= +10% and (c) R= +10% and J= +10% for the step changes in load torque

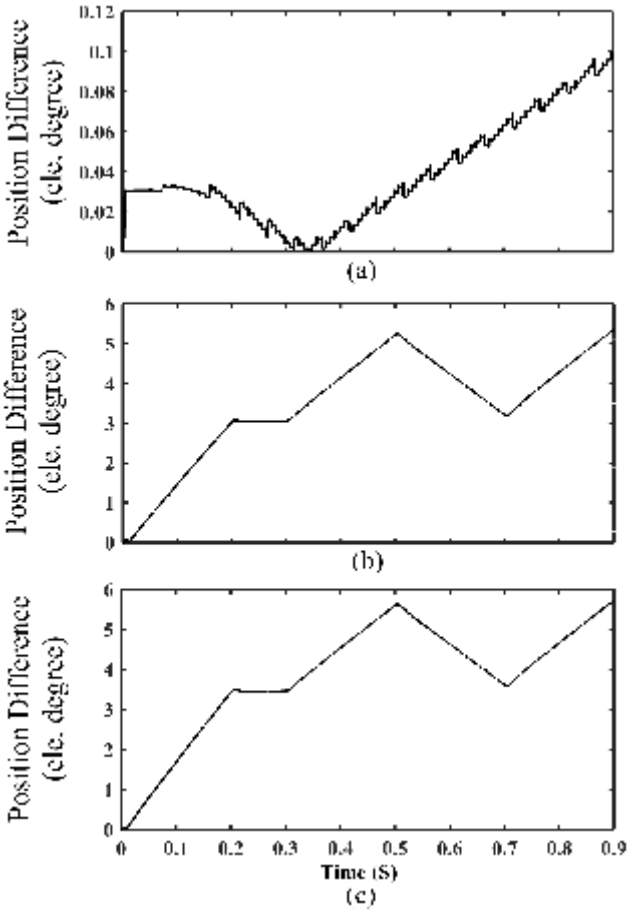

Fig. 8 Position Difference for the variations in (a) J= +10% (b) R= +10% and (c) R= +10% and J= +10% for the step changes in load torque

the step changes is applied to load and this difference is reduced below 1 rpm in steady state. From Fig. 6(e) and 6(f), it is observed that the actual rotor position successfully tracks the estimated rotor position and the maximum difference between the two rotor positions is around 0.07 electrical degree.

The variations in moment of inertia and stator resistance are applied in BLDC motor along with the step changes in load torque. The effect of these variations are observed in terms of speed difference and rotor position difference as shown in Fig. 7 and 8 respectively.

It can be seen from Fig. 7(a) and 8(a) that the effect of variation in J on speed difference and position difference are almost same as they were obtained in Fig. 6(d) and 6(f) respectively. From Fig. 7(b) and 7(c), it can be seen that the speed difference is around 6 rpm during starting and oscillations are increased but the speed difference is only 2 rpm during running conditions. From Fig. 8(b) and 8(c), it can be observed that the maximum position difference is 6 electrical degrees even variations are applied in R and J by +10% each.

Comparative evaluation of the proposed scheme with the existing schemes

Comparative evaluation of the proposed scheme has been carried out with the existing schemes (Terzic and Jadric (2001); Asaei and Rostami (2008); Stirban et. al. (2012) and Rostami and Asaei (2009)) in terms of estimated rotor position error.

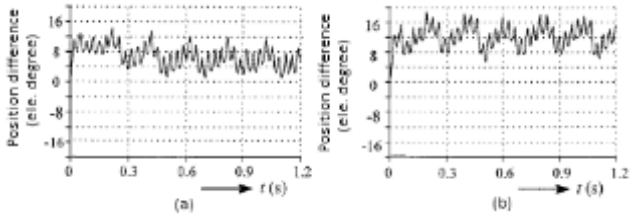

Fig. 9 Position Difference of the existing scheme (Terzic and Jadric) when motor runs at 100 rpm with load torque (a) 0.8 Nm and (b) 4 Nm

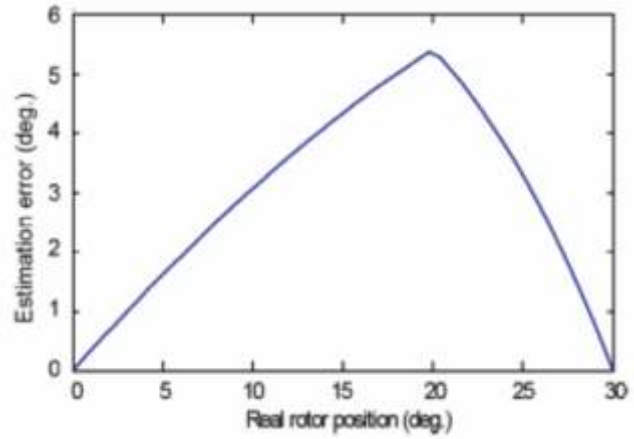

Fig. 10 The estimation error versus real rotor position of the existing scheme (Asaei & Rostami)

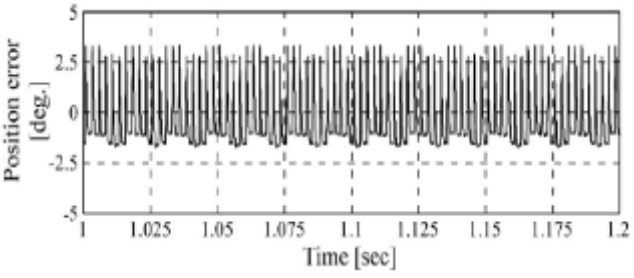

Fig. 11 Position error of the existing scheme (Stirban et. al.)

Table 3. Actual and estimated rotor position w.r.t. current space vector of the proposed scheme (Rostami and Asaei)

If	The rotor position	Estimated rotor position (°)
$i_\beta(30°) > i_\alpha(45°)$	$30° < \theta_r < 37.5°$	33.75
$i_\alpha(45°) > i_\alpha(30°)$ and $i_\alpha(30°) > i_\alpha(60°)$	$37° < \theta_r < 45°$	41.25
$i_\beta(45°) > i_\alpha(60°)$ and $i_\beta(60°) > i_\alpha(30°)$	$45° < \theta_r < 52.5°$	48.75
$i_\alpha(60°) > i_\alpha(45°)$	$52.5° < \theta_r < 60°$	56.25

It has been observed from Fig. 9 to 11 and Table 3 that the maximum estimated rotor position error is 12-16, 5.5, 3-4 & ±4.25 electrical degree, respectively. These errors may be increased if the parameter variations are applied. Conversely, the error given by proposed scheme is less than 1 electrical degree for nominal parameters and around 6 electrical degrees for +10% variation applied in resistance and moment of inertia during transient as well as steady-state conditions for speed variations even with no-load/full load situation. This shows the effectiveness of the controller and observer design.

CONCLUSION

This paper presents an approach for sensorless control of BLDC motor using disturbance torque estimation. The estimated disturbance torque is the sum of proportional and integral of estimation error of current. The speed of the motor is estimated with the help of disturbance torque estimation without any additional hardware. The speed of BLDC motor is controlled using a new controller scheme based on Modified Hybrid Fuzzy PI (MHFPI) controller. From simulation results, it can be seen that maximum starting and steady-state speed difference between actual and estimated speed are around 3% and 1% respectively even for variation in parameters of BLDC motor. The difference between actual and estimated rotor position is less than 1 electrical degree for nominal parameters and around 6 electrical degrees for +10% variation in resistance and moment of inertia each in transient as well as in steady state conditions. Obtained results have been validated for below rated and rated speed of BLDC motor under different loading conditions.

REFERENCES

1. Akrad A., Hilairet, M. and Diallo, D. (2010), 'Performance enhancement of a sensorless PMSM drive with load torque estimation', 36th Annual Conference on IEEE Industrial Electronics Society, pp. 945-950.
2. Arulmozhiyal, R. (2012), 'Design and implementation of fuzzy PID controller for BLDC motor using FPGA', *IEEE International Conference on Power Electronics and Energy System*, pp. 1-6.
3. Asaei, B. and Rostami, A. (2008), 'A novel starting method for BLDC motors without the position sensors', *Energy Conversion and Management*, Vol 50, pp. 337-343.
4. Bernat, J. and Stepien, S. (2011), 'Application of optimal current driver for the torque control of

BLDC motor', *Archives of Electrical Engineering*, Vol. 60, pp. 149-158.

5. Buja, G.S., Menis, R. and Valla, M.I. (1995), 'Disturbance torque estimation in a sensorless DC drive', *IEEE Trans. Industrial Electronics*, Vol. 42, pp. 351-357.
6. Chen, C-Y. and Cheng, M-Y. (2012), 'Adaptive disturbance compensation and load torque estimation for speed control of a servomechanism', *International Journal of Machine Tools & Manufacture, Elsevier*, Vol. 59, pp. 6-15.
7. Ghassemi, H. and Vaez-Zade, S. (2005), 'A very fast direct torque control for interior permanent magnet synchronous motors startup', *Energy Conversion and Management,* Vol. 46, pp. 715-726.
8. Lee, D.-H. and Ahn, J.-W. (2009), 'A Current ripple reduction of a high-speed miniature brushless direct current motor using instantaneous voltage control', *IET Electric Power Applications*, Vol. 3, pp. 85-92.
9. Mandal, A.K. (2006), *Introduction to Control Engineering – Modeling, Analysis and Design*: New Age International Pvt. Ltd.
10. Park, J.-W., Hwang, S.-H. and Kim, J.-M. (2012), 'Sensorless control of brushless DC motors with torque constant estimation for home appliances', *IEEE Trans. Industry Applications,* Vol. 48, pp. 677-684.
11. Park, K-H., Kim, T-S., Ahn, S-C. and Hyun, D-S. (2003), 'Speed control of high-performance brushless DC motor drives by load torque estimation', *34th IEEE annual* Power Electronics Specialist Conference, pp. 1677-1681.
12. Rodriguez, F. and Emadi, A. (2006), 'A novel digital control technique for brushless DC motor drives: steady state and dynamics', 32nd Annual Conference on IEEE Industrial Electronics, pp. 1545-1550.
13. Rostami, A. and Asaei, B. (2009), 'A novel method for estimating the initial rotor position of PM motors without the position sensor', *Energy Conversion and Management*, Vol. 50, pp. 1879-1883.
14. Rubaai, A., Ricketts, D. and Kankam, D. (2001), 'Experimental verification of a hybrid fuzzy control strategy for a high-performance brushless DC drive system', *IEEE Trans. Industry Applications,* Vol. 32, pp. 503-512.
15. Sant, A.V. and Rajagopal, K.R. (2009), 'PM synchronous motor speed control using hybrid fuzzy-PI with novel switching functions', *IEEE Trans. on Magnetics,* Vol. 45, pp. 4672-4675.
16. Shanmugasundram, R., Zakariah, K. and Yadaiah, N. (2014), 'Implementation and performance analysis of digital controllers for brushless DC motor drives', *IEEE/ASME Trans. Mechatronics*, Vol. 19, pp. 213-224.
17. Stirban, A., Boldea, I. and Andreescu, G.D. (2012), 'Motion sensorless control of BLDC-PM motor with offline FEM information assisted position and speed observer', *IEEE Trans. Industry Applications,* Vol. 48, pp. 1950-1958.
18. Terzic, B. and Jadric, M. (2001), 'Design and implementation of the extended kalman filter for the speed and rotor position estimation of brushless DC motor', *IEEE Trans. Industrial Electronics,* Vol. 48, pp. 1065-1073.
19. Xia, C.-L. (2012), *Permanent Magnet Brushless DC Motor Drives and Controls*, Singapore: John Wiley & Sons.
20. Zerikat, M. and Chekroun, S. (2007), 'Design and implementation of a hybrid fuzzy controller for a high performance induction motor', *Proc. World Academy of Science, Engineering and Technology,* pp. 263-269.

Research Article

Isolation and characterization of bacteria associated with sunscald-affected Capsicum annuum L.

Vaishnawi Gupta[1] Aditi D Buch*

[1]Department of Biological Sciences, P. D. Patel Institute of Applied Sciences, Charotar University of Science and Technology, Changa-388 421, Dist. Anand, Gujarat, India.

Received: 07/07/2018
Revised: 31/10/2018
Accepted: 04/12/2018

Correspondence to:
*Aditi D Buch:
aditibuch.biochem@charusat.ac.in

Abstract:

Bell pepper is a crop with high economic value and its productivity in India is low due to numerous biotic and abiotic diseases, managed through various chemical and biological treatments. Present work includes isolation and characterization of selected bacterial species from pepper and monitoring their growth in presence of representative chemical and biocontrol agents. Fifteen isolates from different parts of sunscald-affected capsicum were microbially characterized, of which three isolates forming yellow mucoid colonies were selected, so as to include pathogenic bacteria if any. These isolates, identified as Rosenbergiella epipactidis, Acinetobacter sp. and Bacillus aquimaris based on partial 16S rDNA sequencing, did not show significant pathogenicity on capsicum fruit when tested in an in vivo infection assay; suggesting their neutral or beneficial nature. While CuSO4 could drastically inhibit the growth of all the isolates in an in vitro plate assay, two biocontrol isolates, P4 and FS2 showed varied degree of effect on the growth of capsicum-associated isolates. Overall, the study reports yet unknown occurrence of R. epipactidis as capsicum-associated bacteria, perhaps endophyte, and develops an insight over probable impact of chemical and biocontrol agents used in pepper disease management on the abundance and diversity of inherent bacteria.

Keywords: Capsicum annuum L., Rosenbergiella epipactidis, Bacillus aquimaris, abundance and diversity of inherent bacteria in capsicum

INTRODUCTION

Bell pepper (*Capsicum annuum* L.), a member of *Solanaceae* family, is one of the most economically important crops across the world. In India, it is commercially cultivated in Karnataka, Tamil Nadu, Himachal Pradesh, Uttar Pradesh as well as in Rajasthan, at temperatures less than 30 °C (Jadon et al., 2016; Negi et al., 2018). Bell peppers have high nutritional value being rich source of vitamins A, B6 and C, calcium, and folic acid and have high urban consumption. Besides, the crop also finds pharmaceutical and cosmetic applications (Manoj Kumar et al., 2008). Therefore, despite lesser favourable natural climatic conditions in India, bell pepper is increasingly cultivated in greenhouses and naturally ventilated polyhouses under milder climatic conditions across Goa, Maharashtra and other regions including Gujarat. Under open field cultivation conditions, capsicum yields are up to 20-40t/ha, whereas in a greenhouse the yield could mount up to 100-120t/ha. However, major limitation to productivity of this crop is frequent occurrence of various biotic and abiotic diseases.

Fruit-associated microbiota plays a significant role in maintaining plant health. While numerous fungal pathogens, both surface-associated and endophytic,

are well-known pathogens of bell pepper, affecting stem, leaves and fruits of pepper plant (Jadon et al., 2016; Mmbaga et al., 2018), few bacterial pathogens like *Xanthomonas campestris*, *Ralstonia solanacearum* and *Clavibacter michiganensis* are also identified (Huang et al., 2017). On the other hand, several bacterial endophytes are also associated beneficially with pepper, mainly including members of genus *Pseudomonas, Bacillus, Burkholderia, Paenibacillus, Pandoraea, Enterobacter, Rhizobium* and *Serratia* to name a few (Paul et al., 2013; Irabor and Mmbaga, 2017). These endophytic bacteria present in varying abundance in pepper plants, either prevent the colonization and spread of pathogenic microbes by acting as biocontrol agents or could confer resistance against abiotic stress (Sziderics et al., 2007).

Commonly, the microbial diseases of pepper plant are controlled by interventions involving use of various chemicals mainly including the copper-based compounds (Rather et al., 2012). More eco-friendly management of capsicum diseases is increasingly preferred using biocontrol agents which include *Bacillus*, *Pseudomonas*, *Paenibacillus Flavobacterium* and *Trichoderma* spp (King and Parke, 1993; Manoj Kumar et al., 2008; Chandra et al., 2010; Seggara et al., 2013; Torres et al., 2016). While both these approaches could reduce the disease incidences, they could significantly affect the inherently associated microbiota.

Interestingly, a commonly encountered climatic disease, sunscald caused by persistent exposure of pepper fruit to sunlight and heat (Borkar and Yumlembam, 2016), is likely to influence the abundance and nature of both beneficial and pathogenic bacteria associated with the fruit. Hypothetically, sunscald-damaged tissue with wrinkled surface becomes more prone to bacterial infections and at the same time the hardened sunscald-affected area could show enrichment of endophytic bacteria more tolerant to abiotic stresses. The present work involves isolating and identifying selected bacteria from sunscald-affected capsicum fruits, *in vivo* assessment of their pathogenicity for capsicum and testing the effects of chemical and biocontrol agents on their growth.

MATERIALS AND METHODS

Sampling of capsicum fruits

Surface properties of the fruits with reference to standard manuals available for management of capsicum crop, were used to sample sunscald-affected fruits from greenhouse facility in Ajarpura Village, Anand district, Gujarat. Healthy fruits from the same cultivation system were obtained for use as controls in experiments.

Isolation of bacteria and their preliminary microbial characterization

Within 24 h of sampling the diseased capsicum fruits, approximately 0.5 x 0.5 cm of piece was cut from infected fruit, stem and peduncle using sterilized knife and was mounted on nutrient agar and potato dextrose agar slants prepared earlier. Infected tissue from three different sites on a single fruit were used as microbial source and the slants were then incubated at 30 °C for 48 h to ensure optimum isolation of distinct microbial species. In parallel, similarly derived infected tissue was suspended in 1 ml sterile normal saline pre-dispensed in sterilized centrifuge tubes. The tubes were mildly vortexed for 1 minute, centrifuged at 8,000 rpm for 5 minutes and resultant supernatant was subsequently serially diluted. A volume of 100 µl of 10^{-1}, 10^{-2} and 10^{-3} dilutions were spread on the nutrient agar plates which were subsequently incubated overnight at 30 °C. Distinct bacterial colonies obtained were selected based on visual analysis of colony characteristic and were subjected to further microscopic analysis based on Gram staining, endospore staining and cell shapes by standard procedures. Selected individual colonies were maintained as a pure culture for further study.

Extraction of genomic DNA from isolates

Single colony was inoculated into 3 ml nutrient broth and incubated at 30°C for overnight under shaking conditions (150 rpm). A 1.5 ml of overnight grown culture was harvested by centrifugation of 8,000 rpm for 5 minutes at room temperature. After discarding the supernatant, pellet was washed thrice with 1 ml of SET buffer (pH=8.0) and finally resuspended in 100 µl of the same with addition of 50 µl of lysozyme (10 mg/ml) and mixed properly. After subsequent addition of 30 µl of RNase A (2 mg/ml), the volume was made upto 500 µl with SET buffer. Subsequently, 50 µl of Proteinase K (10 mg/ml) and 50 µl of 10% SDS were added and contents were incubated at 37 °C for 1 h. Followed by this, 100 µl of 5M NaCl and 80 µl of cetyltrimethylammonium bromide solution were added and incubated for 10 min at 55°C. The mixture was extracted with equal volume of Tris-saturated phenol and Chloroform:Isoamyl alcohol (24:1) and centrifuged at 10,000 rpm for 10 min at 4 °C. Aqueous phase was transferred in fresh sterile centrifuge tubes, and again was extracted with equal volume of chloroform followed by centrifugation at 10,000 rpm for 10 min at 4 °C. The resultant aqueous

phase was transferred to fresh sterile tube and genomic DNA was precipitated overnight by adding 0.8 volume of isopropanol. Precipitated DNA was pelleted by centrifugation at 10,000 rpm for 5 min at 4 °C, washed twice with 70% ethanol, air-dried and was dissolved in 50 µl TE buffer. Isolation of genomic DNA was confirmed using agarose gel electrophoresis.

Molecular characterization of selected isolates

16S rRNA gene was amplified using universal primers 8F (5'-AGAGTTTGATCCTGGCTCAG-3') and 1492R (5'-ACGGCTACCTTGTTACGACTT-3'), in PCR reactions performed in 20 µl of volume containing 20 picomoles of each primer, 0.2 mM dNTPs each, 30 ng of template genomic DNA, 1U of Taq DNA polymerase and 1X PCR buffer (used as per manufacturer's instructions). Amplifications were achieved in Biorad thermocycler with following program: initial denaturation at 94 °C for 3 minutes followed by 35 cycles each consisting of denaturation at 94 °C for 30 s, primer annealing temperature at 58 °C for 30 s, primer extension at 72 °C for 1 min 30 s and a final extension of 72 °C for 10 min. PCR amplicons of desired size (~1500 bp size) were confirmed on 1 % agarose gel. Partial DNA sequence of the confirmed PCR product was obtained as outsourced service (1st Base, Singapore) and were subjected to BLAST analysis for identification of the isolates (http://www.ncbi.nlm.nih.gov).

***In vivo* infection assay**

The infection assay was set up using a method used by Fieira et al. (2013) with necessary modifications. Single colony of the selected isolate was inoculated in 3 ml Luria broth and culture was allowed to grow overnight under shaking conditions (30 °C, 150 rpm). Resultant cells were harvested by centrifugation at 8,000 rpm for 2 minutes, washed with 1 ml of sterile normal saline and finally resuspended in the same to prepare the active inoculum. Three microlitres of this inoculum was mixed with 10 µl of 0.4 % agar and the total volume was spotted on a healthy capsicum fruit, surface sterilized using ethanol. The inoculated fruits were incubated at 30 °C and infection was monitored over a period of 6 days, with exposure of sunlight on 5th and 6th days.

***In vitro* antimicrobial assay**

Ability of Cu^{2+} as well as laboratory isolates *Pseudomonas aeruginosa* P4 (P4) and FS2 to inhibit the growth of isolated bacteria was tested by modified dual culture plate assay. Cells harvested from 3 ml overnight Luria broth-grown P4 and FS2 cultures were subsequently washed twice by and re-suspended in 1 ml normal saline aseptically, to prepare inoculum. Similarly prepared cell suspension of the pepper-derived bacterial isolate was diluted 1:1000 times and 0.1 ml of it was spread uniformly on nutrient agar medium. Subsequently, 3 µl of freshly prepared P4 and FS2 inoculum was spotted in two quadrants of the plate. Five microliters of 0.1 mM $CuSO_4$ was spotted in third quadrant as chemical agent while 3 µl of freshly prepared *E. coli* DH5α inoculum was spotted in the fourth quadrant as negative control. Formation of clear zone of inhibition around the zone of bacterial growth after 72 h incubation at 30 °C was taken as a measure of antimicrobial ability.

RESULTS

Preliminary disease analysis of capsicum fruit, isolation and characterization of bacteria

Capsicum fruits with a typical phenotype of white patch with wrinkled surface and edges, depending on the extent of disease, were obtained from local polyhouse plantations of capsicum. Visual analysis of the infected area could classify the disease as sunscald (Fig. 1A) (Borkar and Yumlembam, 2016). Tissues including affected patch, peduncle and stem of the diseased fruit were used to isolate bacteria. Fungal isolates obtained were not carried forward in the study.

Figure 1: Selected bacterial isolates obtained from sunscald-affected capsicum (A) Suncald-affected capsicum fruit used as source of isolation (B) Three distinct yellow and mucoid colonies selected for further studies

Fifteen visually distinct colonies from across all tissues and isolation conditions were considered for further study (Table 1). Six of these isolates were Gram positive and endospore positive while remaining 9 isolates were Gram negative and endospore negative. Most isolates showed short rods and cocci cell types. After comparing the preliminary colony characteristics of all 15 colonies, 3 distinct isolates I-1, I-3 and I-9 were selected for further analysis (Fig. 1B). These isolates were selected on the basis of pale to bright yellow colour and mucoid colony features displayed by commonly known bacterial pathogens of capsicum, so as to possibly include both pathogenic and beneficial bacteria.

Table 1: Characterization of bacterial isolates obtained from sunscald-affected capsicum

Isolate [1]	Gram reaction	Endospore staining	Cell shape
I-1	-ve	-ve	Short rods
I-2	-ve	-ve	Cocci
I-3	-ve	-ve	Short rods
I-4	-ve	-ve	Cocci
I-5	+ve	+ve	Rods
I-6	+ve	+ve	Rods
I-7	-ve	-ve	Short rods
I-8	+ve	+ve	Short rods
I-9	+ve	+ve	Short rods
I-10	+ve	+ve	Short rods
I-11	+ve	+ve	Rods
I-12	-ve	-ve	Cocci
I-13	-ve	-ve	Cocci
I-14	-ve	-ve	Short rods
I-15	-ve	-ve	Short rods

[1] Isolates I-1, I-2, I-3, I-6, I-7, I-8 are isolated from fruit rot on nutrient agar plates, I-4, I-5, I-10, I-11 and I-12 are isolated from fruit rot on nutrient agar slants, I-9 is from rotten peduncle on agar plate, I-13 and I-14 are from stem rot on nutrient agar plate, I-15 is from healthy fruit on agar plate; +ve -positive, -ve –negative

Molecular identification of the selected isolates

Genomic DNA from these isolates was isolated and subjected to amplification of 16S rDNA gene as ~1500 bp amplicon. Partial DNA sequence analysis using BLAST tool revealed maximum identity of I-1, I-3 and I-9 to *Rosenbergiella epipactidis, Acinetobacter sp.* and *Bacillus aquimaris,* respectively (Table 2). Of these, isolate I-1 with similar extent of query cover but relatively lesser Max. Score of BLAST output, also showed a significant homology to *Phaseolibacter flectens*, a probable plant pathogen.

Table 2: BLAST analysis-based molecular identification of selected isolates

Isolate	Identified	Query length	% Identity
I-1	*Rosenbergiella epipactidis/ Phaseolibacter flectens*	1270 (97%)/ 1270 (98%)	97% / 96%
I-3	*Acinetobacter sp.*	1167	99%
I-9	*Bacillus aquimaris*	1077	96%

***In vivo* evaluation of efficacy of selected isolates as bacterial pathogen for capsicum**

Pathogenicity of isolates I-1, I-3 and I-9 for capsicum was monitored using an *in vivo* infection assay as described in 'Materials and Methods' section. Figure 2 depicts that none of the isolates could show any infection phenotype till 96 h, until and unless exposed to sunlight. From fifth day onward, gradual development of disease phenotype on healthy fruit at the site of inoculation was observed which invigorated upon further exposure to sun on sixth day.

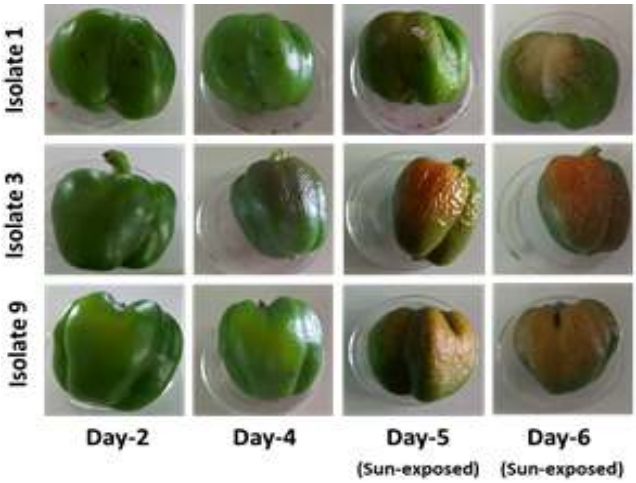

Figure 2: *In vivo* assay to monitor efficacy of selected isolates to infect capsicum.

Advancement of disease phenotype as monitored up to 6 days with last two days of sunlight exposure post inoculation

Effect of chemical and biological disease management agents on growth of selected isolates

All the three pepper-derived isolates were subjected to *in vitro* plate assay to monitor effects of representative chemical agent $CuSO_4$ as well as biological agents P4 and FS2 (rhizospheric lab isolates) on their growth. $CuSO_4$ could inhibit the growth of all the three tested isolates I-1, I-3 and I-9 to drastic extents, with I-9 showing maximum growth inhibition. Biocontrol isolate P4 could significantly inhibit growth of I-1 and I-9 but not I-3 while FS2 failed to inhibit growth of any of the three isolates (Fig. 3). Negative control *E. coli* DH5α showed no antibiosis of isolates.

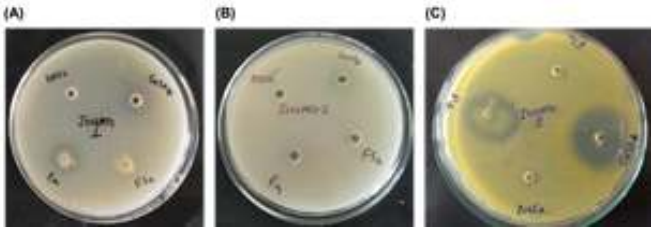

Figure 3: *In vitro* inhibition of growth of selected bacterial isolates from pepper.

In vitro antimicrobial activity of P4 and FS2 as monitored by dual culture plate assay for isolates (A) I-1 (B) I-3 and (C) I-9. $CuSO_4$ was used as chemical inhibitor of bacterial growth.

DISCUSSION

Bell pepper disease management practices involve use of various chemical-based and eco-friendly biocontrol agents. Understanding the influence of these treatments on abundance and diversity of neutral or beneficial endophytic bacteria could not only help the choice of treatment but could also reveal novel endophytes with diverse roles. The present study reports isolation of selected bacterial spp. from sunscald-affected capsicum fruit and their microbial and molecular characterization. Subsequently, effect of representative chemical and biological agents used in disease management of pepper, on growth of these isolates was also tested.

Sunscald-affected capsicum was sampled based on simple symptoms such as occurrence of a white hardened and wrinkled patch on the fleshy surface (Borkar and Yumlembam, 2016). Considering that this environmentally affected area could not only be prone to microbial infections but could also harbour exclusive endophytic population, it was used in the experiments to isolate bacterial spp. selectively. Of around 15 bacterial colonies isolated, only three I-1, I-3 and I-9 were selected for further studies. In order to ensure that bacterial pathogens were not missed out, these colonies were shortlisted based on pale-bright yellow colour and mucoid appearance, common to known bacterial pathogens of pepper i.e. *X. campestris, R. solani* and *C. michiganensis* (Huang *et al*., 2017). However, these colony characteristics could be also displayed by beneficial inherent endophytic bacteria. 16S rDNA sequencing-based analysis identified the selected isolates as *Rosenbergiella epipactidis*, *Acinetobacter spp.* and *Bacillus* spp. respectively. While *Bacillus* and *Acinetobacter,* besides several others, are commonly known endophytes of plants including capsicum (Paul et al., 2013; Irabor and Mmbaga, 2017), occurrence of *Rosenbergiella* spp. in capsicum hasn't been reported. *Rosenbergiella* spp. have been earlier isolated from floral nectar (Halpern et al., 2013; Lenaerts et al., 2014). Isolate I-1 identified as *R. epipactidis,* also showed significant identity to *Phaseolibacter flectens,* a known pathogen of beans albeit not capsicum (Aizenberg-Gershtein et al., 2016). However, *in vivo* infection assay almost ruled out this possibility of pathogenicity as evident from poorly developed infection phenotype, 4 days post inoculation with all the three isolates including I-1. The observed development of sunscald-like disease was only due to exposure to sunlight. Thus, the three isolates were most likely to be neutral or beneficial endophytes of pepper. Since such endophytes share the niche with pathogens, they often possess efficient biocontrol properties thus capably influencing the metabolism and physiology of the host plant (Amaresan et al., 2013; Paul et al., 2013). However, these beneficial effects of inherent endophytes are subject to their abundance which can be largely affected by disease management practices.

Rhizospheric biocontrol isolates P4 and FS2, respectively identified as fluorescent pseudomonads and *Enterobacteriaceae* (unpublished lab data) were used as representatives to understand their ability to affect the growth of selected isolates, in comparison with Cu^{2+} based chemical. The results overall indicated that topically applied biocontrol agents could differentially affect the growth and hence abundance, of endophytic spp of capsicum, with *Enterobacteriaceae* being relatively lesser capable of modulating the same. On the other hand, chemical pesticides which are largely Cu^{2+} -based, could cause drastic adverse effect on the endophytic bacteria.

CONCLUSIONS

Overall, this study reports otherwise unknown occurrence of *Rosenbergiella epipactidis* as capsicum-fruit associated bacteria, mostly endophytic. This study further indicated that biocontrol agents although relatively eco-friendly as compared to chemical pesticides, both these modes of disease control could modulate the abundance and diversity of inherent beneficial endophytes of capsicum; an aspect which is seldom considered before employing disease control treatments.

ACKNOWLEDGEMENTS

The authors are thankful to Dr. K. C. Dave of Agronomy Agribiotech LLP, for access to the greenhouse capsicum plantations and inputs towards understanding of disease conditions.

REFERENCES

1. Aizenberg-Gershtein, Y., Izhaki, I., Lapidus, A., Copeland, A., Reddy, T.B.K., Huntemann, M., Pillay, M., Markowitz, V., Göker, M., Woyke, T., Klenk, H-P., Kyrpides, N. C. and Halpern, M. (2016) 'High quality permanent draft genome sequence of *Phaseolibacter flectens* ATCC 12775T, a plant pathogen of French bean pods.' *Standards in Genomic Sciences*, vol.11, January, pp. 4.

2. Amaresan, N., Jayakumar, V. and Thajuddin, N. (2014) 'Isolation and characterization of endophytic bacteria associated with chilli (*Capsicum annuum*) grown in coastal agricultural ecosystem.' *Indian Journal of Biotechnology*, vol. 13, April, pp. 247-255.
3. Borkar, S. G. and Yumlembam, R. A. (2016) *Bacterial Diseases of Crop Plants*, USA: CRC Press Book
4. Chandra, S., Chatterjee, s and Acharya, K (2010) 'Biological control of fruit rot and die back disease of *Capsicum annuum* with *Pseudomonas aeruginosa* WS-1.' *The Asian and Australasian Journal of Plant Science and Biotechnology*, vol. 4, May, pp. 38-42.
5. Fieira, C., Oliveira, F., Calegari, R. P., Machado, A. and Coelho, A. R. (2013) '*In vitro* and *in vivo* antifungal activity of natural inhibitors against Penicillium expansum.' *Food Science and Technology*, vol. 33, February, pp. 40-46.
6. Halpern, M., Fridman, S., Atamna-Ismaeel, N. and Izhaki, I. (2013) '*Rosenbergiella nectarea* gen. nov., sp. nov., in the family *Enterobacteriaceae*, isolated from floral nectar. International Journal of Systematic and Evolutionary Microbiology, vol. 63, November, pp. 4259-4265.
7. Huang, Y., Wu, Z., He, Y., Ye, B-Ce and Li, C. (2017) 'Rhizospheric *Bacillus subtilis* exhibits biocontrol effect against *Rhizoctonia solani* in pepper (*Capsicum annuum*).' *Biomed Research International*, vol. 2017, December, pp. 9397619.
8. Irabor, A. and Mmbaga, M. T. (2017) 'Evaluation of selected bacterial endophytes for biocontrol potential against *Phytophthora* blight of bell pepper (*Capsicum annuum* L.).' Journal of Plant Pathology and Microbiology, vol. 8, October, 424. doi: 10.4172/2157-7471.1000424
9. Jadon, K. S. Shah, R., Gour, H. N. and Sharma, P. (2016) 'Management of blight of bell pepper (*Capsicum annuum var. grossum*) caused by *Drechslera bicolo*.' *Brazilian Journal of Microbiology*, vol. 47, Oct-Dec, pp. 1020–1029.
10. King, E.B. and Parke, J.L. (1993) 'Biocontrol of Aphanomyces root rot and Pythium damping-off by Pseudomonas cepacian AMMD on four pea cultivars.' *Plant Disease*, vol. 77, 1185–1188.
11. Lenaerts, M., Alvarez-Pérez, S., de Vega, C., Van Assche, A., Johnson, S. D., Willems, K. A., Herrera, C. M., Jacquemyn, H. and Lievens, B. (2014) *Rosenbergiella australoborealis* sp. nov., *Rosenbergiella collisarenosi* sp. nov. and *Rosenbergiella epipactidis* sp. nov., three novel bacterial species isolated from floral nectar.' *Systematic and Applied Microbiology*, vol. 37, September, pp. 402-411.
12. Manoj Kumar, A., Ganeshan, G., Reddy, K.N. and Ramchandra, Y. L., (2008) 'Integrated disease management for the control of powdery mildew (*Levelillula taurica* (*Lev*.) *Arn*.) in bell pepper.' *The Asian and Australasian Journal of Plant Science and Biotechnology*, vol. 2, October, pp. 107-112.
13. Mmbaga, M. T., Gurung, S. and Maheshwari, A. (2018) 'Screening of plant endophytes as biological control agents against root rot pathogens of pepper (*Capsicum annum* L.).' *Journal of Plant Pathology and Microbiology*, vol. 9, March, pp. 435.
14. Negi, R., Thakur, S and Sharma, P. (2018) 'Advances in the breeding of bell pepper - A review.' *International Journal of Current Microbiology and Applied Sciences*, vol. 7, November, pp. 2272-2281.
15. Paul, N. C., Ji, S. H., Deng, J. X. and Yu, S. H. (2013) 'Assemblages of endophytic bacteria in chili pepper (*Capsicum* annuum L.) and their antifungal activity against phytopathogens *in vitro*.' *Plant Omics Journal*, vol. 6, September, pp. 441-448.
16. Rather, T. R., Razdan, V. K., Tewari, A. K., Shanaz, E., Bhat, Z. A., Hassan, Mir G. and Wani, T. A. (2012) 'Integrated management of wilt complex disease in bell pepper (*Capsicum annuum* L.).' *Journal of Agricultural Science*; vol. 4, May, pp. 141-147.
17. Segarra, G., Avilés, M., Casanova, E., Borrero, C. and Trillas, I. (2013) 'Effectiveness of biological control of *Phytophthora capsici* in pepper by *Trichoderma asperellum* strain T34.' *Phytopathologia Mediterranea*, vol.52, April, pp. 77−83.
18. Sziderics, A. H., Rasche, F., Trognitz, F., Sessitsch, A. and Wilhelm, E. (2007) 'Bacterial endophytes contribute to abiotic stress adaptation in pepper plants (Capsicum annuum L.).' *Canadian Journal of Microbiology*, vol. 53, November, pp.1195-1202.
19. Torres, M. J., Pérez Brandan, C., Petroselli, G., Erra-Balsells, R. and Audisio, M. C. (2016) 'Antagonistic effects of *Bacillus subtilis* subsp. *subtilis* and *B. amyloliquefaciens* against *Macrophomina phaseolina*: SEM study of fungal changes and UV-MALDI-TOF MS analysis of their bioactive compounds.' *Microbiological Research*, vol. 182, August, pp. 31-39.

Review Article

Analytical Methods for Quantitative Estimation of Montelukast Sodium: A Review

Kunti Shah[1]*, Vijaykumar Parmar[2]

[1]Thermo Fisher Scientific, Mississauga, Canada,
[2]Department of Pharmaceutical Sciences, Sardar Patel University, Anand, India

Received: 22/02/2017
Revised: 10/01/2018
Accepted: 23/01/2018

Correspondence to:
*Kunti Shah:
vijayparmar.ph@charusat.ac.in

Abstract:

Background: Montelukast sodium is a potent and selective orally active leukotriene receptor anatagonist. It is used for the treatment of asthma and allergic rhinitis in adults as well as children. It was first approved by FDA in 1998 under the trademark Singulair. This literature review summarizes the variety of analytical techniques that have been applied for the estimation of montelukast sodium.

Method: Various analytical techniques for the quantification of montelukast sodium for bulk, pharmaceutical formulations and biological samples have been reported. Assay methods include UV-spectroscopy, high performance liquid chromatography, high performance thin layer chromatography, capillary electrophoresis, spectrofluorimetry, super critical fluid chromatography.

Results: Literature review reveals that methanol is the most commonly used solvent for the analysis of montelukast sodium by spectroscopic technique. For estimation of montelukast sodium by high performance liquid chromatography, methanol and acetonitrile are the commonly used organic solvents in the mobile phase and phosphate buffer or trifluoroacetic acid is used to maintain the pH of the mobile phase. Protein precipitation technique is used widely for extraction of the montelukast from biological samples though liquid-liquid extraction and solid phase extraction has also been reported in fewer articles. The electroanalytical techniques reported for the analysis of the drug have provided methods with lower analysis time.

Conclusion:Amongst all the developed analytical methods, HPLC has been reported extensively for the quantification for montelukast sodium.

Keywords: montelukast sodium, analytical methods, HPLC

1. INTRODUCTION

Montelukast sodium (MON), chemically 1-[[[(1R)-1-[3-(1E)-2-(7-chloro-2-quinolinyl) ethenyl] phenyl]-3-[2-(1-hydroxy-1-methylethyl) phenyl] propyl]thio]-methyl] –cyclopropaneacetic acid, monosodium salt (Figure 1), is a potent and selective leukotriene receptor antagonist (1). It is used for the treatment of asthma and allergic rhinitis for adults as well as children (2-3).

MON was discovered in the Montreal labs of Merck and with the suffix-lukastthe generic name montelukastwas obtained.MON was approved by FDA in 1998 under the trademark Singulair(4). Singulair was covered by U.S. Patent No. 5,565,473(5)which expired on August 3, 2012 (6).Several generics of MON received approval by FDA after that. MON is available as solid oral dosage form as

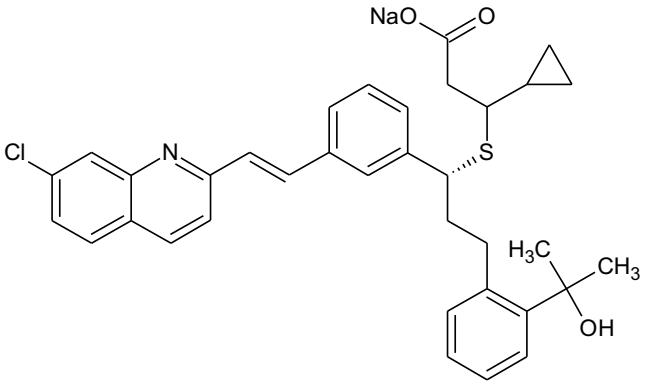

Figure 1 Chemical structure of Montelukast sodium

film coated tablets, chewable tablets and oral granules having strength 4mg, 5mg and 10mg (7). MON is available either individually or in combination with other APIs like levocetrizine, fexofenadine, bambuterolHCl, doxofylline, acebrophylline, desloratadine, ambroxol, etc are available in the market (8-9).

The drug is official in the Indian Pharmacopoeia 2014 (10), British Pharmacopeia 2016 (11),US Pharmacopoeia 2016 (12).The molecular weight of MON is 608.2 and it is a white to pale yellow(10). The drug is ahygroscopic powder and an optically active molecule. It is light sensitive and requires protective handling and storage. It is freely soluble in ethanol,methanol, and water while practically insoluble in acetonitrile (7). It is a lipophilic drug (logP=8.79) having a pka of 2.7 and 5.8 (13).

The present review of literature is based on the several reported analytical methods for estimation of MON in bulk, pharmaceutical formulations as well as biological samples. Methods like spectrophotometry, chromatography including HPLC, HPTLC, UPLC and LC-MS, electrochemical methods and capillary electrophoresis have been reported. HPLC methods have been extensively used (Figure 2).

2. SAMPLE PREPARATION

MON is unstable in the presence of light and moisture thus the monograph in the pharmacopoeia indicates special storage condition. As per the Indian Pharmacopoeia MON is required to be stored protected from light as well as moisture and at a temperature not exceeding 30°C(10). U.S. Pharmacopoeia indicates preserve the API in tight containers(12). Thus sample preparation is required to be done in amber glassware. It has been mentioned to use freshly prepared solvents always for the drug (10-11). Methanol has been used as a diluent for majority of the spectrophotometric methods of analysis for MON.Extraction of the drug from the biological sample includes sample preparation via protein precipitation, liquid liquid extraction and solid phase extraction (44-57). Acetonitrile has been reported extensively for the sample preparation by protein precipitation.

3. ANALYTICAL METHODS

3.1 SPECTROPHOTOMETRY

In the literature, different UV-spectrophotometric methods have been explored for the quantitative estimation of MON in combination with other drugs, including simultaneous equation method, Q-absorbance Ratio method and derivative method. Methanol is commonly used as a solvent for MON in the spectrophotometric methods.J.V. Shanmukhakumar et al.(14) and M. SaeedArayne et al. (15) have reported method for estimation of MON alone while other have reported simultaneous estimation with other API.Table 1 lists the spectrophotometric methods for analysis of MON.

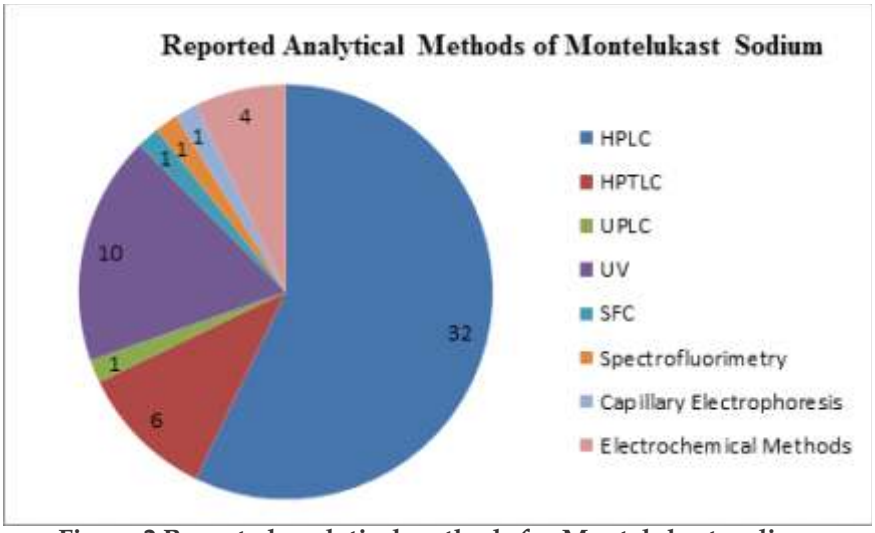

Figure 2 Reported analytical methods for Montelukast sodium

Table 1 Reported spectrophotometric methods for determination of Montelukast sodium individually or in combination with other drugs from the Pharmaceutical Dosage Forms.

API	Method	Solvent	Detection Wavelength (λ,nm)	Ref
Montelukast Sodium	A: Reduction of FE(III) to FE(II) by MTK B: MTK coupling with MBTH C: MTK reaction with 2, 2'-Bipyridyl	Ferric Chloride	A: 510 B: 610 C: 430	14
Montelukast	Spectrophotometric Method	Methanol	283	15
Montelukast Sodium and Theophylline	Simultaneous Equation and Q-Absorbance Ratio method	Water	287(MON) 271(THEO) 280 (isoabsorptive point)	16
Montelukast Sodium and Desloratadine	Q-Absorbance Ratio Method and Dual Wavelength Method	Methanol	283(MON) 263.6 (isoabsorptive point); 345 (MON) 265.6 and 294 (DESLO)	17
Montelukast Sodium and Desloratadine	RatioSpectra Derivative Spectrophotometric Method	Methanol	first derivative amplitudes: 218.6(MON), 262(DESLO)	18
Theophylline, Montelukast and Loratadine	Multivariate Spectrophotometric Calibration-partial least-squares, principal component regression and hybrid linear analysis.	Methanol	275 (THEO), 276(MKST), 251 (LORA)	19
Montelukast Sodium and LevocetirizineDihydrochloride	Derivative and Absorption Factor Spectrophotometric Method	Methanol	first derivative amplitudes: 340(MON), 331 (LEV); 232 (MON), 279 (LEV)	20
RupatadineFumarate and Montelukast Sodium	Q Analysis method	Methanol	260 (Isoabsorptivepoint) 244(RUPA)	21
Acebrophylline and Montelukast Sodium	Simultaneous Equation Method	Methanol	313 (ACBR) 344.5 (MTKT)	22
Rupatadine and Montelukast	First-order derivative UV spectroscopy	Methanol	first derivative amplitudes: 273.46 (MON) 297.27 (RUPA)	23

3.2 Chromatography

3.2.1 HPLC

Among the chromatographic methods employed for the analysis of pharmaceuticals, high performance liquid chromatography is the most widely used technique. Several assay procedures and analysis of related substances mentioned in the pharmacopoeias comprise the HPLC technique. More than twenty HPLC methods for the estimation of montelukast sodium have been summarized in table 2 and fourteen methods for estimation of the drug in biological samples have been summarized in table 3.

Analyte and Matrix	Mobile Phase	Stationary Phase	Detector	Detection Wavelength (nm)	Flow rate (mL/min)	Rt (min)	LOD (µg/ml)	Ref
Montelukast Sodium and its impurities from bulk	Gradient elution: solution A (0.1% OPA), solution B (water:acetonitrile, 5:95 v/v)	C18 column 250 x 4.6 mm i.d, 5 µm particle size	PDA	225	1.5	13.89	0.034	24
Montelukast Sodium from bulk and tablet	Acetonitrile: 1 mM sodium acetate buffer (pH 6.3 adjusted with acetic acid), 90:10v/v	C 18 column 250×4.6 mmi.d, 5 µm particle size	UV	285	1.5	3.4	1.31	25
Motelukast sodium and Theophylline in tablet	Methanol	C18 column 250 ×4.6mmi.d , 5 µm particle size	UV	210	1.0	4.17 (THEO) 2.91 (MON)	0.0073 (THEO), 0.0434 µg/ml (MN)	26
Montelukast Sodium and Doxofylline in tablet	Methanol:sodium phosphate buffer (pH 6.5 adjusted with orthophosphoric acid), 75:25 v/v	C8 column 250× 4.6 mm i.d, 5 µm particle size		230	1.0	3.4(DOXO), 5.5 (MON)	--	27
Montelukast and its degradation products in tablet	Acetonitrile: 0.01M potassium dihydrogen phosphate buffer (pH 4.0), 3:7 v/v	C18 column 250 × 4.6 mm i.d, 5 µm particle size	SPD-M20A photodiode	355nm	1.0	--	5.51	28
Montelukast sodium in oral granules	0.05M Potassium dihydrogen phosphate buffer (pH 3.5) : acetonitrile, (30:70 v/v)	C18 column 50 × 4.6 mm i.d, 5 µm particle size	PDA	225	1.8	--	--	29

Analyte and Matrix	Mobile Phase	Stationary Phase	Detector	Detection Wavelength (nm)	Flow rate (mL/min)	Rt (min)	LOD (µg/ml)	Ref
Montelukast and Theophylline in tablet	0.3 % TFA in water (pH 2.5) : acetonitrile, 20:80 %v/v	C18 column 150 × 4.6 mm i.d, 5 µm particle size	UV	230	1.0	4.20 (THEO), 6.12 (MON)	0.521(THEO), 0.013 (MON)	30
Montelukast Sodium in tablet	Methanol: 0.02 M sodium phosphate buffer (pH 3.5 adjusted by 0.01 M Phosphoric acid), 15:85v/v	C8 column 250 × 4.6 mm i.d, 5 µm particle size	SPD-20 A VP	218	1.0	3.017	--	31
Montelukast Sodium in tablet	Methanol: TFA, 90:10 v/v.	C18 column 250 × 4.6 mm i.d, 5 µm particle size	UV	350	1.0	7.9	--	32
Montelukast Sodium and LevocetirizineDihydrochloride in bulk and tablet	0.02M Disodium hydrogen phosphate buffer : Methanol (7.0 pH adjusted ortho-phosphoric acid, 25:75 v/v	C18 column 250 × 4.6 mm i.d, 5 µm particle size	UV/Vis	231	1.0	3.55(LEVO), 7.45 (MON)	--	33
Montelukast Sodium and Fexofenadinehydrochloride in tablet	50 mM Sodium acetate buffer:acetonitrile: methanol(8.2 pH adjusted with 5% o-phosphoric acid, 25:35:40 v/v	C18 column 250 × 4.6 mm i.d, 5 µm particle size	UV/Vis detector	210	1.0	3.43 (MONT), 8.22(FEXO)	0.29 (MONT), 3.00 (FEXO)	34
Montelukast Sodium and BambuterolHydrochloride in tablet	Gradient elution: Solution A (0.025 M sodium phosphate buffer: methanol, 85:15v/v);Solution B (Acetonitrile:methanol85:15v/v)	C18 column 250 × 4.6 mm i.d, 5 µm particle size	UV/Vis detector	218	1.5	21.2 (MTK), 5.8 (BBL)	--	35
MontelukastSodium and Desloratadine in tablet	Orthophosphoric acid : water, 20:80v/v	C18 column 250 × 4.6 mm i.d, 5 µm particle size	UV/Visible dual absorbance detector	280	1.0	2.92(MON), 4.43(DES)	0.176 (MON), 0.087 (DES)	36

Analyte and Matrix	Mobile Phase	Stationary Phase	Detector	Detection Wavelength (nm)	Flow rate (mL/min)	Rt (min)	LOD (µg/ml)	Ref
MontelukastSodium and Rupatadine fumarate in tablet	Methanol: Potassium dihydrogenphosphate buffer: Acetonitrile (3.0 pH adjustedwith 1% orthophosphoric acid), 50:30:20v/v/v	C18 column 250 × 4.6 mm i.d, 5 µm particle size	PDA	226	1.0	2.48(RPM), 6.38 (MLT)	1.56 (RPM), 1.08 (MLT)	37
Montelukast Sodium and FexofenadineHydrochloride in tablet	0.1M potassium dihydrogen orthophosphate buffer (5.0 pH): methanol, 60:40 v/v	C18 column 250 × 4.6 mm i.d, 5 µm particle size	UV-Visible detector	220	1.0	2.17 (MON), 6.24 (FEX)	0.1 (MON), 1.0 (FEX)	38
Montelukast Sodium in tablet	Water: acetonitrile (modified with 0.2% TFA), 50:50 v/v	Phenyl column 100×3.0 mm i.d, 5 µm particle size	variable wavelength UV detector	389	--	--	--	39
Montelukast and Ebastine in bulk and tablet	Methanol and water (3.0 pH adjusted by ortho phosphoric acid, 80: 20 v/v	C18 column 250 × 4.6 mm i.d, 5 µm particle size	UV detector	268	1.0	6.58 (MTS), 2.98 (EBS)	1.05 (MTS), 1.13 (EBS)	40
Montelukast Sodium in tablet	Acetonitrile: 0.2% TFA, 50:50 v/v	Phenylcolumn 100 × 3.0 mm i.d, 5 µm particle size	UV detector	389	0.9	--	--	13
Montelukast and Loratadine in tablet	Sodium phosphate buffer (3.7 pH adjusted): Acetonitrile, 20:80 v/v	C18 column 250 × 4.6 mm i.d, 5 µm particle size	PDA	225	1.0	--	--	41
Montelukast Sodium in tablet	Acetonitrile:Methanol:Water (pH 3.8), 75:10:15 v/v/v	C18 column 150 × 4.6 mm i.d, 5 µm particle size	PDA	280	0.8	--	--	42

Analyte and Matrix	Mobile Phase	Stationary Phase	Detector	Detection Wavelength (nm)	Flow rate (mL/min)	Rt (min)	LOD (µg/ml)	Ref
MontelukastSodium in bulk and tablet	n-hexane: ethanol: 1,4-dioxane: TFA: diethylamine , 65:25:10:0.3:0.05 v/v	Cellulose tris (3,5-dimethylphenylcarbamate) coated on silica-gel column 25 × 4.6 mmi.d, 5 µm particle size	PDA	280	1.0	15	0.07	43

Table 3 Review of HPLC methods for estimation of Montelukast sodium in biological samples

Matrix	Internal Standard	Sample preparation	Mobile phase	Column	Detector and detection wavelength	Flow rate (ml/min)	Rt and LOD	Ref.
Human Plasma	Mefenamic acid	Protein Precipitation with Acetonitrile	Methanol: Acetonitrile:0.04M disodium hydrogen orthophosphate (4.9 pH), 22:22:56 v/v	C8 column 150mm×4.6mm i.d, 5µm particle size	fluorescence detector, em= 350nm ex=450nm	1.0	7.7 min; LLQC 5ng/ml	44
Human Plasma	Montelukast-*d*6	Protein Precipitation with Acetonitrile	10mM Ammonium formate (pH 4.0): Acetonitrile, 20:80 v/v	C18 column250 x 4.6 mmi.d,5µm particle size	ESI–MS/MS ;	0.8	2.8 ± 0.2; 0.20pg/ml LOD	45
human plasma	--	--	Gradient elution: Acetonitrile:0.1 MAmmonium acetate	C18 column 250×4.6 mm i.d	fluorescence detector, em= 350nm ex=400nm	1.0	1ng/ml LOQ	46
Human Plasma	--	Protein Precipitation with Acetonitrile	Acetonitrile: 0.02 M Ammonium phosphate (3.5 pH), 65:35 v/v	C18 column504.6 mm i.d,3µm particle size	fluorescence detector, em= 350nm ex=400nm	1.5	3.2min; 3ng/ml LLOQ	47
Human Plasma	Imipramine	Protein precipitation	Acetonitrile: Methanol: Water (containing 0.05% (v/v) formic acid),70:20:10 v/v/v	C8 column 50×4.6mm i.d, 5 µm particle size	LC-MS/MS-ESI	1.2	0.76min	48

Matrix	Internal Standard	Sample preparation	Mobile phase	Column	Detector and detection wavelength	Flow rate (ml/ min)	Rt and LOD	Ref.
Human Plasma	Quinine sulphate	Liquid Liquid Extraction	10 mMAmmonium acetate buffer (3.0 pH) : Acetonitrile, 35:65 v/v	C8 column 150 × 4.6 mmi.d, 5µm particle size	fluorescence detector, em=350nm ex=400nm	1.0	12 min; 5ng/ml LOD	49
Human Plasma	amlodipine	Liquid Liquid Extraction	10mM Ammonium acetate (6.4 pH): acetonitrile 15:85 v/v	C18 column 50 × 4.6 mmi.d, 5 µm particle size	MS (ESI)	0.5	2.77min; 0.25ng. ml LLOQ	50
Human Plasma	Zafirlukast	Protein Precipitation with Acetonitrile	Acetonitrile: 0.1% Formic acid, 84:16 v/v	C18 column 50 × 4.6 mm i.d, 1.8 µm particle size	MS	0.6	0.11ng/ ml LOQ	51
Human Plasma	montelukast-d6	Liquid Liquid extraction	20 mM Ammonium formate: Acetonitrile , 20:80 v/v	RP18e column 100× 4.6 mmi.d, 5 µm particle size	LC-MS/MS-ESI	1.2	2.5min	52
human plasma	montelukast d6	solid phase extraction	Acetonitrile: 5mM Ammonium acetate, 80:20 v/v	Phenyl column 75× 4.6 mmi.d, 3.5 µm particle size	LC-MS/MS-ESI	0.8	1.30min; 4.57 0.10 ng/ml LLOQ	53
Sheep plasma	montelukastd6	Protein Precipitation with Acetonitrile	mobile phase A (0.5% Formic acid: water) Mobile Phase B (0.5% Formic acid:Acetonitril)	RP18e column 25×4.6 mm i.d	LC-MS/MS-ESI	2.0	0.36 ng/mL LOQ	54
Human Plasma	--	Protein Precipitation with Acetonitrile	Acetonitrile : 0.05 M Ammonium phosphate buffer (pH 3.5), 62:38 v/v	C18 column 50 x4.6 mm i.d, 3µm particle size	fluorescence detector, em= 350nm ex=400nm	--	4.0min; 5ng/ml LOD	55
human plasma	--	Protein Precipitation with Acetonitrile	Solution 1: Methanol: 10mM Ammonium acetate (3.6 pH), 10:100 v/v Solution 2: Acetonitrile-10mM Ammonium acetate (5.8 pH), 32.5:100 v/v	Chiral AGP column 100× 4.0mmi.d, 5 µm particle size	fluorescence detector, em= 350nm ex=400nm	1.0	23min; 9.6ng/ ml	56

Matrix	Internal Standard	Sample preparation	Mobile phase	Column	Detector and detection wavelength	Flow rate (ml/ min)	Rt and LOD	Ref .
human plasma	Quinine bisulfate	Protein Precipitation with Acetonitrile	0.025 M Sodium acetate (4.0 pH): Acetonitrile, with 50 ml triethylamine (20:80% v/v)	C8 column 100 ×8 mm i.d, 4 µm particlesize	fluorescence detector, em= 350nm ex=400nm	1.0	1ng/ml LOD	57

3.2.2 HPTLC

High performance thin layer chromatographic technique has been widely accepted for drug analysis. It provides the advantages of ease of handling, short analysis time and flexibility to study a wide variety of compounds. About six HPTLC methods have been reported for quantitative analysis of montelukast sodium (Table 4). Mobile phase consisting of a combination of three or more solvents have been reported for montelukast sodium estimation(33, 58-62). The lowest detection limit reported is 1.536ng/spot (61). The detector involved in all the methods is UV detector.

Table 4 Reported HPTLC methods for determination of Montelukast sodium

Analyte and Matrix	Mobile Phase	Detector	Detection Wavelength (nm)	Rf	LOD (ng/spot)	Ref
Montelukast and Theophylline in bulk and tablet	Ethylacetate: Chloroform: Ethanol: Ammonia(6:4:3:1v/v/v/v)	UV	254	0.32 ± 0.01 (MONT) and 0.52 ±0.01 (THEO)	131.01 (MONT) and 597.82 (THEO)	58
Montelukast Sodium and LevocetirizineDihydrochloride in bulk and tablet	Toluene:EthylAcetate: Methanol:Ammonia (2.5: 7: 2.5: 1, v/v/v/v)	UV	231	0.31 (LEVO) 0.44 (MON)	90 (LEVO) 50 (MON)	33
Montelukast and Cetirizine in tablet	Ethyl Acetate : Methanol : Ammonia solution (25%) (14 : 3 : 2 v/v/v)	UV	230	0.30 ± 0.01 (CET) 0.52 ± 0.02 (MON)	3.94 (CET) 2.08 (MON)	59
Montelukast Sodium and Levocetirizine Dihydrochloride in tablet	ethyl Acetate: Methanol:Triethylamine (5:5:0.02 v/v/v)	UV	240	0.29±0.02 (MLS) 0.50±0.02 (LCD)	20.63 (MLS) 21.12 (LCD)	60
Montelukast Sodium and LevocetirizineDihydrochloride in tablet	Chloroform: Methanol: Toluene: Glacial acetic acid (10:5:3:0.5 v/v/v/v)	UV	269	0.89 (MON) 0.64 (LEVO)	1.536 (MON) 2.864 (LEVO)	61
Montelukast Sodium in bulk and tablet	Toluene:EthylAcetate: Glacial acetic acid (6.0:3.4:0.1 v/v/v)	UV	344	--	--	62

3.2.3 Ultra Performance Liquid Chromatography (UPLC)

Hanimi Reddy Bapatu*et al.* have developed a stability indicating UPLC method for montelukast impurities in montelukast sodium(MON) oral granules(63). The separation of the pure API and impurities were obtained on Acquity C18, 1.7µm (100 x 2.1 mm)column with a gradient elution of two solutions; mixture of buffer and acetonitrile (70:30 v/v) and mixture of buffer and acetonitrile in (30:70 v/v). The buffer composed 0.03M phosphate buffer and 1% of Sodium perchlorate and pH was adjusted to 4.9with ortho-phosphoric acid. Flow rate was 0.5mL/min, detection wavelength was 225nm and column temperature was maintained at 30°C. The method demonstrates quantitative determination of six montelukast impurities in pharmaceutical oral dosage forms in a run time of 45min. Specificity of the method has been evaluated by Forced degradation studies to generate the degradation products of the API and known impurities were spiked to the standard solution. Pure peak of MON is reported at 21.29min.

3.4 Electrochemical Analysis

Electrochemical methods of analysis posses the advantage of lesser analysis time and cost, higher sensitivity, wider linearrange, lower detection limits and portability in comparison to the other instrumental analytical techniques that require prior sample preparation, sophisticated instruments, reagents, precautions and experience (64).

N. Aslan*et al.* have for the first time published a potentiometric titration method for the estimation of montelukast sodium[MON] in a pharmaceutical preparation as well as its protonation constant (65). MON was titrated potentiometrically with hydrochloric acid as a titrant in 40% ethanol and 60% water (v/v) mixture. Potentiometric titration curve has been given and Gran's method was used for the determination of equivalence points from the potentiometric data. Authors have indicated that the similarity of the potentiometric titration curve of pure API and marketed formulations prove that the excipients added to the pharmaceutical formulation do not affect the titration curve.

I. Alsarra*et al.*reported the electrochemical property of montelukast sodium [MKST] and specifically its voltammetric behaviour(66) for the first time. Differential pulse polarographic analysis was performed on MKST in 0.1N HCl having 25% methanol as solubiliser. At pH values above 5, a decrease in diffusion current of MKST has been reported. The polarograms were generated at a scan rate 10mV/s with pulse amplitude of -50mV.The authors have demonstrated the cathodic reduction response of MKST and the involvement of reducible ethenyl group in conjugation with the quinoline nucleus and the phenyl group. The proposed method is free from interference of other API in combined pharmaceutical formulations.The limit of detection was found to be 3.41×10^{-7} M.

Ali F. Alghamdi et al. have published quantitative analysis of montelukast sodium by adsorptivestripping voltammetric method (67). The optimised experimental parameters for the voltammetric measurements were accumulation at -0.4V for 180secwith stirring at 3000rpm. The supporting electrolyte used was Britton-Robinson buffer at pH10. The applied potential was scanned at 650 mV/s, 130 Hz SW frequencyrate and 50 mV pulse amplitude. The detection limit for the proposed method was found to be 4×10^{-9} mol/L.

BernuColkesen*et al.*for the first time have reported investigation of montelukat sodium (MKST) using zinc oxide nanoparticles modified carbon paste electrode (ZnO-NP-CPE) (64).The use of mercury having toxic properties in the dropping mercury electrode has been avoided. The authors have explored the use of the ZnO nanoparticles having unique properties like fastelectron transfer kinetics and electrochemical activities. A square wave cathodicadsorptive stripping voltammeric method (SWCAdSV)was developed for estimation of MKST in pharmaceutical preparations as well as biological fluids. The LOD for the proposed method was found to be 7.7×10^{-9}mol/L.

3.5 Capillary Electrophoresis

YuliyaShakalisava et al. studied the separation of montelukast (MON) from its impurities by capillary electrophoresis and HPLC method (68). The authors found cyclodextrins had a positive effect on separation of compounds with structural similarity. Separation of MON from the impurities and it cis-isomer were obtained by using 20 mM borate buffer (pH 9.2) with 10 mM SDS and 10 mM (2-hydroxypropyl)-γ-CD (2HP-γ-CD). The results indicate that the analysis time for a single sample was 9min by the optimised CD-modified MEKC(Micellarelectrokinetic chromatography) method in comparison to the HPLC method having a run time of about 33min to resolve MON from its impurities. The Efficiency of the electrophoretic method (936859±34080 theoretical plates) was found to be higher in comparison to that of the HPLC method (3544±10 theoretical plates).

3.6 Spectrofluorometric

I. Alsarra et al. have developed a spectrofluorometric for estimation of montelukast (MKST) in dosage forms and human plasma (69). Methanol has been used as a solvent as MKST showed maximum fluorescence intensity in methanol compared to other solvents. The excitation and emission wavelengths were 340nm and 390nm respectively. Authors have reported the effects of different surfactants on the fluorescence intensity of MKST. Triton X 100 and β-cyclodextrin showed positive effect on fluorescence intensity of MKST while gelatine, CMC and sodium dodecyl sulphate showed negative effect. The authors have reported the effect of artificial daylight on the stability of MKST solution. Exposure to deuterium lamp did not affect the fluorescence intensity of the drug while the exposure to xenon lamp showed a decrease in fluorescence intensity by 50% in 25min. The LOD for the proposed method was found to be 0.02µg/ml for MKST. The proposed method was applied to paediatric tablets, chewable tablets and human plasma for assay of MKST.

4. CONCLUSION

This review is aimed at focussing on the thorough literature survey of the various analytical techniques reported for the assay of montelukast solid from different sample matrices. The literature review supports the fact that for estimation of montelukast sodium from biological samples where the concentration of the drug is in very small amount, the choice of detector becomes crucial. Reported methods show that only fluorescence detector (up to nanogram level) and mass spectrometer (up to picogram level) are effective for detection of the drug in the biological matrix. PDA detector has been reported for estimation of the drug in bulk and pharmaceutical dosage form only. The conventional UV spectroscopy has been used for assay of the drug individually or in combination with other API from bulk or a dosage form where the concentration of the analyte is higher in comparison to the biological sample. The presence of multiple drugs in a formulation causes a crucial challenge to the analyst during the selection of spectrophotometric methods of analysis. The review has summarised the simultaneous estimation methods developed for the assay of montelukast sodium in presence of multiple drugs in a formulation. For such cases, chemometric techniques for quantitative analysis can be considered (70-71, 19).The review also highlights the use of electroanaytical techniques for the assay of montelukast sodium. These techniques provide the advantage of analysis of multiple samples in a short duration with specific and lower detection limits.

5. CONFLICT OF INTEREST

The authors declare that there is no conflict of interest.

6. ACKNOWLEDGEMENT

Dr. Vijaykumar Parmar and Ms. Kunti A. Shah has received research grant from GUJCOST (GUJCOST/MRP/2016-17/651), Department of Science and Technology, Government of Gujarat, India. Authors acknowledge Charotar University of Science and Technology for providing infrastructural and financial support for completion of the research project.

7. REFERENCES

1. Jones,T. R., Labelle, M., Belley, M., Champion, E., Charette, L., Evans, J., Ford-Hutchinson, A. W., Gauthier, J. Y., Lord, A. and Masson, P. (1995) 'Pharmacology of montelukast sodium (Singulair), a potent and selective leukotriene D4 receptor antagonist', *Canadian Journal of Physiology and Pharmacology*, vol. 73, February, pp. 191–201.
2. Nayak, A. (2004) 'A review of montelukast in the treatment of asthma and allergic rhinitis', *Expert Opinion on Pharmacotherapy.*,vol. 5, March, pp. 679-686.
3. Jarvis, B. and Markham, A. (2000) Montelukast. *Drugs*, vol. 59,pp. 891-928.
4. Huang, X., and Aslanian, R.G. (ed) (2012) *Case studies in modern drug discovery and development*, New Jersey: John Wiley & Sons, Inc.
5. Belley, M.L., Leger, S., Labelle, M., Roy, P., Xiang, Y.B. and Guay, D., inventor; Merck Frosst Canada, Inc., assignee. Unsaturated hydroxyalkylquinoline acids as leukotriene antagonists. United States Patent 5,565,473. 1996 Oct 15.
6. Staton, T. *Merck - 10 Largest U.S. Patent Losses*, [online], Available: https://www.fiercepharma.com/special-report/merck-10-largest-u-s-patent-losses [02 Dec 2017].
7. https://www.accessdata.fda.gov/drugsatfda_docs/ label/2009/020829s051_020830s052_021409s028lbl.pdf[02 Dec 2017].
8. http://www.medlineindia.com/respiratory/montelukast.htm[02 Dec 2017].
9. http://www.drugsupdate.com/brand/showavailablebrands/327/1[02 Dec 2017].

10. Indian Pharmacopoeia 2014. Volume 2. Ghaziabad: The Indian Pharmacopoeia Commission; 2014.Montelukast sodium; p. 2247-2248.
11. British Pharmacopoeia 2016. Volume 2. London: The Stationery Office; 2015. Montelukast sodium; p. 317-319.
12. U.S. Pharmacopoeia-National Formulary [USP 39 NF 34] 2016. Volume 3. Rockville, Md: United States Pharmacopeial Convention, Inc; 2015.Montelukast sodium; p. 4930-4938.
13. Okumu, A., DiMaso, M. and Lobenberg. R. (2008) 'Dynamic Dissolution Testing To Establish In Vitro/In Vivo Correlations for Montelukast Sodium, a Poorly Soluble Drug', *Pharmaceutical Research*, Vol. 25, December, pp. 2778-2785.
14. Shanmukhakumar, J.V., Ramachandran, D., Settaluri, V.S. and Felice, C.S. (2010) 'Spectrophotometric methods for estimation of leukotriene receptor antagonist in bulk dosage forms', *Rasayan journal of chemistry*, vol. 3, January, pp. 166-171.
15. Arayne, M.S., Sultana, N. and Hussain F. (2009) 'Spectrophotometric Method for Quantitative Determination of Montelukast in Bulk, Pharmaceutical Formulations and Human Serum', *Journal of Analytical Chemistry*, vol. 64, July, pp. 690-695.
16. Patel, R.B., Parmar, R.R., Patel, V.M. and Shah, D.A. (2012) 'Simultaneous estimation of montelukast sodium and theophylline in pharmaceutical dosage form by UV spectrophotometric method', *International Journal of Institutional Pharmacy and Life Sciences*, vol. 2, March, pp. 150-160.
17. Bankar, R.M. and Patel, D.B. (2013) 'Spectrophotometric Determination of Montelukast Sodium and Desloratadine in Combined Dosage Form', *International Journal of ChemTech Research*, vol. 5, January, pp. 136-141.
18. Bankar, R.M. and Patel, D.B. (2013) 'Simultaneous estimation of montelukast sodium and desloratadine by ratio spectra derivative spectrophotometry method in combined dosage form', *Journal of Chemical and Pharmaceutical Research*, vol. 5, pp. 193-199.
19. Hassaninejad-Darzi, S.K., Maybodi, A.S. and Nikou, S.M. (2016) 'UV-Vis Spectrophotometry and Multivariate Calibration Method for Simultaneous Determination of Theophylline, Montelukast and Loratadine in Tablet Preparations and Spiked Human Plasma', *Iranian Journal of Pharmaceutical Research*, vol. 15, pp. 379-391.
20. Choudhari, V.P., Kale, A.N., Polshettiwar, S.A., Sutar, A.S., Patel, D.M. and Kuchekar, B.S. (2011) 'Derivative and Absorption Factor Spectrophotometric Estimation of Montelukast Sodium and LevocetirizineDihydrochloride from Pharmaceutical Formulations', *Research Journal of Pharmacy and Technology*, vol. 4, March, pp. 389-392.
21. Choudekar, R.L., Mahajan, M.P. and Sawant, S.D. (2012) 'Spectrophotometric Estimation of RupatadineFumarate and Montelukast Sodium in Bulk and Tablet Dosage Form', *International Journal of Pharmacy and Pharmaceutical Sciences*, vol. 4, May, pp. 737-740.
22. Maniya, J., Raj, H., Vaghani, H., Mangukiya, M. andDudhat, P. (2012) 'Development and Validation of Spectroscopic Method for Simultaneous Estimation of Acebrophylline and Montelukast Sodium in Combined Dosage Form', *Indo American Journal of Pharmaceutical Research*, vol. 2, October, pp. 1027-1036.
23. Patel, P.G., Vaghela, V.M., Rathi, S.G., Rajgor, N.B. and Bhaskar, V.H. (2009) 'Derivative Spectrophotometry Method for Simultaneous Estimation of Rupatadine and Montelukast in their Combined Dosage Form', Journal of Young Pharmacists, Vol.2, October, pp. 354-358.
24. Rashmitha, N., Sunder Raj, T.J., Srinivas, C.H., Srinivas, N., Ray, U.K., Sharma, H.K. and Mukkanti, K. (2010) 'A Validated RP-HPLC Method for the determination of Impurities in Montelukast Sodium', E-Journal of Chemistry, vol. 7, pp. 555-563.
25. Singh, R.M., Saini, P.K., Mathur, S.C., Singh, G.N. and Lal, B. (2010) 'Development and Validation of a RP-HPLC Method for Estimation of Montelukast Sodium in Bulk and in Tablet Dosage Form', *Indian Journal of Pharmaceutical Sciences*, vol. 72, March, pp. 235-237.
26. Jain, P., Rajoriya, V. and Kashaw, V. (2015) 'Development and Validation of Simultaneous RP-HPLC Method for the Estimation of Theophylline and Motelukast in Pharmaceutical Formulation', Analytical Chemistry Letters, vol. 5, November, pp. 172-182.
27. Revathi, R., Ethiraj, T., Thenmozhi, P., Saravanan,

V.S. and Ganesan, V. (2011) 'High performance liquid chromatographic method development for simultaneous analysis of doxofylline and montelukast sodium in a combined form', Pharmaceutical Methods, vol. 2, October, pp. 223-228.

28. Eldin, A.B., Shalaby, A.A. and El-Tohamy, M. (2011) 'Development and validation of a HPLC method for the determination of montelukast and its degradation products in pharmaceutical formulation using an experimental design', ActaPharmaceuticaSciencia, vol. 53, pp. 45-56.
29. Garg,L.K., Reddy, V.S., Sait, S.S., Krishnamurthy, T., Vali, S.J. and Reddy, A.M. (2013) 'Quality by Design: Design of Experiments Approach Prior'to the Validation of a Stability-Indicating HPLC Method for Montelukast', Chromatographia, vol. 76, August, pp. 1697-1706.
30. Chauhan, P.H., Jani, H.D., Luhar, S.V. and Pirani, N.A. (2016) 'Development and Validation of Analytical Method for Simultaneous Estimation of Theophylline and Montelukast in Pharmaceutical Dosage Form', Journal of Pharmaceutical Science and Bioscientific Research, vol. 6, April, pp. 315-321.
31. Shanmukha Kumar, J.V., Ramachandran, D. and Saradhi, S.V. (2010) 'RP-HPLC Method for the Estimation of Montelukast Sodium in Pharmaceutical Dosage Forms', Current Trends in Biotechnology and Pharmacy, vol. 4, October, pp. 943-946.
32. Kanakadurgadevi, N., Rani, A.P., Madhavi, B.R. and Mrudula, B.S. (2010) 'New RP- HPLC Method for the Analysis of Montelukast Sodium in Pharmaceutical Dosage Forms', *International Journal of ChemTech Research*, vol. 2, January, pp. 471-475.
33. Rathore, A.S., Sathiyanarayanan, L. and Mahadik, K.R. (2010) 'Development of Validated HPLC and HPTLC Methods for Simultaneous Determination of LevocetirizineDihydrochloride and Montelukast Sodium in Bulk Drug and Pharmaceutical Dosage Form', *PharmaceuticaAnalyticaActa*, vol. 1, September, pp. 1-6.
34. Vekaria, H., Limbasiya, V. and Patel, P. (2013) 'Development and validation of RP-HPLC method for simultaneous estimation of Montelukast Sodium and Fexofenadine hydrochloride in combined dosage form', *Journal of Pharmacy Research*, vol. 6, January, pp. 134-139.
35. Patil, S., Pore, Y.V., Kuchekar, B.S., Mane, A. and Khire, V.G. (2009) 'Determination of Montelukast Sodium and Bambuterol Hydrochloride in Tablets using RP HPLC', Indian *Journal of Pharmaceutical Sciences*, vol. 71, January, pp. 58-61.
36. Gandhi, B.M., Rao, A.L. and Rao, J.V. (2015) 'Method Development and Validation forSimultaneous Estimation of Montelukast Sodium and Desloratadine by RP-HPLC',*American Journal of Analytical Chemistry*, vol. 6, July, pp. 651-658.
37. Gandla, K., Spandana, R., Kumar, J.M.R., Surekha, M.L. and SheshgiriRao, J.V.L.N. (2012) 'Simultaneous RP-HPLC method for estimation of rupatadinefumarate and montelukast sodium in tablet dosage form', *Der Pharma Chemica*, vol. 4, pp. 1819-1825.
38. Kumar, K.P., Haque, M.A., Kumar, T.P., Nivedita, G., Amrohi, S.H., Prasad, V.V.L.N and Diwan, P.V. (2012) 'Simultaneous Determination of Montelukast Sodium and Fexofenadine Hydrochloride in Combined Dosage Form by Using RP-HPLC Method', *World Journal of Chemistry,* vol. 7, July, pp.42-46.
39. Hoang, T.H., Farkas, R., Wells, C., McClintock, S. and Di Maso, M. (2002) 'A pplication of pressurized liquid extraction technology to pharmaceutical solid dosage form analysis', Journal of Chromatography A, vol. 968, August, pp. 257-261.
40. Shrikrishna, B. and Nisharani, R. (2015) 'Analytical Method Development and Validation for Simultaneous Estimation of Montelukast and Ebastine by HPLC', *Research Journal of Pharmacy and Technology*, vol. 8, January, pp. 01-05.
41. Radhakrishna, T., Narasaraju, A., Ramakrishna, M. and Satyanarayana, A. (2003) 'Simultaneous determination of montelukast and loratadine by HPLC and derivative spectrophotometric methods', *Journal of Pharmaceutical and Biomedical Analysis*, vol. 31, February, pp359-368.
42. Roman, J., Breier, A.R. and Steppe, M. (2011) 'Stability Indicating LC Method to Determination of Sodium Montelukast in Pharmaceutical Dosage Form and its Photodegradation Kinetics', Journal of Chromatographic Science, vol. 49, August, pp. 540-546.
43. Radhakrishnanand, P., SubbaRao, D.V., Surendranath, K.V., Subrahmanyam, D. and Himabindu, V. (2008) 'A Validated LC Method for

Determination of the Enantiomeric Purity of Montelukast Sodium in Bulk Drug Samples and Pharmaceutical Dosage Forms', Chromatographia, vol. 68, June, pp. 263-267.

44. Sripalakit, P., Kongthong, B. and Saraphanchotiwitthayad, A. (2008) 'A simple bioanalytical assay for determination of montelukast in human plasma: Application to a pharmacokinetic study', Journal of Chromatography B, vol. 869, June, pp. 38-44.
45. Challa, B.R., Awen, B.Z., Chandu, B.R., Khagga, M. and Kotthapalli, C.B. (2010) 'Method Development and Validation of Montelukast in Human Plasma by HPLC Coupled with ESI-MS/MS: Application to a Bioequivalence Study', ScientiaPharmaceutica, vol. 78, July, pp411-422.
46. Ochiai, H., Uchiyama, N., Takano, T., Hara, K. and Kamei, T. (1998) 'Determination of montelukast sodium in human plasma by columnswitching high-performance liquid chromatography with fluorescence detection', Journal of Chromatography B: Biomedical Sciences and Applications, vol. 713, August, pp. 409-414.
47. Kitchen, C.J., Wang, A.Q., Musson, D.G., Yang, A.Y. and Fisher, A.L. (2003) 'A semi-automated 96-well protein precipitation method for the determination of montelukast in human plasma using high performance liquid chromatography/fluorescence detection', *Journal of Pharmaceutical and Biomedical Analysis*, vol. 31, March,pp. 647-654.
48. Patel, N.K., Subbaiah, G., Shah, H., Kundlik, M., Sanyal, M. and Shrivastav, P.S. (2009) 'Rapid Determination of Montelukast in Human Plasma by LC-ESI-MS/MS and Its Application to a Bioequivalence Study', *Analytical Letters*, vol. 42, September, pp. 2041-2059.
49. Chauhan, B., Rani, S., Nivsarkar, M. And Padh, H. (2006) 'A new liquid liquid extraction method for determination of Montelukast in Small Volume Human Plasma Samples Using HPLC with Fluorescence detector', Indian Journal of Pharmaceutical Sciences, vol. 68, July, pp. 517-520.
50. Bharathi, D.V., Hotha, K.K., Jagadeesh, B., Mullangia, R. and Naidu, A. (2009) 'Quantification of montelukast, a selective cysteinyl leukotriene receptor (CysLT1) antagonist in human plasma by liquid chromatography–mass spectrometry: validation and its application to a human pharmacokinetic study', *Biomedical Chromatography*, vol. 23, March, pp. 804-810.
51. Ezzeldin, E., Abo-Talib, N.F., Tammam, M.H. and Shahat, A.A. (2014) 'Development and validation of LC/MS/MS method for the simultaneous determination of montelukast, gliclazide, and nifedipine and its application to a pharmacokinetic study', Chemistry Central Journal, vol. 08, March, pp. 17-25.
52. Muppavarapua, R., Guttikara, S., Rajappanb, M., Kamarajanb, K. and Mullangic, R. (2014) 'Sensitive LC-MS/MS-ESI method for simultaneous determination of montelukast and fexofenadine in human plasma: application to a bioequivalence study', *Biomedical Chromatography,* vol. 28, August, pp. 1048-1056.
53. Katteboinam M.Y., Pilli, N.R. and Satla, S.R. (2015) 'LC-MS/MS method development and validation of Montelukast in human plasma and its clinical application', *AmericanJournal of PharmTech Research*, vol. 5, June, pp. 646-657.
54. Papp, R., Luk, P., Mullett, W.M. and Kwong, E. (2007) 'A rapid and sensitive method for the quantitation of montelukast in sheep plasma using liquid chromatography/tandem mass spectrometry', *Journal of Chromatography B*, vol. 858, August, pp. 282-286.
55. Amin, R.D., Cheng, H. and Rogers, J.D. (1995) 'Determination of MK-0476 in human plasma by liquid chromatography', *Journal of Pharmaceutical & Biomedical Analysis*, vol. 13, February, pp. 155-158.
56. Liu, L., Cheng, H., Zhao, J.J. and Rogers, J.D. (1997) 'Determination of montelukast (MK-0476) and its S-enantiomer in human plasma by stereoselective high-performance liquid chromatography with column-switching', Journal of Pharmaceutical and Biomedical Analysis, vol. 15, February, pp. 631-638.
57. Al-Rawithia, S., Al-Gazlanb, S., Al-Ahmadia, W., Alshowaier, I.A., Yusuf, A. and Raines, D.A. (2001) 'Expedient liquid chromatographic method with fluorescence detection for montelukast sodium in micro-samples of plasma', *Journal of Chromatography B*, vol. 754, April, pp. 527-531.

58. Sangeetha, M. and Mahendran, C. (2016) 'Development and Validation of HPTLC Method for Simultaneous Estimation of Montelukast and Theophylline in Bulk and Pharmaceutical Dosage Form', *Journal of Chemical and Pharmaceutical Research*, vol. 8, pp. 203-208.

59. Haghighia, S., Shapouria, M.R., Divab, M.A., Pourghazia, K. and Afruzia, H. (2013) 'HPTLC-Densitometric Determination of Cetirizine and Montelukast Analysis in Combined Tablet Dosage Forms', *Iranian Journal of Pharmaceutical Research*, vol. 12, Spring, pp. 303-309.

60. Rote, A.R. and Niphade, V.S. (2011) 'Determination of Montelukast Sodium and LevocetirizineDihydrochloride in Combined Tablet Dosage Form by HPTLC and First-Derivative Spectrophotometry', *Journal of Liquid Chromatography & Related Technologies*, vol. 34, February, pp. 155-167.

61. Sharma, S., Sharma, M.C., Kohlib, D.V. and Sharma, A.D. (2010) 'Development and Validation of TLC-Densitometry Method for Simultaneous Quantification of Montelukast Sodium and LevocetirizineDihydrochloride Pharmaceutical Solid dosage form', *Der Pharmacia Lettre*, vol. 2, pp. 489-494.

62. Sane, R.T., Menezes, A., Mote, M., Moghe, A. and Gundi G. (2004) 'HPTLC determination of montelukast sodium in bulk drug and in pharmaceutical preparations', Journal of Planar Chromatography – Modern TLC, vol. 17, January, pp. 75.

63. Bapatua, H.R., Kumar, M.R., Garg, L.K., Venugopal, D. and Reddy, A.M. (2012) A Validated Stability Indicating UPLC Method for Montelukast Impurities in Montelukast Sodium Oral Granules',International Journal of Pharma and Bio Sciences', vol. 3, January, pp. 345-355.

64. Colkesen, B., Ozturk, F. and Erdenb, P.E. (2016) 'Electroanalytical Characterization of Montelukast Sodium and Its Voltammetric Determination in Pharmaceutical Dosage Form and Biological Fluids', *Journal of the Brazilian Chemical Society,* vol. 27, May, pp. 849-856.

65. Aslan, N., Erden, P.E., Canel, E. and Kilic, E. (2014) 'Development and validation of a potentiometric titration method for the determination of montelukast sodium in a pharmaceutical preparation and its protonation constant', Bulgarian Chemical Communications, vol. 46, pp. 497-502.

66. Alsarra, I., Al-Omar, M., Gadkariem, E.A. and Belal, F. (2005) 'Voltammetric determination of montelukast sodium in dosage forms and human plasma', Il Farmaco, vol. 60, May, pp. 563-567.

67. Alghamdi, A.F. (2014) 'Voltammetric Analysis of Montelukast Sodium in Commercial Tablet and Biological Samples Using the Hanging Mercury Drop Electrode', *PortugaliaeElectrochimicaActa*, vol. 32, January, pp. 51-64.

68. Shakalisava, Y. and Regan, F. (2008) 'Determination of montelukast sodium by capillary electrophoresis', *Journal of Separation Science*, vol. 31, April, pp. 1137-1143.

69. Alsarra, I., Khalil, N.Y., Sultan, M., Al-Ashban, R. and Belal, F. (2005) 'Spectrofluorometric determination of montelukast in dosage forms and spiked human plasma', *Pharmazie*, vol. 60, November, pp. 823-826.

70. Ragab, M.A. and Youssef, R.M. (2013) 'Simultaneous Determination of Montelukast and Fexofenadine using Fourier Transform Convolution Emission Data under Non-Parametric Linear Regression Method', *Journal of Fluorescence*, vol. 23, November, pp. 1329-1340.

71. Darzi,H. and Karim, S. (2017) 'Rapid and Simultaneous Determination of Montelukast, Fexofenadine and Cetirizine Using Partial Least Squares and Artificial Neural Networks Modeling', *Iranian Journal of Chemistry and Chemical Engineering*, vol. 36,Spring, pp. 81-96

Review Article

Microbial Chitinase and its potential application for biological control of plant parasites

Farhat Z Marchawala[1], Seema R Amin[1]*

[1]Department of Biological Sciences, P.D.Patel Institute of Applied Sciences, Charotar University of Science and Technology (CHARUSAT), Changa-388421, Gujarat, India.

Received: 25/01/2018
Revised: 10/05/2018
Accepted: 17/12/2018

Correspondence to:
*Amin Seema R.:
seemaamin.bt@charusat.ac.in

Abstract:

Chitin is the second most abundant polysaccharide in nature after cellulose, which is mainly found in the exoskeleton of insects, fungi, yeast, algae, and in the internal structures of other vertebrates, which are mostly plant parasites. At present, chemical pesticides are the major means of controlling these disease-causing agents. However, as these chemicals cause potential harm to the environment, human and animal health, new strategies are being developed to replace or reduce the use of such compounds in agriculture. Chitinase are enzymes that degrade chitin, resulting in severe damage and even death in pathogens and pests whose external and internal surfaces contain this polymer. In this perspective, chitinolytic microorganisms are likely to play an important role as biological control agents in agriculture fields against plant pathogens. In this review, various types of microbial chitinase and their role as biological control agents are thoroughly discussed.

Keywords: Microbial chitinase, fungicidal, pesticidal, nematicidal

INTRODUCTION

Chitin, a linear polymer of β-1, 4-N-acetylglucosamine (GlcNAC), is the second most abundant biopolymer on the planet after cellulose (Shahidi and Abozaytoun 2005). It is found in the shells, exoskeletons, and gut linings of arthropods mainly crustaceans and insects. It also comprises the cell walls of many fungi, including some yeasts, and makes up the structural frameworks of certain Protista as well as of nematode eggs (Stoykov et al. 2015). According to previous studies, estimated amount of crop loss due to diseases in the field was up to 40% preharvest- and additionally 10% postharvest (Chandler et al. 2011). The main cause of these losses are insects, weeds, and plant parasites. Subsequently, crops worldwide are completely dependent on the use of chemical pesticides to reduce crop loss, but the major problem of using these chemicals is that the target organisms often develop resistance to them (Russell, P.E. 2006), and non-target organisms and the surrounding environment too face the hazardous effects of chemicals employed. Many human health problems have been linked to pesticide use. Hence, it is important to find out an alternative to these chemical pesticides that is not harmful to humans and to the surrounding environment, besides degrading the chitin present in various plant parasites.

STRUCTURE OF CHITIN

Chitin is a white, hard, inelastic polysaccharide having high percentage of nitrogen (6.89%). It exists in three crystalline forms i.e. α-chitin, β-chitin γ-chitin, which differ in the arrangement of polymer chains

giving them different mechanical properties (Jang et al. 2004). These forms of chitin vary in packing and polarities of adjacent chains in the succeeding sheets (Chen et al. 2010). In the environment, chitin is found in fully acetylated state to its completely deacetylated form which is known as chitosan (Beier and Bertilsson 2013). Because of the ubiquity of chitin in the environment, its degradation has been extensively considered (Nagpure et al. 2014). There is a dire need of a biological substitute for harmful chemicals used as chitin degraders. Insect cuticle, fungal cell wall and nematodes eggshells comprises chitin biopolymer as a protective barrier against harmful chemicals and environmental factors. So based on these findings, microbial chitinase can be employed to degrade chitin to control these plant parasites.

DEGRADATION OF CHITIN BY CHITINASE

Chitinase enzyme degrades chitin. It is secreted by a wide range of organisms for carrying out various functions such as morphogenesis, nutrient cycling, as well as in defense against chitin containing pests and parasites (Dahiya et al. 2006). The catabolism of chitin takes place in 2 steps involving the initial cleavage of the chitin polymer by chitinase into chitin oligosaccharides, and further cleavage to N-acetylglucosamine. Whereas, monosaccharides are cleaved by chitobiases (Suginta et al. 2000). Chitinase (E.C 3.2.2.14) are glycosyl hydrolases with their size ranging from 20 kDa to about 90 kDa (Bhattacharya et al. 2007). Chitinase have been divided into 2 main groups *viz* endochitinase and exochitinase. The endochitinase randomly split chitin at internal sites, thereby forming the dimer di-acetylchitobiose and soluble low molecular mass multimers of GlcNAc such as chitotriose, and chitotetraose. The exochitinase have Chitobiosidases, which are involved in catalyzing the progressive release of di-acetylchitobiose cleaving the oligomeric products of endochitinase and chitobiosidases, thereby generating monomers of GlcNAc (Sahai et al. 1993).Based on amino acid sequence of the enzyme, chitinases are grouped into different categories of glycoside hydrolase (GH) families such as GH18, GH19, and GH20. Most bacterial chitinase belong to the GH18 family (Adrangi and Faramarzi 2013). Chitinase are produced by wide range of organisms such as bacteria, fungi, plants, arthropods, and humans. Chitinase have been receiving an increased attention due to their role in the biocontrol of plant parasites (Mathivanan et al. 1998). Microbial chitinase weaken and degrade the important structures of many pests and pathogens, thereby exhibiting fungicidal, insecticidal, or nematicidal activity (Edreva, A. 2005). Chitinolytic enzymes will become a more obvious and important solution towards overcoming the environmental hazards that result from the application of synthetic pesticides and fungicides. Chitinase producing bacteria have been isolated from soil, shellfish waste, garden and park waste compost, and hot springs (Yuli et al. 2004). In marine environments, they are involved in the nutrient cycling of the substantial amount of chitin derived from arthropod shells and other sources (Souza et al. 2011). In the soil and rhizosphere, bacteria use chitin from insects and fungi as a carbon and nitrogen source (Cohen-Kupiec and Chet 1998, Geisseler et al. 2010).

In this review, we intent to broaden the understanding regarding chitinase, how it degrades the chitin, microbial chitinase and its potent application as biological control agents against plant parasites.

MICROBIAL SOURCES OF CHITINASE

Bacterial Chitinase

Microorganisms, particularly bacteria, form one of the major sources of chitinase (Bhattacharya et al. 2007). Bacteria produce chitinase mainly to degrade chitin and utilize it as an energy source. Microbial chitinase can hydrolyze chitin and partially N-acetylated chitosan as well (Mitsutomi et al. 1995). Bacterial chitinases are receiving increased attention due to their wide range of biotechnological applications especially in the production of chito-oligosaccharides and N-acetyl D-glucosamine (Pichyangkura et al. 2002), biocontrol of pathogenic fungi, preparation of sphaeroplast and protoplasts from yeast and fungal species (Balasubramanian et al. 2003), bioconversion of chitin waste to single cell protein (Dahiya et al. 2005), as well as one of the potential enzymes for applications in agriculture, pharmaceutical, waste management, biotechnology and industry (Gupta et al. 1995). Their high demand and varied uses has led to the discovery of new strains of microorganisms that are capable to produce enzymes with novel properties and the development of low cost industrial media formulations
(Saito et al. 2009).

Fungal Chitinase

Fungal chitinase, like bacterial chitinase, have multiple functions as they play an important role in nutrition, morphogenesis, and fungal development processes. Chitin is a major cell wall component of fungi (Sahai et al. 1993). The chitinase production in

filamentous fungi is seen throughout its life cycle. The main role of this enzyme is to help the fungi in releasing the spores and in hyphal elongation and branching (Muzzarelli et al. 2012). In yeast, chitinase helps in budding especially in cell separation. It also plays an important role in septa dissolution and gamete fusion (Gooday and Gow 1990). Chitinase is essential not only in the various developmental stages of fungi but also in fungal nutrition (Gunaratna and Balasubramanian 1994). It helps in utilization of chitin for its carbon and nitrogen requirements. In certain cases, it is also associated with pathogenicity of the organisms (Narayana and Vijayalakshmi 2009).

CHITINOLYTIC MICROORGANISMS AS POTENTIAL BIOLOGICAL CONTROL AGENTS

Among the bacteria used as biocontrol agents, the primary ones are species of *Streptomyces*, *Bacillus*, and *Pseudomonas* (Bélanger, R.R. 2001). Recent studies are focused on the search for alternatives to chemical pesticides and *B. thuringiensis* toxin, since plant parasites have developed resistance against both control agents. To this end, bacteria from different orders have been found to be effective biocontrol agents (Kalia and Gosal 2011).

Actinobacteria are important saprophytic soil bacteria which are known for antibiotic and secondary metabolite production, as well as for the synthesis of chitinolytic enzymes (Barka et al. 2016). They are among the most important taxa in the soil microbial chitinolytic community (Gonzalez-Franco et al. 2003). The purified chitinase from *Streptomyces rimosus* exhibited in vitro antifungal properties against *Fusarium solani* and *Alternaria alternate* (Brzezinska et al. 2013). Similarly, *Streptomyces viridificans* was found to lyse the fungal cell walls of *Rhizoctonia*, *Colletotrichum*, *Aspergillus*, *Fusarium*, *Sclerotinia*, *Curvularia*, and *Pythium* in vitro (Gupta et al. 1995).

Bacillus thuringiensis is a well-known biocontrol agent that has been in use for decades for pest control in agriculture. Many *B. thuringiensis* strains that constitutively express chitinase have been described (Liu D et al. 2010, Chen et al. 2007). Hollensteiner et al. (2017) isolated *B. thuringiensis* from tomato roots which exhibited in vitro antifungal activity against *Verticillium spp. Paenibacillus illinoisensis* isolated from coastal soil in Korea was reported to have strong in vitro chitinolytic activity when assayed on colloidal chitin. It also deformed and destroyed the eggshell of the root-knot nematode *Meloidogyne incognita* (Jung et al. 2002).

BIOCONTROL OF FUNGAL PHYTOPATHOGEN BY MICROBIAL CHITINASE

The fungal phytopathogens cause severe problems worldwide in the cultivation of economically important plants (Brimner and Boland 2003). Chitinase enzymes are able to lyse the cell wall of numerous fungi and the microbes which produce these enzymes are capable of eradicating these fungal pathogens. Normally chemical fungicides are used to reduce

Table: 1 Chitinase producing key agents for biocontrol of fungal plant pathogens (published from 2007 onwards)

Microbial antagonist	Fungal pathogen	References
Bacillus licheniformis	*Gibberella saubinetii, Aspergillus niger, Rhizoctonia solani*	Xiao et al 2009, Kamil et al 2007
Bacillus pumilus	*Rhizoctonia solani, Verticillium spp., Nigrospora sp., Stemphyllium botryosum, Bipolaris spp. Alternaria brassicicola*	Ghasemi et al 2010
Bacillus subtilis	*Aspergillus niger, Aspergillus flavus, Penicillium chrysogenum.*	Karunya S.K 2011
Pseudomonas spp	*Fusarium oxysporum*	Velusamy et al 2011
Serratia marcescens	*Rhizoctonia solani, Bipolaris spp., Alternaria raphanin, Fusarium solani, Aspergillus flavus*	Zarei et al 2011, Zeki and Muslim 2017
Aspergillus niger	*Fusarium culmorum, Fusarium solani, Rhizoctonia solani*	Brzezinska and Jankiewicz 2012
Trichoderma viride	*Rhizoctonia solani, Fusarium oxysporum, Pythium ultimum*	Fahmi et al 2012
Streptomyces griseus	*Fusarium oxysporum, Alternari alternate, Rhizoctonia solani, Fusarium solani, Aspergillus flavus*	Anitha and Rabeeth 2010

Table: 2 Microbial agents for pest management (published from 2007 onwards)

Microbial antagonist	Insect/Pest	Reference
Bacillus subtilis	*Spodoptera litura*	Chandrasekaran et al 2012
Bacillus thuringiensis subsp. *colmeri*	*Spodoptera exigua, Helicoverpa armigera*	Liu et al 2010
Pseudomonas fluorescens MP-13	*Helopeltis theivora*	Suganthi et al 2017
Serratia marcescens SEN	*Spodoptera litura*	Aggarwal et al 2015
Isaria fumosorosea	*Plutella xylostella*	Huang et al 2016
Pochonia chlamydosporia	*Bombyx mori*	Mi et al 2010
Trichoderma harzianum	*Helicoverpa armigera*	Binod et al 2007
Trichoderma viride	*Bombyx mori*	Berini et al 2016

fungal pathogens. But the extreme use of chemical fungicides had led to environmental problems along with induced pathogen resistance. These chemical compounds may be toxic to beneficial insects and microorganisms in the soil, and may also enter into the food chain (Budi et al. 2000). Biological control of plant pathogens by soil bacteria is a well-known fact and chitinase production by these bacteria has been shown to play an important role in suppressing them (Hong and Hwang 2006). Bolar et al. (2001) studied synergistic activity of endochitinase and exochitinase from *Trichoderma atroviride* against the pathogenic fungus *Venturia inaequalis* in transgenic apple plants. The principal chitinase producers for controlling fungal phytopathogens are enlisted in Table: 1.

MIRCOBIAL CHITINASE AS A BIOPESTICIDE

In an agricultural system, pesticides are used to protect plants/crops from damage by disease causing plant pathogens. Acknowledging the side effects of these chemicals, control of crop pests by use of biological agents is prerequisite (Table: 2). In insects, chitin functions as scafflold material that supports the cuticles of epidermis and trachea as well as the gut epithelium lining. Hence if chitin is targeted it would result in degradation of insect's

structures. Chitinase produced by *Bacillus spp*. is found to control *Aphis gossypii* (Nurdebyandaru et al. 2010). Daizo K (2005) sprayed chitinase directly to the strawberry plants and observed that plants were free from insects. Recently, Suganthi et al. (2017) isolated chitinase from *Pseudomonas fluorescens* that showed insecticidal activity against tea mosquito bug. These findings open up the possibility of using chitinase as a biopesticidal agent for integrated pest management strategies.

MICROBIAL CHITINASE AS A NEMATICIDAL AGENT

Global estimates of agricultural losses due to infections by plant-parasitic nematodes are of $ 130 billion annually (Becker, J.O. 2014). At present, chemical pesticides control nematodes but enzymes and the microbes which produce these enzymes (Table: 3) having nematicidal action are receiving an augmented attention. Cuticle in adult nematodes and eggshell play an important role in preventing nematophagous infection. The main component of cuticle is collagen which is degraded by microbial proteases during infection of adult nematodes. Eggshell is a more complex protective structure resulting in the increased survival rate of enveloped eggs, embryos or larvae against chemical and biological nematicides. In many studies, it was found that the chitinase has nematicidial effect on eggshell of nematodes (Wharton, D. 1980), and it was first investigated by (Mankau and Das 1969). They found that the chitin amendments controlled the citrus nematode *Tylenchulus semipenetrans* and the root-knot nematode *Meloidogyne incognita*. Later, chitin amendments were used to control *Tylenchorhynchus dubius* (Miller et al. 1973), *M. arenaria* (Mian et al. 1982), *M. javanica*, and the cereal cyst nematode *Heterodera avenae* (Spiegel et al. 1989). Purified chitinase inhibited egg hatch of *Globodera rostochiensis* up to 70% in vitro, and the chitinase-producing bacteria *Stenotrophomonas maltophilia* and *Chromobacterium sp*. reduced egg hatch of nematode both in vitro and in soil (Cronin et al. 1997). *Pseudomonas chitinolytica* reduced *M. javanica*

Table: 3 Microbial agents for biocontrol of plant parasitic nematodes (published from 2007 onwards)

Microbial antagonist	Target Nematode	Reference
Bacillus thuringiensis subsp. *tenebrionis*	*Caenorhabditis elegans* (juveniles)	Ni et al 2015
Pseudomonas aeruginosa	*Caenorhabditis elegans* (eggs, adult)	Chen et al 2017, Chen et al 2015
Pseudomonas fluorescens HN1205	*Meloidogyne incognita* (eggs)	Lee and kim 2015
Monacrosporium thaumasium NF34	*Panagrellus redivivus* (juveniles)	Soares et al 2015
Paecilomyces javanicus	*Meloidogyne incognita* (eggs, juveniles)	Chan et al 2010
Pochonia chlamydosporia	*Meloidogyne incognita* (eggs)	Mi et al 2010
Verticillium psalliotae	*Meloidogyne incognita* (eggs)	Gan et al 2007

infection and improved growth of tomato, *Lycopersicon esculentum* (Spiegel et al. 1991). The chitinolytic fungus, *Paecilomyces lilacinus*, destroyed nematode eggs and efficiently controlled *M. incognita* (Morgan-Jones et al. 1984).

CONCLUSION

Application of biological agents as a substitute to chemicals pesticides holds great possibilities to control a range of plant pathogens. More study on microbial chitinase by using genetic engineering tools will offer better understanding about chitinase genes, its overexpression resulting in better yield of enzymes and biotechnological applications in agriculture sector. By understanding biochemistry and protein engineering, one can produce microbial chitinase with specific functions that will make them more useful for various processes in near future.

REFERENCES

1. Adrangi, S., and Faramarzi, M. A. (2013). From bacteria to human: a journey into the world of chitinases. *Biotechnology advances*, *31*(8), 1786-1795.
2. Aggarwal, C., Paul, S., Tripathi, V., Paul, B., and Khan, M. A. (2015). Chitinase producing *Serratia marcescens* for biocontrol of *Spodoptera litura (Fab)* and studies on its chitinolytic activities. *Annals of Agricultural Research*, *36*(36), 132-137.
3. Anitha, A., and Rabeeth, M. (2010). Degradation of fungal cell walls of phytopathogenic fungi by lytic enzyme of *Streptomyces griseus*. *African Journal of Plant Science*, *4*(3), 061-066.
4. Balasubramanian, N., Juliet, G. A., Srikalaivani, P., and Lalithakumari, D. (2003). Release and regeneration of protoplasts from the fungus *Trichothecium roseum*. *Canadian journal of microbiology*, *49*(4), 263-268.
5. Barka, E. A., Vatsa, P., Sanchez, L., Gaveau-Vaillant, N., Jacquard, C., Klenk, H. P., ... and Van Wezel, G. P. (2016). Taxonomy, physiology, and natural products of Actinobacteria. *Microbiology and Molecular Biology Reviews*, *80*(1), 1-43.
6. Becker, J. O. (2014). Plant health management: crop protection with nematicide, *Encyclopedia of Agriculture and Food Systems*, 4, 400-407.
7. Beier, S., and Bertilsson, S. (2013) Bacterial chitin degradation—mechanisms and ecophysiological strategies. *Frontiers in Microbiology,* 4, 149.
8. Bélanger, R. R. (2001) Biological control in greenhouse systems. *Annual Review of Phytopathology,* 39, 103–133.
9. Berini, F., Caccia, S., Franzetti, E., Congiu, T., Marinelli, F., Casartelli, M., and Tettamanti, G.
(2016). Effects of *Trichoderma viride* chitinases on the peritrophic matrix of *Lepidoptera*. *Pest management science*, 72(5), 980-989.
10. Bhattacharya, D., Nagpure, A., and Gupta, R. K. (2007). Bacterial chitinases: properties and potential. *Critical reviews in biotechnology*, *27*(1), 21-28.
11. Binod, P., Sukumaran, R. K., Shirke, S. V., Rajput, J. C., and Pandey, A. (2007). Evaluation of fungal culture filtrate containing chitinase as a biocontrol agent against *Helicoverpa armigera*. *Journal of applied microbiology*, *103*(5), 1845-1852.
12. Bolar, J. P., Norelli, J. L., Harman, G. E., Brown, S.

K., and Aldwinckle, H. S. (2001). Synergistic activity of endochitinase and exochitinase from *Trichoderma atroviride* (*T. harzianum*) against the pathogenic fungus (*Venturia inaequalis*) in transgenic apple plants. *Transgenic research*, *10*(6), 533-543.

13. Brimner, T. A., and Boland, G. J. (2003). A review of the non-target effects of fungi used to biologically control plant diseases. *Agriculture, Ecosystem and Environment,* 100(1), 3-16.
14. Brzezinska, M. S., and Jankiewicz, U. (2012). Production of antifungal chitinase by *Aspergillus niger* LOCK 62 and its potential role in the biological control. *Current microbiology*, *65*(6), 666-672.
15. Brzezinska, M. S., Jankiewicz, U., and Walczak, M. (2013) Biodegradation of chitinous substances and chitinase production by the soil actinomycete *Streptomyces rimosus*. *International Biodeterioration and Biodegradation,* 84, 104–110.
16. Budi, S. W., Van Tuinen, D., Arnould, C., Dumas-Gaudot, E., Gianinazzi-Pearson, V., and Gianinazzi, S. (2000). Hydrolytic enzyme activity of *Paenibacillus sp.* strain B2 and effects of the antagonistic bacterium on cell integrity of two soil-borne pathogenic fungi. *Applied Soil Ecology*, *15*(2), 191-199.
17. Chan, Y. L., Cai, D., Taylor, P. W. J., Chan, M. T., and Yeh, K. W. (2010). Adverse effect of the chitinolytic enzyme PjCHI 1 in transgenic tomato on egg mass production and embryonic development of *Meloidogyne incognita*. *Plant pathology*, *59*(5), 922-930.
18. Chandler, D., Bailey, A. S., Tatchell, G. M., Davidson, G., Greaves, J., and Grant, W. P. (2011). The development, regulation and use of biopesticides for integrated pest management. *Philosophical Transactions of the Royal Society B, Biological Sciences*, *366*(1573), 1987-1998.
19. Chandrasekaran, R., Revathi, K., Nisha, S., Kirubakaran, S. A., Sathish-Narayanan, S., and Senthil-Nathan, S. (2012). Physiological effect of chitinase purified from *Bacillus subtilis* against the tobacco cutworm *Spodoptera litura (Fab)*. *Pesticide biochemistry and physiology*, *104*(1), 65-71.
20. Chen, J. K., Shen, C. R., and Liu, C. L. (2010). N-acetylglucosamine: production and applications. *Marine drugs*, *8*(9), 2493-2516.
21. Chen, Y. L., Lu, W., Chen, Y. H., Xiao, L., and Cai, J. (2007). Cloning, expression and sequence analysis of chiA, chiB in *Bacillus thuringiensis* subsp. *colmeri* 15A3. *Wei sheng wu xue bao= Acta microbiologica Sinica*, *47*(5), 843-848.
22. Chen, J., An, Y., Kumar, A., and Liu, Z. (2017). Improvement of chitinase Pachi with nematicidal activities by random mutagenesis. *International journal of biological macromolecules*, *96*, 171-176.
23. Chen, L., Jiang, H., Cheng, Q., Chen, J., Wu, G., Kumar, A., ... and Liu, Z. (2015). Enhanced nematicidal potential of the chitinase pachi from *Pseudomonas aeruginosa* in association with Cry21Aa. *Scientific reports*, *5*, 14395.
24. Cohen-Kupiec, R., and Chet, I. (1998). The molecular biology of chitin digestion. *Current opinion in biotechnology*, *9*(3), 270-277.
25. Cronin, D., Moënne-Loccoz, Y., Dunne, C., and O'gara, F. (1997). Inhibition of egg hatch of the potato cyst nematode *Globodera rostochiensis* by chitinase-producing bacteria. *European Journal of Plant Pathology*, *103*(5), 433-440.
26. Dahiya, N., Tewari, R., and Hoondal, G. S. (2006). Biotechnological aspects of chitinolytic enzymes: a review. *Applied microbiology and biotechnology*, *71*(6), 773-782.
27. Dahiya, N., Tewari, R., Tiwari, R. P., and Singh Hoondal, G. (2005). Chitinase from *Enterobacter sp.* NRG4: Its purification, characterization and reaction pattern. *Electronic Journal of Biotechnology*, *8*(2), 14-25.
28. Daizo, K. O. G. A. (2005). Application of chitinase in agriculture. *Journal of Metals, Materials and Minerals*, *15*(1), 33-36.
29. Edreva, A. (2005) Pathogenesis-related proteins: research progress in the last 15 years. *General and Applied Plant Physiology,* 31, 105–124.
30. Fahmi, A. I., Al-Talhi, A. D., and Hassan, M. M. (2012). Protoplast fusion enhances antagonistic activity in *Trichoderma spp*. *Nature and Science*, *105*, 100-106.
31. Gan, Z., Yang, J., Tao, N., Liang, L., Mi, Q., Li, J., and Zhang, K. Q. (2007). Cloning of the gene *Lecanicillium psalliotae* chitinase Lpchi1 and identification of its potential role in the biocontrol of root-knot nematode *Meloidogyne incognita*. *Applied Microbiology and Biotechnology*, *76*(6), 1309-1317.
32. Geisseler, D., Horwath, W. R., Joergensen, R. G., and Ludwig, B. (2010). Pathways of nitrogen utilization by soil microorganisms–a review. *Soil Biology and Biochemistry*, *42*(12), 2058-2067.

33. Ghasemi, S., Ahmadian, G., Jelodar, N. B., Rahimian, H., Ghandili, S., Dehestani, A., and Shariati, P. (2010). Antifungal chitinases from *Bacillus pumilus* SG2: preliminary report. *World Journal of Microbiology and Biotechnology*, *26*(8), 1437-1443.

34. Gonzalez-Franco, A. C., Deobald, L. A., Spivak, A., and Crawford, D. L. (2003). Actinobacterial chitinase-like enzymes: profiles of rhizosphere versus non-rhizosphere isolates. *Canadian Journal of Microbiology*, *49*(11), 683-698.

35. Gooday, G. W., and Gow, N. A. (1990). Enzymology of tip growth in fungi. *Tip growth in plant and fungal cells*, 31-58.

36. Gunaratna, K. R., and Balasubramanian, R. (1994). Partial purification and properties of extracellular chitinase produced by *Acremonium obclavatum*, an antagonist to the groundnut rust, *Puccinia arachidis*. *World Journal of Microbiology and Biotechnology*, *10*(3), 342-345.

37. Gupta, R., Saxena, R. K., Chaturvedi, P., and Virdi, J. S. (1995). Chitinase production by *Streptomyces viridificans*: its potential in fungal cell wall lysis. *Journal of Applied Microbiology*, *78*(4), 378-383.

38. Hollensteiner, J., Wemheuer, F., Harting, R., Kolarzyk, A. M., Valerio, D., Stefani, M., ... and Braus, G. H. (2017). *Bacillus thuringiensis* and *Bacillus weihenstephanensis* inhibit the growth of phytopathogenic *Verticillium* species. *Frontiers in microbiology*, *7*, 2171.

39. Hong, J. K., and Hwang, B. K. (2006). Promoter activation of pepper class II basic chitinase gene, CAChi2, and enhanced bacterial disease resistance and osmotic stress tolerance in the CAChi2-overexpressing Arabidopsis. *Planta*, *223*(3), 433.

40. Huang, Z., Hao, Y., Gao, T., Huang, Y., Ren, S., and Keyhani, N. O. (2016). The Ifchit1 chitinase gene acts as a critical virulence factor in the insect pathogenic fungus *Isaria fumosorosea*. *Applied microbiology and biotechnology*, *100*(12), 5491-5503.

41. Jang, M. K., Kong, B. G., Jeong, Y. I., Lee, C. H., and Nah, J. W. (2004). Physicochemical characterization of α chitin, β chitin, and γ chitin separated from natural resources. *Journal of Polymer Science Part A: Polymer Chemistry*, *42*(14), 3423-3432.

42. Jung, S. J., An, K. N., Jin, Y. L., Park, R. D., Kim, K. Y., Shon, B. K., and Kim, T. H. (2002). Effect of chitinase-producing *Paenibacillus illinoisensis* KJA-424 on egg hatching of root-knot nematode (*Meloidogyne incognita*). *Journal of microbiology and biotechnology*, *12*(6), 865-871.

43. Kalia, A., and Gosal, S. K. (2011). Effect of pesticide application on soil microorganisms. *Archives of Agronomy and Soil Science*, *57*(6), 569-596.

44. Kamil, Z., Rizk, M., Saleh, M., and Moustafa, S. (2007). Isolation and Identification of Rhizosphere Soil Chitinolytic Bacteria and their Potential in Antifungal Biocontrol. *Global Journal of Molecular Sciences*, 2(2), 57-66.

45. Karunya, S. K. (2011). Optimization and purification of chitinase produced by *Bacillus subtilis* and its antifungal activity against plant pathogens. *International Journal of Pharmaceutical and Biological Archive*, *2*(6), 1680-1685.

46. Lee, Y. S., and Kim, K. Y. (2015). Statistical optimization of medium components for chitinase production by *Pseudomonas fluorescens* strain HN1205: role of chitinase on egg hatching inhibition of root-knot nematode. *Biotechnology and Biotechnological Equipment*, *29*(3), 470-478.

47. Liu, D., Cai, J., Xie, C. C., Liu, C., and Chen, Y. H. (2010). Purification and partial characterization of a 36-kDa chitinase from *Bacillus thuringiensis* subsp. *colmeri*, and its biocontrol potential. *Enzyme and Microbial Technology*, *46*(3-4), 252-256.

48. Mankau, R., and Das, S. (1969). Influence Of Chitin Amendments On *Meloidogyne Incognita*. *Journal of Nematology*, 1(1), 15.

49. Mathivanan, N., Kabilan, V., and Murugesan, K. (1998). Purification, characterization, and antifungal activity of chitinase from *Fusarium chlamydosporum*, a mycoparasite to groundnut rust, *Puccinia arachidis*. *Canadian Journal of Microbiology*, *44*(7), 646-651.

50. Mi, Q., Yang, J., Ye, F., Gan, Z., Wu, C., Niu, X., ... and Zhang, K. Q. (2010). Cloning and overexpression of *Pochonia chlamydosporia* chitinase gene pcchi44, a potential virulence factor in infection against nematodes. *Process Biochemistry*, *45*(5), 810-814.

51. Mian, I. H., Godoy, G., Shelby, R. A., Rodriguez-Kabana, R., and Morgan-Jones, G. (1982). Chitin amendments for control of *Meloidogyne arenaria* in infested soil. *Nematropica*, *12*(1), 71-84.

52. Miller, P. M., Sands, D. C., and Rich, S. (1973). Effect of industrial mycelial residues, wood fiber wastes, and chitin on plant-parasitic nematodes and some soilborne diseases. *Plant Disease Reporter*, *57*(5), 438-442.

53. Mitsutomi, M., Kidoh, H., Tomita, H., and Watanabe, T. (1995). The action of *Bacillus circulans* WL-12 chitinases on partially N-acetylated chitosan. *Bioscience, biotechnology, and biochemistry*, *59*(3), 529-531.

54. Morgan-Jones, G., White, J. F., and Rodriguez-Kabana, R. (1984). Phytonematode pathology: Ultrastructural studies. II. Parasitism of *Meloidogyne arenaria* eggs and larvae by *Paecilomyces lilacinus*. *Nematropica*, *14*(1), 57-71.

55. Muzzarelli, R. A., Boudrant, J., Meyer, D., Manno, N., DeMarchis, M., and Paoletti, M. G. (2012). Current views on fungal chitin/chitosan, human chitinases, food preservation, glucans, pectins and inulin: A tribute to Henri Braconnot, precursor of the carbohydrate polymers science, on the chitin bicentennial. *Carbohydrate Polymers*, *87*(2), 995-1012.

56. Nagpure, A., Choudhary, B., and Gupta, R. K. (2014). Chitinases: in agriculture and human healthcare. *Critical reviews in biotechnology*, *34*(3), 215-232.

57. Narayana, K. J., and Vijayalakshmi, M. (2009). Chitinase production by *Streptomyces sp*. ANU 6277. *Brazilian Journal of Microbiology*, *40*(4), 725-733.

58. Ni, H., Zeng, S., Qin, X., Sun, X., Zhang, S., Zhao, X., ... and Li, L. (2015). Molecular docking and site-directed mutagenesis of a *Bacillus thuringiensis* chitinase to improve chitinolytic, synergistic lepidopteran-larvicidal and nematicidal activities. *International journal of biological sciences*, *11*(3), 304.

59. Nurdebyandaru, N., Mubarik, N. R., and Prawasti, T. S. (2010). Chitinolytic bacteria isolated from Chili rhizosphere: Chitinase characterization and application as biocontrol for *Aphis gossypii*. *Microbiology Indonesia*, *4*(3).

60. Pichyangkura, R., Kudan, S., Kuttiyawong, K., Sukwattanasinitt, M., and Aiba, S. I. (2002). Quantitative production of 2-acetamido-2-deoxy-D-glucose from crystalline chitin by bacterial chitinase. *Carbohydrate Research*, *337*(6), 557-559.

61. Russell, P. E. (2006) The development of commercial disease control. *Plant Pathology* 55(5), 585–594.

62. Sahai, A. S., and Manocha, M. S. (1993). Chitinases of fungi and plants: their involvement in morphogenesis and host parasite interaction. *FEMS Microbiology Reviews*, *11*(4), 317-338.

63. Saito, A., Ooya, T., Miyatsuchi, D., Fuchigami, H., Terakado, K., Nakayama, S. Y., ... and Ando, A. (2009). Molecular characterization and antifungal activity of a family 46 chitosanase from *Amycolatopsis sp*. CsO-2. *FEMS microbiology letters*, *293*(1), 79-84.

64. Shahidi, F., and Abuzaytoun, R. (2005). Chitin, chitosan, and co-products: chemistry, production, applications, and health effects. *Advances in food and nutrition research*, *49*, 93-137.

65. Soares, F. E. D. F., de Queiroz, J. H., de Araújo, J. V., Queiroz, P. V., Gouveia, A. D. S., Hiura, E., and Braga, F. R. (2015). Nematicidal action of chitinases produced by the fungus *Monacrosporium thaumasium* under laboratorial conditions. *Biocontrol science and technology*, *25*(3), 337-344.

66. Souza, C. P., Almeida, B. C., Colwell, R. R., and Rivera, I. N. (2011). The importance of chitin in the marine environment. *Marine biotechnology*, *13*(5), 823.

67. Spiegel, Y., Cohn, E., and Chet, I. (1989). Use of chitin for controlling *Heterodera avenae* and *Tylenchulus semipenetrans*. *Journal of nematology*, *21*(3), 419.

68. Spiegel, Y., Cohn, E., Galper, S., Sharon, E., and Chet, I. (1991). Evaluation of a newly isolated bacterium, *Pseudomonas chitinolytica sp.* nov., for controlling the root knot nematode *Meloidogyne javanica*. *Biocontrol science and technology*, *1*(2), 115-125.

69. Stoykov, Y. M., Pavlov, A. I., and Krastanov, A. I. (2015). Chitinase biotechnology: production, purification, and application. *Engineering in Life Sciences*, *15*(1), 30-38.

70. Suganthi, M., Senthilkumar, P., Arvinth, S., and K. N, C. (2017). Chitinase from *Pseudomonas fluorescens* and its insecticidal activity against *Helopeltis theivora*. *The Journal of general and applied microbiology*, *63*(4), 222-227.

71. Suginta, W., Robertson, P. A. W., Austin, B., Fry, S. C., and Fothergill Gilmore, L. A. (2000). Chitinases from *Vibrio*: activity screening and

purification of chiA from *Vibrio carchariae*. *Journal of applied microbiology*, *89*(1), 76-84.

72. Velusamy, P., Ko, H. S., and Kim, K. Y. (2011). Determination of antifungal activity of *Pseudomonas sp.* A3 against *Fusarium oxysporum* by high performance liquid chromatography (HPLC). *Agriculture Food and Analytical Bacteriol*ogy, *1*, 15-23.
73. Wharton, D. (1980). Nematode egg-shells. *Parasitology*, *81*(2), 447-463.
74. Xiao, L., Xie, C. C., Cai, J., Lin, Z. J., and Chen, Y. H. (2009). Identification and characterization of a chitinase-produced *Bacillus* showing significant antifungal activity. *Current microbiology*, *58*(5), 528-533.
75. Yuli, P. E., Suhartono, M. T., Rukayadi, Y., Hwang, J. K., and Pyun, Y. R. (2004). Characteristics of thermostable chitinase enzymes from the Indonesian *Bacillus sp*. 13.26. *Enzyme and microbial technology*, *35*(2), 147-153.
76. Zarei, M., Aminzadeh, S., Zolgharnein, H., Safahieh, A., Daliri, M., Noghabi, K. A., ... and Motallebi, A. (2011). Characterization of a chitinase with antifungal activity from a native *Serratia marcescens* B4A. *Brazilian Journal of Microbiology*, *42*(3), 1017-1029.
77. Zeki, N. H., and Muslim, S. N. (2017). Purification, characterization and antifungal activity of chitinase from *Serratia marcescens* isolated from fresh vegetables. *Ibn AL-Haitham Journal for Pure and Applied Science*, *23*(1), 13-25.

Reflections of Visionaries

"I am happy to know that CHARUSAT has a goal set for mission of social upliftment with components of knowledge acquisition and imparting education."

Dr. APJ Abdul Kalam
Former President of India
Architect of Missile Programme of india

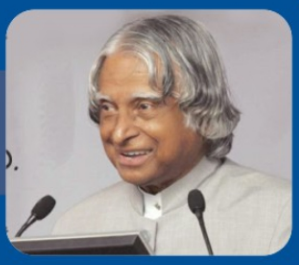

Shri Narendra Modi
Hon. Prime Minister of India

"CHARUSAT is indeed a Golden Truth of Gujarat."

"I am extremely impressed with CHARUSAT as it is driven by Research and innovation."

Dr. Vijay Bhatkar
Padmashri
Architect of India's First Super Computer-PARAM

Dr. R A Mashelkar
Padma Vibhushan
National Research Professor;
National Chemical Laboratory

"I was proud to see that the CHARUSAT has the dream of becoming world class in education and research. This dream can be converted into reality, if we match this 'great ambition' with 'stimulating ambience'. I have no doubt that this dream will become a reality."

CHARUSAT
CHAROTAR UNIVERSITY OF SCIENCE AND TECHNOLOGY

CHAROTAR UNIVERSITY OF SCIENCE AND TECHNOLOGY

CHARUSAT Campus
Off Nadiad – Petlad Highway, Changa, Dist. Anand – 388 421 (Gujarat) India.
Ph # 91 2697 265011, 265021 **Fax** # 91 2697 265007 **Email:** info@charusat.ac.in **Website:** www.charusat.ac.in

Front Cover Design: Aditya Pawar and Farhin Patel (University Students)

Edited by Dr. Palash Mandal, Printed and Published by Dr. Devang Joshi, On behalf of Charotar University of Science and Technology, Changa-388421, Gujarat, India and Printed at Reprography Centre, 1st floor, Administration Block, Charotar University of Science and Technology, CHARUSAT Campus, Changa-388421, Gujarat, India.